Biology and Prognostic Value of N-Myristoyltransferase 1 (NMT1) and NMT2 in Acute Myeloid Leukemia (AML)

by

Ryan Stubbins

A thesis submitted in partial fulfillment of the requirements for the degree of

Master of Science

in

Translational Medicine

Department of Medicine
University of Alberta

Abstract

Myristoylation is the post-translational modification of proteins with a 14-carbon fatty-acid by N-myristoyltransferase 1 (NMT1) or NMT2. Myristoylation is key to protein membrane binding and cell survival. Bioinformatics data suggests NMT mRNA expression impacts overall survival (OS) in AML. We characterized NMT protein levels in AML patients.

We performed a retrospective and prospective cohort study, including adult patients newly diagnosed with AML in Edmonton from April 2014 until September 2016, excluding acute promyelocytic leukemia. In addition, a small group of control marrow aspirates were obtained. We assayed marrow aspirate or peripheral blood for NMT1/2 protein levels by fluorescence activated cell sorting with intracytoplasmic staining by custom mouse anti-NMT1-Alexa-Fluor-647 or anti-NMT2-FITC, expressed as Mean Fluorescent Intensity (MFI) relative to IgG1k isotype control. NMT1/2 MFI was determined for the bulk blast, CD34+, and CD34+38- blast subpopulations. Clinical data was analysed by t-test or ANOVA. Relapse-free survival (RFS) and OS were dichotomized with a receiver operator curve, followed by a Kaplan-Meier analysis with a log-rank test for significance or univariate and multivariate Cox regression, with $p < 0.05$ as significant. Censoring, survival, and clinical parameters were defined by European LeukemiaNet (ELN) guidelines and REMARK criteria.

Recruitment reached 105 patients. Median age was 67.1 years, with 57 ELN intermediate-risk patients. Median follow-up and OS are 1.54 and 0.95 years, respectively. NMT1 MFI was consistent through all samples. NMT2 MFI was higher in lymphocytes (mean MFI = 3.01 ± 0.08) vs. monocytes (mean MFI = 0.98 ± 0.03, $p < 0.001$) NMT2 MFI did not vary between AML bulk blast (mean MFI = 1.13 ± 0.03), CD34+ blast (mean MFI = 1.21 ± 0.03), and CD34+38- blast populations (mean MFI 1.22 ± 0.04) ($p = 0.145$). NMT2 MFI was significantly higher in control CD34+ cells (mean MFI = 1.65 ± 0.11, $p < 0.001$) and CD34+38- cells (mean MFI = 1.91 ± 0.17, $p < 0.001$) versus their AML counterparts. NMT2 MFI was significantly higher in AML with the cytogenetic abnormality inv(16) (mean MFI = 1.67 ± 0.05, $p < 0.001$), and slightly lower with mutated NPM1 (mean MFI = 1.09 ± 0.04, $p = 0.004$). NMT2 MFI was not associated with ELN risk groups or remission status. (p=0.166, 0.303). NMT2 MFI receiver operator curve analysis for OS in ELN intermediate-risk AML in CD34+38- cells generated a

cut-off 1.28 (AUC=0.697, p=0.021) for sensitivity=50% and specificity=80%. Kaplan-Meier analysis was significant with respect to RFS in the CD34+38- population (p = 0.038) and OS in the bulk blast population (p = 0.005). Kaplan-Meier analysis was significant with respect to OS for bulk blast (p = 0.048) and CD34+38- population (p = 0.014) when analyzing the intermediate-risk, age < 65 years patient subgroup. NMT2 was not significant for RFS or OS versus the ELN scheme by univariate or multivariate Cox regression. NMT2 MFI for all intermediate-risk patients was not significant for RFS on univariate Cox regression, but was significant on multivariate regression (p = 0.019). NMT2 MFI for OS in all intermediate-risk patients was significant on univariate Cox regression (p = 0.007) but not significant on multivariate analysis. Age and WBC at diagnosis were used as covariates.

We analyzed how NMT1 and NMT2 MFI relate to clinical factors, cytogenetics, molecular abnormalities, ELN risk group, and clinical outcomes in AML. NMT1 was not associated with any of these factors. NMT2 MFI was intermediate in normal hematopoietic stem cells, higher in lymphocytes, and lower in monocytes. This suggests that regulation of NMT2 protein levels may influence early lymphoid/myeloid lineage commitment, possibly by modulation of the T-cell receptor pathway. The cytogenetic abnormality inv(16) showed significantly higher NMT2 MFI, possibly secondary to control of NMT2 expression by the transcriptional regulators RUNX2 and RUNX3. NMT2 MFI was moderately lower in patients with NPM1. NMT2 MFI was not associated with ELN risk group, or achievement of CR with first induction chemotherapy. Higher NMT2 MFI generally predicted worsened outcomes in the ELN intermediate-risk population, with this effect being driven by the CD34+38- blast subsets. This may represent an indirect measure of the stemness of the blast population, and the LSC burden in patients with AML. NMT2 MFI may be a novel biomarker for prognosis in intermediate-risk AML, and further investigation is warranted.

Preface

All fluorescence activated cell sorting data was generated, interpreted, and gated by Zoulika Zak[1] and Dr. Arthur Szkotak[4], with sample processing assistance provided by Aishwarya Iyer[2] and Megan Yap[2] from the lab of Dr. Luc G. Berthiaume.[2] Additional assistance in processing and running fluorescence activated cell sorting was provided by the diagnostic hematology lab at the University of Alberta Hospital. Preliminary bioinformatics data, mentioned in section 2.3, was provided by Dr. Luc G. Berthiaume[2] or Krista Vincent[3,5], in association with Lynne Postovit.[4] This study was established as a sub-investigation of the minimal residual disease study being run by Dr. Lalit Saini,[1] who provided both logistical support and components of the clinical data. The primary investigator of this study was Dr. Joseph M. Brandwein,[1] working in collaboration with Dr. Luc G. Berthiaume[2] and Dr. John R. Mackey.[3] This study received research ethics approval from the research ethics and management office (REMO) at the University of Alberta.

Department of Medicine[1], Cell Biology[2], Oncology[3], and Laboratory Medicine and Pathology[4], Faculty of Medicine and Dentistry, University of Alberta.
Schulich School of Medicine and Dentistry[5], University of Western Ontario

Acknowledgements

I thank the members of my supervisory committee, Dr. Joseph M. Brandwein, Dr. Luc G. Berthiaume, and Dr. John R. Mackey for their ongoing mentorship and support. In addition, I also extend thanks to Zoulika Zak and Dr. Arthur Szkotak for their role in collecting and interpreting the flow cytometry data that formed the basis of this study. In addition, I thank the members of the Berthiaume Lab, Aishwarya Iyer and Megan Yap, for their assistance with processing samples for flow cytometry analysis. I am also thankful for Krista Vincent, Dr. Lynne Postovit, and Dr. Luc G. Berthiaume, for their contribution of the bioinformatics data that led to the initiation of this study. I also acknowledge and thank Dr. Lalit Saini, who has provided invaluable support in multiple aspects of this study.

Table of Contents

List of Tables

List of Figures

List of Abbreviations

Allo-HSCT, allogeneic hematopoietic stem cell transplant	**M-CSF**, Macrophage colony stimulating factor
AML, acute myeloid leukemia	**MARCKS**, myristoylated alanine-rich C-kinase substrate
AML1-ETO, acute myeloid leukemia 1 protein-eight twenty one oncoprotein	**MDS**, myelodysplastic syndrome
ARF, alternative reading frame tumor suppressor	**MFI**, mean fluorescent intensity ratio
AUC, area under the curve	**MPN**, myeloproliferative neoplasm
BID, BH3 interacting domain death agonist	**NMT**, N-myristoyltransferase
c-Src, proto-oncogene tyrosine-protein kinase Src	**NMT1**, N-myristoyltransferase 1
CBF, core binding factor	**NMT1$^{f/f}$**, floxed NMT1
CBFB-MYH11, core binding factor B-myosin heavy chain 11	**NMT2**, N-myristoyltransferase 2
CEBPA, CCAT/enhancer binding protein	**NMT2$^{f/f}$**, floxed NMT2
CR, complete remission	**NOD-SCID**, non-obese diabetic-severe combined immunodeficiency mice
ELN, European LeukemiaNet	**NPM1**, nucleophosmin 1
FACS, Fluorescent activated cell sorting	**OS**, overall survival
Fbw7γ, F-box and WD repeat domain containing protein 7	**PCR**, polymerase chain reaction
FISH, fluorescence *in-situ* hybridization	**PKCε**, protein kinase C epsilon type
FLAG-IDA, fludarabine, cytarabine, G-CSF, and idarubicin chemotherapy	**PPM1A**, protein phosphatase magnesium dependent 1A
FLT3-ITD, fms-like tyrosine kinase 3 with internal tandem deletion	**PPM1B**, protein phosphatase magnesium dependent 1B
G-CSF, Granulocyte colony stimulating factor	**RD**, resistant disease
GEO, Gene Expression Omnibus	**RFS**, relapse-free survival
GEP, gene-expression profiling	**ROC**, receiver operator curve
GM-CSF, Granulocyte macrophage colony stimulating factor	**RUNX**, runt-related transcription factor
HSC, hematopoietic stem cell	**SMAD6,** mothers against decapentaplegic homolog 6
IDAC, idarubicin and cytarabine	**SMMHC**, smooth muscle myosin heavy chain
Lck, lymphocyte specific protein kinase	**TCGA**, The Cancer Genome Atlas
LDAC, low dose cytarabine	**TCR**, T-cell receptor
LSC, leukemic stem cell	**WBC**, white blood cell

Chapter 1 - Introduction

1.1 - The need for novel prognostic markers

Acute Myeloid Leukemia (AML) is a heterogeneous disease characterized by the uncontrolled proliferation of minimally differentiated hematopoietic precursor cells, known as blasts. This is the result of a diverse array of acquired genetic defects that block the terminal differentiation of hematopoietic stem cells (HSCs). Prognostication in patients with AML is key to optimal management, as risk adapted therapy allows for the maximization of patient benefit, while minimizing the impact of highly toxic treatments. [1-3]

Intensity and duration of therapy, including decisions about stem cell transplant, are currently determined by the European LeukemiaNet (ELN) risk classification scheme. The ELN classification scheme adequately predicts adverse and favorable outcomes, but performs poorly for the 50% of patients who fall into the intermediate-risk categorization. [1-3] As such, new prognostic biomarkers continue to be needed in AML.

1.2 - The nature of current prognostic markers

The ELN classification system is currently predicated on cytogenetic and molecular genetic markers that are identified through a combination of karyotyping, fluorescence *in-situ* hybridization (FISH), and polymerase chain reaction (PCR). [1] Exhaustive investigation has been done to identify genetic markers of prognosis in AML, with one of the most recently developed assays involving a gene expression profiling (GEP) panel examining leukemic stem cell (LSC) signatures in AML patient samples. [4] In addition, recent whole-exome sequencing suggests that several of the high impact gene-level mutations in AML have already been identified. [5] What remains unexplored is the proteome; there currently exists no validated protein based biomarkers in AML. As such, protein based biomarkers represents an attractive and unexplored field for prognosis in AML.

1.3 - Proposing a novel protein based biomarker

Herein we perform an exploratory study examining N-myristoyltransferase (NMT), an enzyme that post-translationally modifies intracellular proteins, resulting in alterations to cellular pathways involved in signal transduction and apoptosis. Building on pre-clinical data, we used patient samples to examine the variations in NMT protein levels between normal controls and patients with AML. We also establish the variation between different blast immunophenotypes, with a focus on those relating to the leukemic stem cell (LSC). Further, we explore the relation of NMT protein levels to established prognostic markers, including the different ELN risk groups, and how these levels relate to clinical outcomes and prognosis in AML.

Chapter 2 - Background

2.1 - The biology of myristoylation and N-myristoyltransferase 1 (NMT1) and NMT2

2.1.1 - The regulation of protein function and cell signaling by NMT1 and NMT2

Myristoylation is a form of protein modification in which the 14-carbon fatty acid myristate is attached to intracellular proteins, either co- or post-translationally, by the enzymes NMT1 and NMT2. Myristate is covalently attached to either an N-terminal glycine shortly after protein translation in a co-translational fashion, or added to an internal glycine in a post-translational fashion after exposure of a cryptic myristoylation consensus sequence by caspase cleavage. [6, 7] The addition of the hydrophobic myristoyl moiety modifies protein activity in a variety of ways. Commonly this results in the reversible targeting of a protein towards cellular membranes and lipid rafts, which can facilitate native activity or result in protein interactions by co-localization at the membrane. Myristoylation can also modify protein activity by inducing weak protein-protein interactions, or stabilizing the tertiary structure of certain proteins. [6-8]

Myristoylation is ubiquitous in eukaryotic cells and has been demonstrated in mammals, yeast, fungi, plants and parasites. In addition to endogenous proteins, it has been demonstrated that some viral proteins, such as HIV-1 *Gag* and *Nef*, are myristoylated *in vivo* by the host NMT, and myristoylation is essential to HIV-1 pathogenesis. NMT has a diverse range of protein targets, with an estimated 0.5 to 3% of all intracellular proteins being myristoylated. [6] These proteins have diverse roles, but they most commonly are involved in either cellular signaling or apoptosis. Examples of NMT targets involved in signaling include tyrosine kinases, such as

proto-oncogene tyrosine-protein kinase Src (c-Src), other protein kinases, such as protein kinase C epsilon type (PKCε), protein phosphatases, such as protein phosphatase magnesium dependent 1A and B (PPM1A and B). Myristoylation is essential for the proper functioning of many of these proteins, and the absence of NMT can impair signaling cascades involving these proteins, resulting in a variety of consequences to cellular function. [6-10] NMT itself is regulated at the gene level by several transcription factors, such as mothers against decapentaplegic homolog 6 (SMAD6), at the epigenetic level by promoter methylation, and at the protein level by both phosphorylation and the intracellular availability of its substrate, myristate. [7, 11]

2.1.2 - The isoforms NMT1 and NMT2

Two isoforms of NMT exists in mammalian cells, N-myristoyltransferase 1 (NMT1) and N-myristoyltransferase 2 (NMT2). These isozymes are encoded by distinct genes, located on chromosomes 17 and 10, respectively. They have overlapping but distinct substrate specificities, while sharing a 77% similar sequence identity. Each individual isozyme is highly conserved amongst different mammalian species, with the human and mouse homologues of NMT1 and NMT2 sharing 97% and 96% identity, respectively. This suggests that each isozyme likely has a specific physiologic role, though the distinct targets and roles of the different isozymes remain to be fully defined. [6] One study utilizing small interfering RNAs to ablate either NMT1 or NMT2 activity in an SK-OV-3 cell line showed that NMT1, particularly, was critical for tumor cell proliferation, though the loss of either isozyme increased apoptosis by downregulating anti-apoptotic pathways. The same study also utilized an *in vivo* assay that suggested silencing either NMT1 alone or NMT1 and NMT2 inhibits tumor growth. Notably, this study also suggested that cell lines could upregulate NMT2 to compensate for a loss of NMT1 activity, though the converse was not true. [12] Another study noted that the presence of NMT2 activity alone did not provide sufficient redundancy to rescue the embryonal development of $NMT1^{-/-}$ knockout mice, further suggesting that each NMT isoform have distinct physiologic roles. [13]

2.1.3 - NMT1 and NMT2 in hematopoiesis and leukocyte function

Limited investigation has been previously performed with regards to potential roles for myristoylation in hematopoiesis, with most previous investigation having primarily targeted NMT1. One previous study demonstrated that heterozygous $NMT1^{+/-}$ knockout mice had

suppressed macrophage colony formation when mice bone marrow cells were stimulated with granulocyte colony stimulating factor (G-CSF), macrophage colony stimulating factor (M-CSF), or granulocyte macrophage colony stimulating factor (GM-CSF). They also demonstrated that homozygous $NMT1^{-/-}$ embryonic stem cells had a severely impaired ability to differentiate into mature macrophages. These results suggest that NMT activity may be necessary for proper myeloid differentiation. [14-16]

NMT activity is critical to T-cell development, with a previous study demonstrating that T-cell receptor (TCR) signaling was disrupted in mice with T-cell lineage specific deficiencies in NMT1 and NMT2 activity, resulting in a developmental blockage of thymocyte development. This was due to mislocalized lymphocyte specific protein kinase (Lck), a member of the Src family of tyrosine kinases, and myristoylated alanine-rich C-kinase substrate (MARCKS), both essential to TCR signaling. [17]

2.1.4 - NMT1 and NMT2 in apoptosis and cancer

Apoptosis, or programmed cell death, is the physiologic mechanism by which cells that have sustained genetic, membrane or metabolic injury are removed from the organism. This involves the activation of a metabolic cascade, mediated by enzymes known as caspases. It is critical to the removal of cells with DNA damage that could lead to malignant proliferation, and dysfunction of apoptosis is characteristic of malignant cells. [6] Myristoylation and NMT activity is known to be central to the apoptosis cascade, with multiple proteins revealing cryptic myristoylation sequences upon caspase cleavage. One example of these is the protein BH3 interacting domain death agonist (BID), which upon cleavage by caspase-8 localized to the mitochondrial membrane, which triggers cellular apoptosis by the cytochrome c pathway. [6, 18-21] Upwards of 15 other proteins also undergo post-translational myristoylation after caspase cleavage, suggesting that this mechanism is widely applicable throughout multiple points in the apoptotic signaling cascades. [6, 19, 21]

There is also substantial evidence that NMT expression is aberrant in cancer, with NMT having been shown to be overexpressed in colorectal adenocarcinomas, gallbladder carcinomas, oral squamous cell carcinomas and brain tumors. In colon adenocarcinoma, there is evidence that

NMT activity is higher overall, with the NMT2 isoform having particularly high expression levels. [22-27] These observations have been entirely restricted to solid tumors, with no literature currently examining NMT in relation to cancers of hematologic origin.

2.2 - Pathogenesis, prognostication, and treatment in AML

2.2.1 - The European LeukemiaNet (ELN) Prognostic Scheme

The current standard for risk stratification in AML is the ELN prognostic scheme, which categorizes patients as either favorable risk, intermediate risk, or unfavorable risk at diagnosis. Survival and relapse rates are dramatically different among the three groups. Patients of age less than 60 who did not receive an allogeneic hematopoietic stem cell transplant (Allo-HSCT) carrying a median overall survival (OS) of 63.6 months for favorable, 13.6 - 18.7 months for intermediate, and 6.0 months in unfavorable. [2] The ELN risk group is established upfront, with karyotyping for recurrent cytogenetic abnormalities, PCR testing for recurrent molecular mutations, and FISH for some recurrent translocations performed on the initial diagnostic bone marrow aspirate. A favorable prognosis is portended by the presence of the core binding factor (CBF) translocations inv(16) or t(8;21). These are typically detected on karyotyping, though a FISH for the RUNX1 translocation associated with t(8;21) is often performed as a complementary test. A favorable prognosis is also noted with the detection of mutated nucleophosmin 1 (NPM1) by PCR, when seen in the context of normal cytogenetics and either negative or low detected levels of fms-like tyrosine kinase 3 with internal tandem deletion (FLT3-ITD) by PCR. Similarly, biallelic mutated CCAT/enhancer binding protein (CEBPA) is noted to have a favorable risk profile when detected by PCR. The presence of the cytogenetic translocations inv(3) or t(3;3), t(6;9), t(v;11), -5 or del(5q), -7, or abnormal(17p) all carry an unfavorable risk profile. Patients who have complex cytogenetics, defined as the presence of three or more cytogenetic abnormalities, fall into the unfavorable risk group and are noted to have a particularly poor prognosis. Additionally, mutated FLT3-ITD at high levels in the presence of wild type NPM1 is thought to be a poor prognosis. [1-3] The remainder of patients, typically about 50%, fall into the intermediate risk prognostic group. [2] Decisions on treatment in this group remain challenging, given that there is significant heterogeneity in their outcomes. [1-3]

2.2.2 - Brief review of current therapy and prognosis for AML

A diagnosis of AML is established when a blast population of greater than 20% occurs *de novo* in peripheral blood or bone marrow aspirate. Initial evaluation includes a bone marrow aspirate and trephine biopsy for pathologic examination, flow cytometry/fluorescent activated cell sorting (FACS) to establish the blast immunophenotype, and additional standard labs and coagulation parameters. Karyotyping, PCR, and FISH are performed on the bone marrow aspirate to establish the presence or absence of the prognostic markers noted in 2.2.4. [1] Adverse clinical prognostic markers at initial diagnosis, other than the previously reviewed ELN scheme, include age, particularly age greater than 65, high initial white blood cell (WBC) count, poor performance status, a history of prior exposure to chemotherapy or radiation, and a history of an antecedent myeloproliferative neoplasm (MPN) or myelodysplastic syndrome (MDS). Age, ELN risk group, and performance status typically have the largest impact on relapse-free survival (RFS) and OS. [1-3]

For patients who are considered fit enough to withstand intensive therapy, the initial treatment regimen typically consists of idarubicin and cytarabine (IDAC) induction chemotherapy. Patients then have a repeat bone marrow aspirate at approximately four weeks to assess whether they have achieved complete remission (CR), defined as the presence of less than 5% residual blasts. Patients who do not achieve this are classified as having residual disease (RD). At this point, further decisions on therapy are made in a risk-adapted manner. Patients with a favorable risk profile will typically receive a course of consolidation chemotherapy with cytarabine alone, whereas patients with an adverse risk profile will receive consolidation chemotherapy in addition to being evaluated for allo-HSCT. Patients in the intermediate risk group will receive consolidation chemotherapy, and have the benefits and risks of allo-HSCT weighed against their risk of disease relapse. Patients who are not fit to receive induction chemotherapy will typically either be treated with a demethylating agent, such as azacytidine, low dose chemotherapy with cytarabine (LDAC), be enrolled into a clinical trial, or receive purely symptom management measures. [1-3]

2.2.3 - The biology of leukemic stem cells (LSC)

The concept of a leukemic stem cell (LSC) refers to a unique subpopulation cells in AML that retain features more like HSC than the bulk of their blast counterparts, having an enhanced capacity for self-renewal and persistence (figure 2.2.1). They are implicated in relapse, and represent a highly attractive therapeutic target. They are typically enhanced within the CD34+38- cell compartment, and represent only a small fraction of the overall population of leukemic blasts. The CD34+38- blast subset can engraft to non-obese diabetic-severe combined immunodeficiency (NOD-SCID) mice, whereas the CD34+38+ blast subset cannot, suggesting that this subset has additional self-renewal properties, in comparison to the larger blast population. [28-31] Given that LSC, like HSC, spend more time in the quiescent phases of the cell cycle, they are intrinsically more resistant to chemotherapeutic agents that primarily target actively dividing cells. They are implicated as being one of the main drivers behind disease relapse in AML. [28, 29] One of the most prominent pathways involved in HSC biology is the Wnt/β-catenin pathway. The human genome contains approximately 20 genes that encode for the Wnt proteins. Wnt proteins are all lipid-modified secreted glycoproteins. [30, 32] Increased Wnt signaling has been shown to be critical to both maintenance and proliferation of HSC's and, being a key mediator of HSC persistence, is also likely critical to LSC pathogenesis. [33-35]

2.2.4 - The pathogenesis of AML with core binding factor (CBF) translocations and mutated nucleophosmin 1 (NPM1)

The CBF family encompasses a group of proteins that act as master transcriptional regulators for hematopoietic growth and differentiation. They are the target of mutations or translocations in 15-20% of AML cases. [36] The CBF complex consists of two subunits, α and β. The α subunit has three members encoded by three separate genes: CBFα1, encoded by runt-related transcription factor 2 (RUNX2), CBFα2, encoded by RUNX1, and CBFα3, encoded by RUNX3. The RUNX family are master transcriptional regulators involved in HSC differentiation, and are critical to hematopoiesis. Members of the RUNX family have diverse interactions, and typically result in transcriptional activation, but can also recruit transcriptional repressors. [11] The β unit has a single subunit, CBFβ. CBFBα must interact CBFβ to both stabilize its interaction with DNA and guard it from ubiquitin mediated degradation. [37] The CBFα and CBFβ complex represents a common pathway for the oncogenic effects of the

recurrent cytogenetic abnormalities t(8;21) and inv(16). The t(8;21) translocation produces a the RUNX1-RUNX1T1 fusion gene, which generates the acute myeloid leukemia 1 protein-eight-twenty one oncoprotein (AML1-ETO) fusion protein. The AML1-ETO fusion retains the DNA binding functionality of wild-type CBFα, while the ETO component of the fusion protein acts as a constituent transcriptional repressor, blocking hematopoietic differentiation and leading to blast proliferation. The inv(16) translocation results in the core binding factor subunit beta-myosin heavy chain 11 (CBFB-MYH11) fusion gene, generating a fusion protein between CBFβ and the smooth muscle myosin heavy chain (SMMHC). The main mechanism by which CBFβ-SMMHC blocks hematopoietic differentiation is thought to be through dominant negative repression of the CBFβ-CBFα interaction, effectively sequestering CBFα and preventing it from inducing normal hematopoietic differentiation. [36-39] Though commonly thought to be a sole driver mutation in AML, recent studies suggest that expression of the CBFB-MYH11 fusion gene potentiates the development of AML, but that an addition "second hit" mutation is required for the development of frank AML. [40, 41] Given that this signaling pathway is critical to hematopoeisis and AML pathogenesis, it is feasible to think NMT may be involved in its regulation.

Nucleophosmin 1 (NPM1) is a ubiquitously expressed nucleolar protein which is mutated in 20-30% of cases of AML. NPM1 has multiple physiologic roles, being involved in the maintenance of genomic stability, regulation of the p53 mediated cellular stress response, and the nuclear export of ribosomal RNA. It also has a role in regulating the apoptotic system, binding to caspase-6 and- 8 to prevent cellular apoptosis. Mutated NPM1 is mislocalized to the cytoplasm, blocking its regulatory functions. This results in a destabilization of key proteins such as the alternative reading frame (ARF) tumor suppressor and the F-box protein F-box and WD repeat domain containing protein 7 (Fbw7γ), resulting in a downstream activation of the c-MYC oncoprotein. Though NPM1 mutations promote the development of hematologic malignancies, additional cooperating events are required for the development of AML. [42]

2.3 - Preliminary NMT mRNA expression data in hematologic malignancies

Given that myristoylation is integral to proliferative signaling and apoptosis, both cellular functions central to cancer pathogenesis, it was postulated by Berthiaume *et al* that altered NMT expression itself could be oncogenic. (manuscript in preparation) Further studies

examining mRNA expression in cell lines from the cancer cell line encyclopedia, a large bioinformatics database of gene expression in multiple different types of cancer cell lines, revealed that NMT2 expression was low with preserved NMT1 expression in several hematological cancer cell lines, particularly Burkitt lymphoma, Diffuse-large B-cell lymphoma, and AML cell lines. This was followed by a study performed by K. Vincent *et al* examining NMT1 and NMT2 mRNA expression in two cohorts of AML patients with available microarray information from The Cancer Genome Atlas (TCGA) and Gene Expression Omnibus (GEO) databases. (manuscript in preparation) Our data suggested that there were significantly worse clinical outcomes for patients with intermediate-risk AML who had low NMT2 mRNA expression. As such, we performed an exploratory study examining NMT1 and NMT2 MFI by FACS with fluorescent anti-NMT1 and anti-NMT2 antibodies to further elucidate the landscape of NMT protein levels in AML, and to correlate this with clinically relevant patient outcomes.

Chapter 3 - Hypothesis

We hypothesized that NMT2 MFI will be independent of the currently known prognostic markers in AML, and will predict clinically relevant outcomes. We hypothesized that NMT1 would be consistent between all cell types and variables. We assessed this by the following specific aims.

3.1 - Primary endpoint: NMT2 levels are independent of ELN risk groups

Based on the mRNA expression data extracted from the GEO and TCGA cohorts, we hypothesized that NMT2 MFI is not associated with the ELN risk groups in newly diagnosed patients with AML.

3.2 - Secondary endpoint: NMT2 levels are associated with CR and survival

3.2.1 - NMT2 levels are associated with achievement of CR

In newly diagnosed patients with AML, we hypothesized that high NMT2 MFI is associated with the achievement of first CR by conventional induction chemotherapy with IDAC.

3.2.2 - NMT2 levels are associated with relapse-free survival (RFS) and overall survival (OS)

In newly diagnosed patients with AML, we hypothesized that high NMT2 MFI is associated with improved RFS and OS in ELN intermediate-risk patients.

3.3 - Exploratory endpoints with regards to NMT1 and NMT2 MFI

3.3.1 - Exploratory endpoints related to the biology of NMT MFI in vivo

We explored blasts and HSC NMT1 and NMT2 MFI in a small cohort of control patients receiving a diagnostic bone marrow aspirate and biopsy for indications other than AML. NMT1 and NMT2 MFI in mature monocytes and lymphocytes in both controls and AML patients was also determined. Additionally, we examined NMT1 and NMT2 MFI in the CD34+ and CD34+38- cell subsets. We predicted NMT1 MFI would be uniform amongst all samples, and hypothesized that NMT2 MFI would vary amongst normal, blast, and CD34+/CD34+38- cell populations.

3.3.2 - Exploratory endpoints related to NMT MFI and patient factors

We explored the relation of NMT1 and NMT2 MFI with AML patient factors, specifically antecedent diagnoses of a MPN or MDS, or previous treatment with chemotherapy or radiation exposure.

3.3.3 - Exploratory endpoints related to NMT MFI and AML factors

We explored the relation of NMT1 and NMT2 MFI with AML biology. The relation to recurrent cytogenetic abnormalities, specifically complex cytogenetics, t(8;21), inv(16), t(15;17), t(6;9), inv(3), t(1;22), t(v;11), t(9;22) and t(v;21) were explored. The relation to recurrent molecular abnormalities, specifically NPM1, FLT3-ITD, and JAK2 were also explored. The relation of NMT1 to ELN risk group was also explored.

3.3.4 - Exploratory endpoints related to NMT MFI, treatment outcomes and survival

We explored the relation of NMT1 MFI to the achievement of CR by standard induction chemotherapy with IDAC, in addition to RFS and OS.

Chapter 4 - Methods

4.1 - Methods for the determination of NMT1 and NMT2 levels, in addition to immunophenotype, by fluorescence activated cell sorting (FACS)

We analyzed bone marrow aspirate or peripheral blood obtained at the time of AML diagnosis from patients who had given written, informed consent. We also analyzed a small subset of control patients who were undergoing a bone marrow aspirate as a diagnostic procedure for a non-AML indications. Samples were obtained either retrospectively from a biobank of bone marrow aspirate cryopreserved at -60°C, or analyzed prospectively immediately after collection.

We determined NMT1 and NMT2 expression and cell immunophenotypes, including markers for CD34+/CD34+38- cell populations, by multicolor FACS with combined cell surface and intracytoplasmic staining. We extracted Peripheral blood mononuclear cells from either peripheral blood or bone marrow aspirate by density gradient centrifugation. We applied a Fc block (Human BD Fc Block #564220, BD Biosciences) to approximately $1x10^6$ cells in 100 μL after washing with PBS buffer. We performed Cell surface staining with CD45-BUV395 (#563791), CD34-PE (#560941), CD38-bv421 (#562445), and CD123-APC (#560087). We permeabilized the cells with IntraPrep Permeabilization Reagent, (#PN IM2389, Beckman Coulter), then added purified mouse anti-NMT2-FITC custom antibody (BD Biosciences) with purified mouse IgG1k-FITC as an isotype control (#556649, BD Biosciences). In samples that had NMT1 levels determined, we used purified custom mouse anti-NMT1-Alexa Fluor 647 custom antibody (Berthiaume lab) with an IgG1k-Alexa Fluor 647 control. We analyzed the samples on a LSR Fortessa cell analyzer.

We gated the resultant dot plots for single, live cells with side scatter (SSC) vs forward scatter (FSC) and vs BV510, respectively. We gated blasts, mature lymphocytes and monocytes with SSC vs CD45-BUV395. We gated primitive blast populations, defined as either CD34+ or CD34+38- immunophenotypes, with a two-parameter density plot generated with CD38-BV421 vs CD34-PE. We generated histograms for intracytoplasmic staining of IgGk-FITC or IgGk-Alexa Fluor 647 and anti-NMT2-FITC or anti-NMT1-Alex Fluor 647. NMT1 and NMT2 protein levels were expressed as a mean fluorescent intensity ratio (MFI), relative to the respective IgGk isotype control. We expressed the MFI for the bulk blast, CD34+, and CD34+38- populations.

The flow cytometry data was gated and minimum events determined by either an experienced hematopathologist (AS) or a research assistant with extensive flow cytometry experience (ZZ). The described FACS methodology for quantitation of NMT1 or NMT2 protein levels was previously validated against Western blot in AML cell lines and found to correlate.

4.2 - Study design, definitions and statistical methods

The study was a combined retrospective and prospective cohort study enrolling all consenting participants over the age of 18 with a new diagnosis of AML, excluding acute-promyelocytic leukemia (APL), at the University of Alberta hospital, from the dates of April, 2014 to September, 2016. This included patients being prospectively followed for a separate study at the same institution, for whom biobanked specimens were available. The initial proposed sample size, calculated based on a preliminary hazard ratio generated from database studies of mRNA expression of NMT1 and 2, was for a total N of 150 to give 80% power to detect an effect size of 0.463.

Data acquisition for patient information was done with multiple modalities, including a review of existing database information, paper chart review, and electronic chart review. All collected patient cytogenetic and molecular data was originally generated for clinical purposes with routine diagnostic assays performed at the University of Alberta Hospital in Edmonton, Alberta. The data analysis software utilized was SPSS (v.23, Armonk, NY: IBM Corp). Patients received routine clinical follow-up, and all treatment decisions were done as per the clinical judgement of the treating physician. Both NMT1 and NMT2 MFI were determined by FACS for all retrospective, biobanked samples, with gating being done by ZZ. All prospectively collected samples had NMT2 MFI alone determined by the same FACS methodology, but utilized a different flow cytometer of the same make and manufacturer, with gating performed by AS. Control samples were collected prospectively and were analyzed on the same flow cytometer utilized for the prospectively collected AML samples, with gating performed by AS. NMT1 and NMT2 MFI were recorded as continuous variables. All MFI values were expressed as mean MFI ± standard error of the mean.

Between group differences with respect to mean NMT MFI for the bulk blast, CD34+ and CD34+38- cell subsets were tested with either a Student's t-test for binomial variables, or Analysis of Variances (ANOVA) for polynomial variables. Groups with $n < 3$ were not statistically analyzed. Statistically significant results were then reanalyzed applying the Bonferroni correction with a total of six hypotheses per variable to correct for the application of multiple comparisons, giving a corrected p of 0.008. This was expressed in the results as the original p value multiplied by six. Variables examined were as per outlined in the hypothesis. NMT1 and NMT2 MFI for bulk blast, CD34+ and CD34+38- cell subsets were then dichotomized by receiver operator curve (ROC) analysis with respect to RFS or OS including either all patients, or ELN intermediate-risk only patients. The breakpoint for high versus low NMT expression was selected as that which maximizes Youden's J statistic, with a minimum specificity threshold of 80%, and was calculated with the ROC curve demonstrating the most discriminatory power, as measured by minimizing the p value for the area under the curve (AUC). A $p < 0.05$ was taken as significant for all statistical tests.

CR was defined as bone marrow blasts < 5%; absence of blasts with Auer rods; absence of extramedullary disease; absolute neutrophil count > 1.0×10^6/L; platelet count > 100×10^9/L; independence of red cell transfusion. Complete remission with incomplete recovery (CRi) was defined as all CR criteria, except for residual neutropenia (ANC < 1.0×10^9/L) or thrombocytopenia. (< 100×10^9/L) Treatment failure was defined as either death or RD, with RD defined as failure to achieve CR or CRi, only including patients surviving ≥ 7 days following initial treatment, with evidence of persistent leukemia by blood or bone marrow examination. OS was defined as the time from the date of the diagnostic bone marrow confirming to the date of death from any cause. RFS was defined as the time from the date of achievement of CR of CRi to the date of relapse or death from any cause. RFS was undefined for patients not receiving induction chemotherapy. Patients were not censored if they received an allo-HSCT. Patients were censored on the date of a defined event or last follow-up. All study definitions are made in compliance with the ELN guidelines for clinical trials in AML, and this study designed in accordance with the REMARK criteria for tumor prognostic studies. [1, 43]

Chapter 5 - Results

5.1 - Performance of the NMT1 and NMT2 FACS assay

A sample of the raw flow cytometry data and gating parameters is displayed in figure 5.1.1. The custom anti-NMT1 Alexa Fluor 647 antibody from the Berthiaume lab versus the anti-IgGk Alexa Fluor 647 isotype control provided sufficient separation of cell populations to facilitate analysis, as demonstrated in figure 5.1.2. Fewer events resulted in the increased noise evident in the represented histograms for the CD34+38- blast population and the mature monocyte population, represented in figure 5.1.2 C and E, respectively. However, we had enough observations to allow analysis of all cell populations for NMT1.

The custom anti-NMT2 FITC antibody from BD biosciences versus the IgGk isotype control provided sufficient separation of cell populations to facilitate analysis, though separation was inferior to that seen with the anti-NMT1 Alexa Fluor 647 antibody, as demonstrated in figure 5.1.3. Fewer events resulted in increased noise in the mature monocyte population, evident in figure 5.1.3 E. However, we had enough observations to allow analysis of all cell populations for NMT2.

In the original protocol, anti-CD123-APC antibody was added to allow for further gating of the blast population for the primitive CD34+38-132+ population. However, gating for this population generally resulted in an insufficient number of events to allow for robust analysis. As such, this data was not further analyzed.

5.2 - Baseline characteristics of the patient population

A total of 105 patients were recruited into the study, with 44 samples being obtained as biobanked samples, and 61 samples obtained prospectively. One patient was excluded from the analysis as they had a diagnosis of acute promyelocytic leukemia, confirmed by a positive fluorescence *in situ* hybridization assay demonstrating the presence of the PML/RαRα translocation, a pre-defined exclusion criteria. Two patients did not have a bone marrow biopsy performed due to patient preference, and had a diagnosis of AML confirmed based on the presence of blasts in the peripheral blood. FACS was performed in the peripheral blood samples of these two individuals, and they were included in the analysis. Two patients were lost to

follow-up shortly after being diagnosed with AML and receiving induction chemotherapy, with both returning to their home provinces outside of Alberta for further therapy after CR was confirmed. These individuals were not considered as having an event, and their date of last follow-up was the time of their last clinical encounter documented in Alberta.

The median age at diagnosis was 67.1 years, with 54% of patients being older than 65 at the time of diagnosis. The cohort was predominantly male, with 68% of patients being male. Prior exposure to chemotherapy was seen in 8% of patients and previous radiation therapy was seen in 5% of patients, with a total of 9% of patients receiving either chemotherapy and/or radiation therapy. An antecedent diagnosis of a MPN or MDS was seen in 13% of patients. Median peripheral WBC at diagnosis was 13.8 x 10^9 cells / L, with 45% of patients having a peripheral WBC of greater than 20.0 x 10^9 cells / L at diagnosis. Median peripheral blast count was 33% of TNC, while median bone marrow blast count was 54% of TNC.

Cytogenetic profiles were variable, with the most common profile being normal cytogenetics (n = 42), followed by complex cytogenetics (n = 16). CBF rearrangements were also prominent, with both inv(16) (n = 6) and t(v;21) (n = 4) represented. MLL rearrangements were also prominent, with t(v;11) (n = 8) being the third most common profile. One case of t(9;22) was noted. All other patients had nonspecific cytogenetic abnormalities that were not considered recurrent cytogenetic abnormalities, per the ELN criteria.

Molecular profiles were similarly variable, with NPM1 (n = 29) and FLT3-ITD (n = 20) mutations being the most common. The combined profile of these mutations included NPM1(+)/FLT3(-) (n = 17), NPM1(+)/FLT3(+) (n = 12), and NPM1(-)/FLT3(+) (n = 8). JAK2 (n = 5) and BCR/ABL (n = 2) mutations were also commonly noted. One c-KIT mutation and one CEBPA mutation were recorded, but these assays were performed on only a minority of patients (n = 5 and n = 3 tests, respectively).

ELN risk groups were balanced, with 22% of patients having favorable-risk profiles, 55% having intermediate-risk profiles, and 21% having adverse risk profiles. Two patients had

unknown risk profiles, due to them not undergoing a diagnostic bone marrow, with the consequent lack of cytogenetic or molecular profiles.

Induction chemotherapy was received by approximately half (n = 58) of patients, with IDAC being almost universally the regimen utilized (n = 55). Two patients received IDAC in addition to a tyrosine kinase inhibitor, given that they were positive for the BCR/ABL transcript, and one patient received fludarabine, cytarabine ,G-CSF, and idarubucin (FLAG-IDA) as an induction regimen. Palliative chemotherapy regimens utilized included azacytidine (n = 13), and LDAC (n = 5). Several patients were on palliative chemotherapy regimens as part of a clinical trial, including LDAC plus volasertib (n = 4) and the SG1-110 trial (n = 9). The remainder of patients received purely palliative and symptom control measures. Most patients who received induction chemotherapy achieved a CR or iCR with first induction (n = 46). The remainder of patients either had resistant disease (n = 8) or died during induction chemotherapy (n = 4). Half of the patients receiving induction chemotherapy had received an allo-HSCT at the time of last follow-up (n = 29).

At last follow-up, approximately one-third of patients who had achieved CR had relapsed (n = 20) or met the RFS endpoint (n = 24). Approximately half of the overall population had met the OS endpoint (n = 59). Median RFS and OS were 1.31 years and 0.95 years, respectively. Median follow-up is currently 1.54 years in surviving patients.

5.3 - NMT MFI variation amongst various cell subsets and disease states

5.3.1 - NMT1 and NMT2 MFI variation amongst lymphocytes, monocytes, blasts, CD34+, and CD34+38- blast subsets

NMT1 MFI was determined in monocytes, lymphocytes, bulk blasts, CD34+, and CD34+38- blast subsets for all patients with biobanked marrow aspirate. (n = 44) NMT1 MFI did not vary amongst AML bulk blast populations (mean MFI = 5.39 ± 0.96) versus CD34+ blasts (mean MFI = 6.02 ± 1.07, p = 0.661), or CD34+ blasts and CD34+38- blasts (mean MFI = 7.23 ±1.79, p = 0.558). NMT1 MFI also did not vary between the three groups. (p = 0.603) No variation was observed between mature monocytes (mean MFI = 5.66 ± 1.00) versus lymphocytes (mean MFI = 6.53 ± 1.02, p = 0.542). This is summarized in figure 5.3.1.

NMT2 MFI was determined in monocytes, lymphocytes, bulk blasts, CD34+, and CD34+38- blast subsets for a cohort of normal patients who underwent marrow biopsy for non-AML indications (n = 16), in addition to patients with a new diagnosis of AML (n = 104). NMT2 MFI was significantly higher in normal samples versus their AML counterparts in the CD34+ population (mean MFI = 1.65 ± 0.11, $p < 0.001$) and the CD34+38- population (mean MFI = 1.91 ± 0.17, $p < 0.001$). NMT2 MFI was not significantly different between normal CD34+ and CD34+38- cells ($p = 0.193$). NMT2 MFI did not vary significantly between the AML bulk blasts (mean MFI = 1.13 ± 0.03), CD34+ blasts (mean MFI = 1.21 ± 0.03), and CD34+38- blasts (mean MFI 1.22 ± 0.04) ($p = 0.145$). NMT2 MFI was significantly lower in mature monocytes (mean MFI = 0.98 ± 0.03) versus mature lymphocytes (mean MFI = 3.01 ± 0.08, $p < 0.001$). This is summarized in figure 5.3.2.

5.3.2 - NMT1 and NMT2 MFI variation in CD34+ blast subsets with premorbid clinical characteristics

NMT1 MFI was determined in CD34+ blast subsets for the overall population of patients with biobanked samples (median MFI = 6.02 ± 1.07, n = 44). NMT1 MFI was not statistically different for patients who had received antecedent chemotherapy (mean MFI = 3.13 ± 0.36, $p = 0.400$) or radiation therapy (mean MFI = 2.70 ± 0.63, $p = 0.505$) versus those who had not. NMT1 MFI was also not statistically different for patients with an antecedent MPN (mean MFI = 4.39 ± 0.988, $p = 0.514$). Only one patient who had NMT1 measured had an antecedent MDS (MFI = 4.55). This is summarized in figure 5.3.3.

NMT2 MFI was determined in CD34+ blast subsets for the overall population of patients with a new diagnosis of AML (mean MFI = 1.21 ± 0.03, n = 104). NMT2 MFI was not statistically different for patients who had received antecedent chemotherapy (mean MFI = 1.20 ± 0.24, $p = 0.962$) or radiation therapy (mean MFI = 0.98 ± 0.08, $p = 0.147$) versus those who had not. NMT2 MFI was statistically higher for patients with an antecedent MPN (mean MFI = 1.60 ± 0.15, $p = 0.016$). However, this was non-significant after application of the Bonferroni

correction (p = (0.016 * 6) = 0.096). NMT2 MFI was not statistically different for patients with an antecedent MDS (mean MFI = 1.11 ± 0.14). This is summarized in figure 5.3.4.

5.3.3 - NMT1 and NMT2 MFI variation in CD34+ blast subsets with recurrent cytogenetic abnormalities

NMT1 MFI was determined in CD34+ blast subsets for the overall population of biobanked patients who had a bone marrow biopsy at diagnosis (mean MFI = 6.15 ± 1.12, n = 43). NMT1 MFI was not significantly different for patients with normal (mean MFI = 3.91 ± 0.44, p = 0.053) or complex cytogenetics (mean MFI = 3.45 ± 1.52, p = 0.510). NMT1 MFI was not statistically different amongst patients with recurrent cytogenetic abnormalities t(v;11) (mean MFI = 10.04 ± 7.27, p = 0.598) or t(v;21) (mean MFI = 5.44 ± 0.81, p = 0.888). Only one patient had NMT1 MFI measured with inv(16) (MFI = 5.41). This is summarized in figure 5.3.5.

NMT2 MFI was determined in CD34+ blast subsets for the overall population of patients who had a bone marrow biopsy at diagnosis (mean MFI = 1.21 ± 0.03, n = 102). NMT2 MFI was statistically lower for patients with normal cytogenetics (mean MFI = 1.13 ± 0.04, p = 0.032). However, this was non-significant after application of the Bonferroni correction (p = (0.032 * 6) = 0.192). NMT2 MFI was not statistically different in patients with complex cytogenetics (mean MFI = 1.14 ± 0.09, p = 0.093). NMT2 MFI was statistically higher in patients with the recurrent cytogenetic abnormality inv(16) (mean MFI = 1.67 ± 0.05, p < 0.001). This remained significant after application of the Bonferroni correction (p = (0.001 * 6) = 0.006). NMT2 MFI was not statistically different in patients with the recurrent cytogenetic abnormalities t(v;11) (mean MFI = 1.14 ± 0.10, p = 0.586) or t(v;21) (mean MFI = 1.17 ± 0.09, p = 0.784). This is summarized in figure 5.3.6.

5.3.4 - NMT1 and NMT2 MFI variation in CD34+ blast subsets with recurrent molecular abnormalities

NMT1 MFI was determined in CD34+ blast subsets for the overall population of biobanked patients who had a bone marrow biopsy at diagnosis (mean MFI = 6.15 ± 1.12, n = 43). NMT1 MFI was not statistically different for patients with the recurrent molecular

abnormalities NPM1 (mean MFI = 5.24 ± 1.63, p = 0.586), FLT3-ITD (mean MFI = 4.91 ± 0.71, p = 0.537), or JAK2 (mean MFI = 5.09 ± 2.46, p = 0.742). This is summarized in figure 5.3.7.

NMT2 MFI was determined in CD34+ blast subsets for the overall population of patients who had a bone marrow biopsy at diagnosis (mean MFI = 1.21 ± 0.03, n = 102). NMT2 MFI was statistically lower in patients with the recurrent molecular abnormality NPM1 (mean MFI = 1.09 ± 0.04, p = 0.004). This remained significant after application of the Bonferroni correction (p = (0.004 * 6) = 0.024). NMT2 MFI was not statistically different for patients with the recurrent molecular abnormalities FLT3-ITD (mean MFI = 1.13 ± 0.05, p = 0.196) or JAK2 (mean MFI = 1.49 ± 0.25, p = 0.179). This is summarized in figure 5.3.8.

5.4 - NMT1 and NMT2 MFI variation in bulk, CD34+, and CD34+38- blast subsets with ELN risk group

NMT1 MFI was determined in bulk, CD34+, and CD34+38- blast subsets for all biobanked patients who had a bone marrow biopsy at diagnosis (n = 43). NMT1 MFI for bulk blast populations was not statistically different between favorable-risk (mean MFI = 3.70 ± 0.39), intermediate-risk (mean MFI = 4.82 ± 0.92), and unfavorable-risk (mean MFI = 10.09 ± 4.26) (p = 0.076). NMT1 MFI for CD34+ blast populations were also not statistically different between favorable-risk (mean MFI = 4.03 ± 0.38), intermediate-risk (mean MFI = 5.23 ± 0.91), and unfavorable-risk (mean MFI = 11.58 ± 4.98) (p = 0.053). NMT1 MFI for CD34+38- blast populations were also not statistically different between favorable-risk (mean MFI = 3.54 ± 0.31), intermediate-risk (mean MFI = 6.23 ± 1.94), and unfavorable-risk (mean MFI = 14.74 ± 7.29) (p = 0.119). This is summarized in figure 5.4.1.

NMT2 MFI was determined in bulk, CD34+, and CD34+38- blast subsets for all patients who had a bone marrow biopsy at diagnosis (n = 102). NMT2 MFI for bulk blast populations was not statistically different between favorable-risk (mean MFI = 1.17 ± 0.07), intermediate-risk (mean MFI = 1.17 ± 0.04), and unfavorable-risk (mean MFI = 1.01 ± 0.08) (p = 0.166). NMT2 MFI for CD34+ blast populations were also not statistically different between favorable-risk (mean MFI = 1.28 ± 0.07), intermediate-risk (mean MFI = 1.20 ± 0.04), and unfavorable-

risk (mean MFI = 1.16 ± 0.08) (p = 0.633). NMT2 MFI for CD34+38- blast populations were also not statistically different between favorable-risk (mean MFI = 1.26 ± 0.07), intermediate-risk (mean MFI = 1.23 ± 0.06), and unfavorable-risk (mean MFI = 1.16 ± 0.10) (p = 0.819). This is summarized in figure 5.4.2.

5.5 - NMT1 and NMT2 MFI variation in CD34+ blast subsets with achievement of CR with first induction chemotherapy

NMT1 MFI was determined in CD34+ blast subsets for all biobanked patients who underwent induction chemotherapy (mean MFI = 6.93 ± 1.82, n = 23). NMT1 MFI was not statistically different between patients who achieved CR or iCR with first induction chemotherapy (mean MFI = 7.87 ± 2.28) versus patients who had RD or death (mean MFI = 3.56 ± 0.50) (p = 0.339). This is summarized in figure 5.5.1.

NMT2 MFI was determined in CD34+ blast subsets for all patients who underwent induction chemotherapy (mean MFI = 1.21 ± 0.05, n = 58). NMT2 MFI was not statistically different between patients who achieved CR or iCR with first induction chemotherapy (mean MFI = 1.23 ± 0.06) versus patients who had RD or death (mean MFI = 1.12 ± 0.07) (p = 0.303). This is summarized in figure 5.5.2.

5.6 - NMT1 and NMT2 MFI variation with regards to survival in AML

5.6.1 - Survival by Kaplan-Meier analysis for RFS and OS with respect to ELN risk group and clinical prognostic factors

Kaplan-Meier analysis was performed for RFS (p = 0.025, n = 52) and OS (p = 0.002, n = 102) with stratification by ELN risk group for the applicable overall population that underwent a bone marrow biopsy. Kaplan-Meier analysis was also performed for patients of age < 65 for RFS (p = 0.025, n = 43) and OS (p < 0.001, n = 48). This is summarized in figure 5.6.1.

Kaplan-Meier analysis was performed for RFS (p = 0.513, n = 52) and OS (p < 0.001, n = 104) with stratification by age greater than 65 at diagnosis. Kaplan-Meier analysis was also performed for RFS (p = 0.161, n = 52) and OS (p = 0.046, n = 104) with stratification by

peripheral white blood cell count (WBC) greater than 20 x 10^9 /L at diagnosis. This is summarized in figure 5.6.2.

Kaplan-Meier analysis was performed for RFS (p = 0.044, n = 52) and OS (p = 0.905, n = 104) with stratification by antecedent exposure to chemotherapy or radiation therapy prior to AML diagnosis. Kaplan-Meier analysis was also performed for RFS (p = 0.009, n = 52) and OS (p = 0.264, n = 104) with stratification by an antecedent diagnosis of MDS or MPN. This is summarized in figure 5.6.3.

5.6.2 - Receiver operator curve (ROC) analysis of NMT1 and NMT2 in bulk, CD34+, and CD34+38- blasts for RFS and OS

NMT1 MFI was examined in bulk, CD34+, and CD34+38- blast subsets by ROC analysis for RFS and OS in the overall population. ROC were generated for RFS in the bulk blast (AUC =0.533, p = 0.815, n = 21), CD34+ blast (AUC = 0.578, p = 0.586, n = 21), CD34+38- blast populations (AUC = 560, p = 0.694, n = 20). ROC were also generated for OS in the bulk blast (AUC = 0.508, p = 0.930, n = 44), CD34+ blast (AUC = 0.496, p = 0.970, n = 44), and CD34+38- blast populations (AUC = 0.556, p = 0.568, n = 42). This is summarized in figure 5.6.4.

NMT1 MFI was examined in bulk, CD34+, and CD34+38- blast subsets by ROC for RFS and OS in the ELN intermediate risk patients. ROC were generated for RFS in intermediate risk patients only in the bulk blast (AUC = 0.350, p = 0.462, n = 9), CD34+ blast (AUC = 0.350, p = 0.462, n = 9), CD34+38- blast populations (AUC = 0.400, p = 0.655, n = 8). ROC were also generated for OS in intermediate risk patients in the bulk blast (AUC = 0.481, p = 0.894, n = 24), CD34+ blast (AUC = 0.398, p = 0.463, n = 24), and CD34+38- blast populations (AUC = 0.400, p = 0.502, n = 23). This is summarized in figure 5.6.5.

NMT2 MFI was examined in bulk, CD34+, and CD34+38- blast subsets by ROC for RFS and OS in the overall population. ROC were generated for RFS in the bulk blast (AUC = 0.615, p = 0.158, n = 52), CD34+ blast (AUC = 0.620, p = 0.160, n = 47), CD34+38- blast populations (AUC = 0.677, p = 0.049, n = 42). ROC were also generated for OS in the bulk blast (AUC =

0.520, p = 0.731, n = 104), CD34+ blasts (AUC = 0.565, p = 0.277, n = 98), and CD34+38- blast populations (AUC = 0.567, p = 0.287, n = 88). This is summarized in figure 5.6.6.

NMT2 MFI was examined in bulk, CD34+, and CD34+38- blast subsets by ROC for RFS and OS in the ELN intermediate risk patients. ROC were generated for RFS in intermediate risk patients only with respect to the bulk blast (AUC = 0.742, p = 0.030, n = 31), CD34+ blast (AUC = 0.675, p = 0.131, n = 28), CD34+38- blast populations (AUC = 0.702, p = 0.108, n = 23). ROC were also generated for OS in intermediate risk patients in the bulk blast (AUC = 0.648, p = 0.057, n = 57), CD34+ blast (AUC = 0.648, p = 0.062, n = 55), and CD34+38- blast populations (AUC = 0.697, p = 0.021, n = 48). This is summarized in figure 5.6.7.

A sensitivity versus specificity table for various NMT2 MFI cut-off values was generated for the receiver operator curve that maximized the area under the curve, as measured by a minimum p value approach. Curve F from figure 5.6.7, which was the receiver operator curve for overall survival in the intermediate risk population for NMT2 MFI amongst the CD34+38- blast subset. Youden's J was then calculated as a composite measure of sensitivity and specificity. Two optimization peaks were observed at an NMT2 MFI of 1.17 (sensitivity = 0.64, specificity = 0.70), which optimizes sensitivity at the expense of specificity, and 1.28 (sensitivity = 0.50, specificity = 0.80), which optimizes specificity at the expense of sensitivity. This is summarized in table 5.6.1 and figure 5.6.9.

5.6.3 - Kaplan-Meier analysis of NMT2 MFI for RFS and OS in bulk, CD34+, and CD34+38- blasts

The ELN intermediate risk population was examined in bulk, CD34+, and CD34+38- blast subsets using a higher sensitivity, lower specificity NMT2 MFI cut-off of 1.17. Kaplan-Meier analysis was performed for RFS in the bulk blast (p = 0.249, n = 30), CD34+ blast (p = 0.249, n = 28), and CD34+38- blast populations (p = 0.285, n = 22). Kaplan-Meier analysis was also performed for OS for bulk blast (p = 0.015, n = 57), CD34+ blast (p = 0.246, n = 55), and CD34+38- blast populations (p = 0.053, n = 47). This is summarized in figure 5.6.10.

The ELN intermediate risk population was examined in bulk, CD34+, and CD34+38- blast subsets using a lower sensitivity, higher specificity NMT2 MFI cut-off of 1.28. Kaplan-Meier survival analysis was performed for RFS for bulk blast (p = 0.084, n = 30), CD34+ blast (p = 0.076, n = 28), and CD34+38- blast populations (p = 0.038, n = 22). Kaplan-Meier analysis was also performed for OS for bulk blast (p = 0.005, n = 57), CD34+ blast (p = 0.088, n = 55), and CD34+38- blast populations (p = 0.086, n = 47). This is summarized in figure 5.6.11.

The ELN intermediate risk, age < 65 population was examined in bulk, CD34+, and CD34+38- blast subsets using a lower sensitivity, higher specificity NMT2 MFI cut-off of 1.28. Kaplan-Meier analysis was performed for RFS for bulk blast (p = 0.203, n = 24), CD34+ blast (p = 0.147, n = 23), and CD34+38- blast populations (p = 0.096, n = 17). Kaplan-Meier survival curves are also displayed for OS for bulk blast (p = 0.048, n = 24), CD34+ blast (p = 0.057, n = 23), and CD34+38- blast populations (p = 0.014, n = 17). This is summarized in figure 5.6.12.

5.6.4 - Cox regression analysis of NMT2 MFI for RFS and OS in bulk, CD34+, and CD34+38- blasts

Univariate and multivariate Cox regression analyses was performed for relapse-free survival, overall survival in patients undergoing induction only, and overall survival in all patients. Variables examined include ELN adverse-risk (vs favorable or adverse), age > 65, peripheral WBC > 20 x 10^9, and NMT2 MFI > 1.28. ELN adverse-risk was a significant variable for relapse-free survival in both univariate (HR 3.361, 95% CI 1.320 - 8.559, p = 0.011) and multivariate (HR 3.076, 95% CI 1.158 - 8.169, p = 0.024) analysis. ELN adverse-risk was also significant for overall survival in patients undergoing induction on univariate (HR 6.141, 95% CI 2.360, p < 0.001) and multivariate (HR 5.813, 95% CI 2.192 - 15.413, p < 0.001) analysis. Overall survival in all patients showed significance on univariate analysis for the variables ELN adverse-risk (HR 2.390, 95% CI 1.374 - 4.158, p = 0.002), age > 65 (HR 3.847, 95% CI 2.154 - 6.873, p < 0.001), and peripheral WBC > 20 x 10^9 /L (HR 1.673, 95% CI 1.003 - 2.791, p = 0.049). This was retained on multivariate analysis for ELN adverse risk (HR 2.232, 95% CI 1.277 - 3.902, p = 0.005), age > 65 (HR 3.805, 95% CI 2.107 - 6.870, p < 0.001), and peripheral WBC > 20 x 10^9 /L (HR 1.902, 95% CI 1.902 - 1.123, p = 0.017). The proportional hazards

assumption was inspected visually and found to be valid in Kaplan-Meier curves 5.6.11 A, D, B, and C, but not for curves E and F. This is summarized in table 5.6.2.

Univariate and multivariate Cox regression analyses were performed for relapse-free survival, overall survival in patients undergoing induction only, and overall survival in ELN intermediate-risk only patients. Variables examined include ELN adverse-risk (vs favorable or adverse), age > 65, peripheral WBC > 20 x 10^9, and NMT2 MFI > 1.28. No variables were significant for relapse-free survival on univariate analysis. On multivariate analysis for relapse-free survival, peripheral WBC > 20 x 10^9 (HR 5.433, 95% CI 1.196 - 24.686, p = 0.028) and bulk blast NMT2 MFI > 1.28 (HR 6.200, 95% CI 1.348 - 28.529, p = 0.019) were significant. No variables were significant on univariate or multivariate analysis for overall survival in intermediate-risk patients undergoing induction only. On univariate analysis for overall survival in all intermediate-risk patients, age > 65 (HR 5.230, 95% CI 2.131 - 12.838, p < 0.001), peripheral WBC > 20 x 10^9 /L (HR 2.302, 95% CI 1.126 - 4.706, p = 0.022), and bulk blast NMT2 MFI > 1.28 (HR 2.683, 95% CI 1.313 - 5.485, p = 0.007) were significant. On multivariate analysis for overall survival in all intermediate-risk patients age > 65 (HR 5.618, 95% CI 2.207 - 14.299, p < 0.001) and peripheral WBC > 20 x 10^9 /L (HR 2.676, 95% CI 1.250 - 5.730, p = 0.011) were significant. The proportional hazards assumption was inspected visually and found to be valid in Kaplan-Meier curves 5.6.11 A, D, B, and C, but not for curves E and F. This is summarized in table 5.6.3.

5.6.5 - Logistic regression of NMT2 MFI for RFS and OS in bulk, CD34+, and CD34+38- blasts

Univariate binary logistic regression of NMT2 MFI was performed with respect to relapse-free survival for intermediate-risk patients in the bulk blast population (OR 67.409, 95% CI 0.959 - 4737.185, p = 0.052), CD34+ blast population (OR 13.979, 95% CI 0.497 - 393.261, p = 0.121), and CD34+38- blast population (OR 13.384, 95% CI 0.533 - 336.019, p = 0.115) is displayed. Logistic regression of NMT2 MFI with respect to overall survival for intermediate risk patients who underwent induction was performed in the bulk blast population (OR 37.102, 95% CI 0.642 - 2145.082, p = 0.081), CD34+ blast population (OR 13.631, 95% CI 0.513 - 362.271, p = 0.119), and CD34+38- blast population (OR 18.144, 95% CI 0.563 - 585.009, p = 0.102) is also displayed. Logistic regression of NMT2 MFI with respect to overall survival for

intermediate-risk patients was also performed in the bulk blast population (OR 10.923, 95% CI 1.091 - 109.318, p = 0.042), CD34+ blast population (OR 8.801, 95% CI 0.861 - 89.916, p = 0.067), and CD34+38- blast population (OR 7.275, 95% CI 1.064 - 49.757, p = 0.043) is also displayed. This is summarized in table 5.6.4.

Chapter 6 - Discussion and Conclusions

6.1 - Assay performance and data set quality

6.1.1 - FACS provides effective measurement of NMT1 MFI

As demonstrated in figures 5.1.1 and 5.1.2, the FACS based assay for measuring NMT1 MFI with intracellular staining by the anti-NMT1 Alexa Fluor 647 antibody (Berthiaume lab) provided excellent separation from the IgG1k isotype control in all cell compartments, with minimal overlap between the isotype control and the fluorophore. When gated for side scatter versus CD45-BUV395, enough events were present to facilitate analysis of the lymphocyte, monocyte, and bulk blast populations in all samples. When gated for CD38-BV421 vs CD34-PE, sufficient events were present to facilitate analysis of these subpopulations in several samples.

6.1.2 - FACS provides effective measurement of NMT2 MFI with a highly translatable assay

As demonstrated in figures 5.1.1 and 5.1.3, the FACS based assay for the measurement of NMT2 MFI with intracellular staining by the anti-NMT2 FITC antibody (BD biosciences) provided reasonable separation from the isotype control in all cell compartments. It is notable that, compared to the NMT1 antibody, this antibody provided inferior separation from the isotype control, as demonstrated by the histogram overlap in the strongly NMT2 positive lymphocyte gate (Figure 5.1.3 D). This likely represents an increased error with the measurement of smaller absolute NMT2 MFI values, relative to NMT1 MFI. Nonetheless, the assay provided NMT2 MFI data that was suitable for analysis. When gated for side scatter versus CD45-BUV395, enough events were present to facilitate analysis of the lymphocyte, monocyte, and bulk blast populations in all samples. When gated for CD38-BV421 vs CD34-PE, sufficient events were present to facilitate analysis of these subpopulations in most samples.

The FACS based assay for measurement of NMT2 MFI has excellent potential for clinical translation. All patients diagnosed with AML undergo FACS as a routine part of their

initial diagnostic workup to determine the blast immunophenotype and characterize the blast population. Addition of another fluorophore would represent only an incremental cost increase, and would not require significantly more technical labor or expertise than is currently applied during the initial diagnostic workup of newly diagnosed AML. As such, this assay is both effective at measuring NMT2 MFI, and has excellent feasibility for clinical applications.

6.1.3 - Our cohort's clinicopathologic characteristics are comparable to the literature

In comparison with the literature, our cohort was slightly older with a median age of 67.1 years, compared to a median age at diagnosis of 65 years, and had a preponderance of males at 68%, compared to a population average of 47-50%. [3, 44-46] The median peripheral WBC at diagnosis in our cohort (13.8 x 10^9 /L) was slightly lower than that found in the literature (18.2 - 18.7 x 10^9 /L), but not to a clinically significant degree. [3, 47] A total of 9% of patients in our cohort had previous exposure to radiation and/or chemotherapy, versus 3% in the literature, and 13% had an antecedent diagnosis of MDS or a MPN, versus 13% in the literature. [3] The distribution of cytogenetic abnormalities between our cohort versus the literature was similar with normal (40% vs 48%), complex (15% vs 11%), t(v;11) (8% vs 6%), inv(16) (6% vs 7.9%), and t(v;21) (4% vs 6.7%).[42] Recurrent molecular abnormalities were similarly distributed vs the literature between NPM1 (28% vs 30%) and FLT3 (19% vs 20%). [42, 48] The ELN risk groups in our study were balanced and similar to the literature between favorable (22% v 26.9%), intermediate (55% vs 50.2%), and unfavorable (21% vs 22.8%), with a similar rate of allogenic HSCT (28% vs 22.5%). [2]

Our survival outcomes were concordant with expectations for the ELN risk groups (figure 5.6.0). It is notable that for RFS with the ELN risk groups in both the overall population, as well as RFS and OS in patients of age < 65 (figure 5.6.0 A, C, and D), that the favorable curve does cross the intermediate curve. For RFS, this likely represents the impact of allo-HSCT performed on intermediate risk patients in first CR, versus being performed in second CR for the favorable risk patients, thus resulting in early censoring for their relapse event. For OS in patients of age < 65, this may represent an early statistical fluctuation relating to mortality during initial induction chemotherapy. Nonetheless, the ELN classification retains statistical significance for both RFS and OS, including in individuals aged below 65. Our survival

outcomes were also as expected for age and peripheral WBC at diagnosis (figure 5.6.1) with respect to OS, but not for RFS. With respect to age, this is because many older individuals did not receive induction chemotherapy, and thus did not have the RFS endpoint defined, and is likely related to the impact of induction chemotherapy and transplant for peripheral WBC. Our survival data behaved as expected for antecedent chemotherapy/radiation or MDS/MPN (figure 5.6.2) with respect to RFS, but not for OS. This again likely reflects the impact of patient age and treatment selection in the group that had a RFS endpoint defined.

As such, our study cohort is generally consistent with the literature with regards to known prognostic factors, with some minimal deviations not being of significant magnitude to constitute clinically significant. In addition, our survival data generally behaves as expected with regards to known clinical, cytogenetic, and molecular prognostic markers, with some exceptions secondary to the impact of treatment heterogeneity, thus establishing the integrity of our dataset. Our median follow-up now is 1.54 years, which is slightly short of the desired median follow-up of 2 years in AML, but sufficient for analysis.

6.2 - Insights into the biology of NMT1

6.2.1 - NMT1 MFI is higher at baseline than NMT2 MFI, and does not vary between cell type, clinical, cytogenetic, or molecular factors related to AML

NMT1 MFI was found to be highly consistent between various cell types and cell compartments (figure 5.3.1), with no statistical variation between mature cell types, or primitive CD34+ or CD34+38- blasts. Overall, the mean NMT1 MFI was higher in absolute terms relative to that seen with the NMT2 MFI, suggesting that there may be higher physiologic level of NMT1 present, or that the NMT1 antibody was more efficient. NMT1 MFI was also found to be consistent between groups of clinical factors in AML (figure 5.3.0), recurrent cytogenetic abnormalities (figure 5.3.2), and molecular abnormalities (figure 5.3.4). This suggests that NMT1 MFI does not fluctuate during hematopoietic differentiation, or with the development of AML.

6.2.2 - NMT1 MFI does not associate with ELN risk group, and does not predict achievement of CR, nor is predictive of survival in AML

NMT1 MFI was consistent between ELN risk groups (figure 5.4.0) and did not predict achievement of CR versus RD/death (figure 5.5.0). Similarly, NMT1 MFI was not found to predict RFS or OS in either the overall population, or the ELN intermediate-risk population (figure 5.6.4 and 5.6.5). Overall, these results suggest that NMT1 appears to play a physiologic role in hematopoiesis, and does not appear to influence AML pathogenesis or prognosis based on our data.

6.3 - Insights into the biology of NMT2

6.3.1 - NMT2 MFI is high in lymphocytes, low in monocytes, and intermediate in normal HSC populations, suggesting NMT2 may influence early lymphoid/myeloid lineage commitment in normal hematopoiesis

The most notable trend amongst the control samples tested, as well as the mature monocytes and lymphocytes in patients with AML, was the statistically significantly higher NMT2 MFI in mature lymphocytes versus monocytes, having an approximately threefold increase in mean MFI. In the CD34+38- cell subsets from normal control samples, a compartment enriched for HSCs, there was a statistically significant increase in the NMT2 MFI relative to the mature monocytes and corresponding AML blast populations, by approximately twofold (figure 5.3.2). This would suggest that altered NMT2 protein levels may play a role in early lymphoid/myeloid lineage commitment in HSC, where an HSC with intermediate NMT2 protein levels will either upregulate NMT2 to commit to the lymphoid lineage, or downregulate NMT2 to commit to the myeloid lineage. There is previous evidence suggesting that abrogation of NMT activity impairs thymocyte development and function. [17] In this study, the investigators examined the effects on thymocyte development in mice with floxed NMT1 and NMT2 genes, with a Lck-Cre promoter. The effect of this was to turn off NMT1 and/or NMT2 production once the cell starting producing Lck, a c-Src related protein. They demonstrated that in the presence of $NMT1^{f/f}$ or $NMT1^{f/f}$ and $NMT2^{f/f}$ that both Lck and MARCKS, both essential proteins for the TCR signal transduction cascade and lymphocyte maturation, were mislocalized to the cytoplasm rather than the plasma membrane, resulting in a loss of TCR mediated signaling

and a developmental block in lymphocyte development. Unusually, $NMT2^{f/f}$ alone did not have as major of an impact on lymphocyte development as did $NMT1^{f/f}$ or $NMT1^{f/f}$ and $NMT2^{f/f}$. [17]

The effect of myristoylation on the TCR signaling cascade is an example of one mechanism by which NMT2 may influence lymphoid/myeloid lineage commitment. Particularly, the downregulation of NMT2 as a HSC becomes committed to the myeloid lineage could block the TCR signaling cascade by mislocalizing Lck and MARCKS to cytoplasm, thus ensuring myeloid development. However, this would not be consistent with the finding of Rampoldi *et al* suggesting that $NMT2^{f/f}$ did not impact lymphocyte development to the same degree $NMT1^{f//f}$ and $NMT2^{f/f}$ does. This could be explained if either the effect of NMT2 on lineage commitment occurs proximal in the differentiation cascade to the initiation of the Lck promoter, or if there are species differences in HSC lineage commitment between mice and humans.

A mechanism such as this would not account for blockage of B-cell differentiation, and there remain many different possible pathways by which NMT2 could mediate myeloid/lymphoid lineage commitment. However, it is certainly plausible that NMT2 could modulate lineage commitment, as demonstrated by our TCR example. Overall, this remains undefined at this point in time, and warrants further investigation.

It was also notable that normal HSC have an intermediate level of NMT2 activity. It should be considered whether this may relate to the self-renewal capabilities of the HSC. This could involve the Wnt/β-catenin pathway, known to both be central to HSC self-renewal and to involve several proteins that are lipid modified by either palmitoylation or myristoylation. [33-35] This too remains undefined currently, and warrants further investigation.

6.3.2 - NMT2 MFI is strongly associated with the cytogenetic abnormality inv(16), weakly with mutated NPM1, and is not associated with other clinical, cytogenetic, or molecular abnormalities in AML

There was a strong correlation, which persisted after application of the Bonferroni correction, noted between the cytogenetic abnormality inv(16) and higher NMT2 MFI, at similar levels that were seen in control CD34+38- populations (figure 5.3.6). This cannot be explained

by chromosomal disruption, given that NMT2 resides on chromosome 10. [49] One possible explanation for this is that NMT2 expression is modulated by a member of the RUNX family of transcriptional regulators. As reviewed in 2.2.4, inv(16) results in the aberrant fusion gene CBFB-MYH11, the product of which causes the dominant negative inhibition of the proteins CBFα1, CBFα2, and CBFα3. These are encoded by RUNX2, RUNX1, and RUNX3, respectively. The RUNX family of transcriptional regulators act as master transcriptional regulators for hematopoietic growth and differentiation. [36-38] Given that we suspect NMT2 protein levels are related to early lymphoid/myeloid lineage commitment, it would be fitting if modulation of NMT2 expression occurred through one of these transcriptional regulators.

It is notable, though, that patients with the CBF abnormalities t(v;21) did not have a similar increase in NMT2 MFI, as did their inv(16) counterparts. Only two of these patients were true t(8;21) translocations, with the other two being less specific t(v;21) translocations. Nonetheless, the two patients with t(8;21) did not have an increased NMT2 MFI. This may be explained by the fact that t(8;21) specifically targets the RUNX1 transcriptional regulator, while the inv(16) protein product would repress all three members of the RUNX family. [36-38] As such, we suspect that the NMT2 protein levels may be modulated by either the RUNX2 or RUNX3 transcriptional regulators.

There was also noted a statistically significant decrease in NMT2 MFI in AML with mutated NPM1 that persisted after application of the Bonferroni correction (figure 5.3.8). The reasons for this are less clear, however we do note that this association was less robust than that seen for inv(16), with a significant amount of measurement variability. This may be attributable to sampling error, though it could be considered that NPM1 either directly or indirectly plays a role in the transcriptional regulation of NMT2. Neither NPM1 itself or any of its major protein interaction partners are known to be myristoylated. Nonetheless, NPM1 has such a diverse range of interactions that it may yet be shown interact with myristoylated partners. [42]

Statistical significance was initially noted for an antecedent diagnosis of an MPN (figure 5.3.4) and for normal cytogenetics (figure 5.3.6), however both observations lost statistical significance after the Bonferroni correction was applied to compensate for the multiple

comparisons being performed on each variable. All other statistically significant values retained significance after application of the Bonferroni correction.

6.4 - NMT2 MFI and prognosis in AML

6.4.1 - NMT2 MFI is independent of ELN risk groups and the achievement of CR with first induction chemotherapy

As we had originally predicted in our hypothesis, NMT2 MFI was not associated with the current ELN risk groups (figure 5.4.2). Despite inv(16) having a higher NMT2 MFI relative to baseline, this was not sufficient to make the NMT2 MFI statistically higher in the favorable risk group. This suggests that NMT2 MFI is generally independent of the current classification scheme, which makes it relevant as a potential novel prognostic biomarker.

In contrast to our original prediction, NMT2 MFI was not associated with achievement of first CR with induction chemotherapy (figure 5.5.2). Patients who had RD or death with first induction had a similar NMT2 MFI to those who achieved CR with first induction chemotherapy, suggesting that NMT2 MFI is not a useful biomarker to predict achievement of CR.

6.4.2 - NMT2 MFI predict RFS and OS by in intermediate-risk AML, and this may represent a measure of the LSC burden of the blast population

We utilized ROC analysis to determine the utility of the continuous variable NMT2 MFI as a predictor for the dichotomous variables of RFS or OS. For the overall population, including the adverse and favorable risk groups, NMT2 MFI did not predict either RFS or OS in a statistically significant manner (figure 5.6.6). This is unsurprising, however, given that the impact of other prognostic factors likely outweighed that of NMT2 MFI for the favorable and adverse risk groups.

For the ELN intermediate-risk group, our main population of interest, NMT2 MFI did predict RFS and OS by ROC analysis (figure 5.6.7). The ROC for RFS in the bulk blast population (5.6.7 A) was significant and, though the AUC was above 0.7 in the CD34+38- blast population (5.6.7 C), this lost statistical significance due to a decreased sample size, as some

patients had insufficient events available for analysis in the CD34+38- subpopulation. The AUC for OS in the bulk blast population trended towards significance (figure 5.6.7 D), but became statistically significant once observing the CD34+38- blast subpopulation (figure 5.6.7 F). The overall trend was towards improved discrimination in the CD34+38- blast subpopulation with respect for OS. Interpretation of this trend for RFS is limited by sample size constraints.

The curve that demonstrated the best discrimination (figure 5.6.7 F) was then used to generate a sensitivity versus specificity table for various cut-off points of NMT2 MFI (table 5.6.1, figure 5.6.9). Two optimization peaks were demonstrated, one optimizing sensitivity at the expense of specificity, and one optimizing specificity at the expense of sensitivity. Both had reasonable discriminatory characteristics for both specificity and sensitivity. Kaplan-Meier analysis was done for both the higher sensitivity cut-off value (figure 5.6.10) and the higher specificity cut-off value (figure 5.6.11). This demonstrated that the higher specificity cut-off value was generally superior at defining survival. In addition, a higher specificity cutoff is more sensible from a clinical standpoint, as a false-positive would be more harmful in this clinical scenario than a false-negative, particularly if it were to result in committing a patient to a more aggressive therapy with major morbidity. As such, the higher specificity cut-off was utilized for further analysis.

Patients with a higher NMT2 MFI, using a cut-off value of 1.28, did appear to have a worsened RFS and OS by Kaplan-Meier analysis, particularly when utilizing the cut-off value in the CD34+38- blast subsets (figure 5.6.11). This was statistically significant for RFS in the CD34+38- population (figure 5.6.11 C), and showed a trend towards significance for RFS in the CD34+ population (figure 5.6.11 B) and for OS in the CD34+ and CD34+38- population (figure 5.6.11 E and F). An NMT2 MFI of greater than 1.28 was statistically significantly worse for OS in the bulk blast population (figure 5.6.11 D). Significance was narrowly lost for OS in the CD34+ and CD34+38- blast subsets (figure 5.6.11 E and F) due to an early crossing of the curves before 0.50 years of follow-up. We hypothesized this was secondary to the population we analyzed for OS being highly heterogeneous, and likely related to individuals with advanced age being censored at an early time point.

As such, we examined RFS and OS after restricting to the subpopulation of intermediate-risk, age < 65 patients only (figure 5.6.12). This eliminated the previously noted curve crossing, and resulted in a statistically significantly worse OS in the bulk blast and CD34+38- blast populations (figure 5.6.12 D and F), with a trend towards worsened OS in the CD34+ blast population (figure 5.6.12 E). RFS was not statistically significant in this subgroup, due to sample size limitations (figure 5.6.12 A, B, and C).

NMT2 MFI was evaluated in both the overall population and intermediate risk patients only for RFS and OS by univariate and multivariate Cox regression analysis with respect to the bulk blast populations. Variables included age > 65 and peripheral WBC > 20 x 10^9 /L at diagnosis (figure 5.6.3), with additional inclusion of ELN adverse-risk (vs favorable or intermediate) for the overall population (figure 5.6.2). The bulk blast subset was chosen for this analysis, as the CD34+ and CD34+38- groups violated the proportional hazards assumption.

ELN adverse-risk was the only significant variable with respect to RFS and OS for patients who had received induction on both univariate and multivariate analysis (figure 5.6.2 A and B). ELN adverse-risk, age > 65, and peripheral WBC > 20 x 10^9 /L were significant on univariate and multivariate analysis for OS in the overall population, but not NMT2 MFI (figure 5.6.2 C). For ELN intermediate-risk patients, we chose not to analyze the age < 65 and intermediate-risk subgroup, to allow for a more robust sample size and the use of age as a covariate. For RFS, no variables were significant by univariate analysis, with peripheral WBC > 20 x 10^9 /L and NMT2 MFI > 1.28 being significant on multivariate analysis (figure 5.6.3 A). No variables were significant on univariate or multivariate analysis for OS in the induction only population (figure 5.6.3 B). For OS in the overall population the variables age > 65, peripheral WBC > 20 x 10^9 /L, and NMT2 MFI > 1.28 were all significant on univariate analysis, with NMT2 MFI > 1.28 losing significance on the multivariate analysis (figure 5.6.3 C). These results are likely due to the population for whom RFS and OS with induction was defined being generally younger with more uniform treatment, giving advanced age less of an impact. Losing significance for NMT2 MFI > 1.28 on multivariate analysis for OS in the overall population was likely due to the heterogeneity of this, with the outsized effects of advanced age clouding the analysis.

A univariate binomial logistic regression was performed to evaluate the utility of NMT2 MFI as a continuous variable in predicting RFS, OS in induction patients only, or OS in the overall population. NMT2 MFI in either the bulk, CD34+, or CD34+38- blasts was not statistically significant for predicting RFS or OS in the induction population (figure 5.6.4 A and B). NMT2 MFI was statistically significant in the bulk blasts and CD34+38- blasts for OS in the overall population, but not in the CD34+ blasts (figure 5.6.4 C).

Overall, though limitations exist to the survival analysis due to the heterogeneity of the cohort analyzed and sample size constraints, the overall trend is towards a high NMT2 MFI portending a worse prognosis in patients with AML. This could represent a novel, highly translatable biomarker for prognosis in intermediate-risk AML. However, this result was the inverse of our original hypothesis based on the previous bioinformatics analysis by K. Vincent *et al* (manuscript in preparation), which found that higher NMT2 expression was associated with improved survival. It should be considered, though, that the mRNA data collected for the TCGA and GSE databases was based on expression in the overall peripheral blood mononuclear cell fractions. What we are observing in our study is, rather, is that it is primarily the NMT2 MFI in the CD34+38- blast subpopulation that is driving prognosis. This element would not have been observable in the original mRNA bioinformatics studies, due to aggregated RNA signals from various cell populations.

It is then interesting to consider what it is that we are measuring in the CD34+38- blast subset that is contributing to prognosis in AML. As reviewed in 2.2.3, the CD34+38- blast subset in AML is enriched with LSC, but is not the sole defining features of LSC. [28-30] The presence of LSC are thought to strongly influence prognosis in AML, and recent GEP panels have emerged to evaluate the stemness of blast populations, which refers to how closely a blast population genotypically resembles LSCs, and have been shown to be effective at predicting survival in AML. [4] Given our previous observations that NMT2 MFI is higher in control HSC like populations, this would suggest that a higher NMT2 MFI may be a feature of cells that more closely resemble primitive HSC progenitors. As such, a higher NMT2 MFI may represent an indirect measure of either the stemness of the blast population, particularly in the CD34+38-

blast subsets, or of the LSC burden, thus explaining the observed worsened RFS and OS in patients with higher NMT2 MFI.

6.5 - Future directions with NMT2 and AML

Further investigation is warranted into the utility of NMT2 MFI as prognostic biomarker in intermediate-risk AML. While the survival data in this study are suggestive, limitations exist with the significant heterogeneity of the study cohort. We suggest that a follow-up retrospective or prospective cohort study with inclusion criteria of ELN intermediate-risk, age < 65, and receipt of induction chemotherapy would provide confirmation that the measurement of NMT2 MFI by FACS has utility as a prognostic biomarker for intermediate-risk AML.

Further investigation is also warranted into the biology and role of NMT2 in both normal and malignant hematopoiesis. Particularly, the specific protein targets and mechanism by which NMT2 protein levels regulate early lymphoid/myeloid lineage commitment would be of great interest. Additionally, confirmatory investigation into the biology of NMT2 protein levels as they relate to inv(16) would be of great interest. Examination of the correlation between NMT2 protein levels and both the stemness of AML blast populations and LSC burden would also be valuable.

6.6 - Summary and conclusion

We analyzed how NMT1 and NMT2 MFI relate to clinical factors, recurrent cytogenetic and molecular abnormalities, ELN risk group, and clinical outcomes in AML. NMT1 was not associated with any of these factors, and was consistent throughout all samples. NMT2 MFI was moderately higher in normal hematopoietic stem cells, significantly higher in mature lymphocytes, and significantly lower in mature monocytes. This suggests that regulation of NMT2 protein levels influence early lymphoid/myeloid lineage commitment, possibly by modulation of the T-cell receptor pathway. The cytogenetic abnormality inv(16) showed significantly higher NMT2 MFI, possibly secondary to control of NMT2 expression by the transcriptional regulators RUNX2 and RUNX3. NMT2 MFI was moderately lower in patients with NPM1. NMT2 MFI was not associated with ELN risk group, or achievement of CR with first induction chemotherapy. Higher NMT2 MFI predicted worsened outcomes in the ELN

intermediate-risk population, with this effect being driven by the CD34+38- blast subsets. This may represent an indirect measure of the stemness of the blast population or the LSC burden in patients with AML.

References

1. Dohner, H., Estey, EH, Amadori, S, *et al*, *Diagnosis and management of acute myeloid leukemia in adults: recommendations from an international expert panel, on behalf of the European LeukemiaNet.* Blood, 2010. **115**(3): p. 453-474.
2. Rollig, C., Bornhauser, M, Thiede, C, *et al*, *Long-Term Prognosis of Acute Myeloid Leukemia According to the New Genetic Risk Classification of the European LeukemiaNet Recommendations: Evaluation of the Proposed Reporting System.* J. Clin. Oncol., 2011. **29**(20): p. 2758-2765.
3. Pastore, F., Dufour, A, Benthaus, T, *et al*, *Combined Molecular and Clinical Prognostic Index for Relapse and Survival in Cytogenetically Normal Acute Myeloid Leukemia.* J. Clin. Oncol., 2014. **32**(15): p. 1586-1594.
4. Ng, S., Mitchell, A, Kennedy, JA, *et al*, *A 17-gene stemness score for rapid determination of risk in acute leukaemia.* Nature, 2016. **540**(7633): p. 433-437.
5. Kim, T., Tyndel, MS, Kim, HJ, *et al*, *The clonal origins of leukemic progression of myelodysplasia.* Leukemia, 2017: p. 1-8.
6. Wright, M., Heal, WP, Mann, DJ, Tate, EW, *Protein myristoylation in health and disease.* J. Chem. Biol., 2010. **3**(1): p. 19-35.
7. Martin, D., Beauchamp, E, Berthiaume, LG, *Post-translational myristoylation: Fat matters in cellular life and death.* Biochimie, 2011. **93**(1): p. 18-31.
8. Xu, M., Xie, L, Yu, Z, Xie, J, *Roles of protein N-myristoylation and translational medicine applications.* Crit. Rev. Euk. Gene Exp., 2015. **25**(3): p. 259-168.
9. Chida, T., Ando, M, Matsuki, T, *et al Myristoylation is essential for protein phosphatases PPM1A and PPM1B to dephosphorylate their physiological substrates in cells.* Biochem. J., 2013. **449**(3): p. 741-749.
10. Thinon, E., Serwa, RA, Broncel, M, *et al Global profiling of co- and post-translationally N-myristoylated proteoms in human cells.* Nat. Commun., 2014. **5**: p. 4919.
11. Knezevic, K., Bee, T, Wilson, NK, *et al*, *A Runx1-Smad6 rheostat controls Runx1 activity during embryonic hematopoeiesis.* Molecular and Cellular Biology, 2011. **31**(14): p. 2817-2826.
12. Ducker, C., Upson, JJ, French, KJ, Smith, CD, *Two N-myristoyltransferase isozymes play unique roles in protein myristoylation, proliferation, and apoptosis.* Mol. Cancer Res., 2005. **3**(8): p. 463-467.
13. Yang, S., Shrivastav, A, Kosinski, C, *et al*, *N-myristoyltransferase 1 is essential in early mouse development.* J. Biol. Chem., 2005. **280**(19): p. 18990-18995.
14. Shrivastav, A., Varma, S, Lawman, Z, *et al*, *Requirement of N-myristoyltransferase 1 in the development of monocytic lineage.* J. Immunol., 2008. **180**(2): p. 1019-1028.
15. Shrivastav, A., Suri, SS, Mohr, R, Janardhan, KS, Sharma, RK, Singh, B, *Expression and activity of N-myristoyltransferase in lung inflammation of cattle and its role in neutrophil apoptosis.* Vet. Res., 2010. **41**(1): p. 1-12.
16. Kumar, S., Singh, B, Dimmock, JR, Sharma, RK, *N-myristoyltransferase in the leukocytic development process.* Cell Tissue Res., 2011. **345**(2): p. 203-211.
17. Rampoldi, F., Bonrouhi, M, Boehm, ME *et al*, *Immunosuppression and aberrant T-cell development in the absence of N-myristoylation.* J. Immunol., 2015. **195**(9): p. 4228-4243.

18. Zha, J., Weiler, S, Oh, KJ, *et al Post-translational N-myristoylation of BID as a molecular switch for targeting mitochondria and apoptosis.* Science, 2000. **290**(5497): p. 1761-1765.
19. Martin, D., Vilas, GL, Prescher, JA, *et al Rapid detection, discovery, and identification of post-translationally myristoylated proteins during apoptosis using a bio-orthogonal azidomyristate analog.* FASEB J., 2008. **22**(3): p. 797-806.
20. Vilas, G., Corvi, MM, Plummer, GJ, Seime, AM, Lambkin, GR, Berthiaume, LG, *Posttranslational myristoylation of caspase-activated p21-activated protein kinase 2 (PAK2) potentiates late apoptotic events.* Proc. Nat. Acad. Sci., 2006. **103**(17): p. 6542-6547.
21. Perinpanayagam, M., Beauchamp, E, Martin, DD, Sim, JY, Yap, MC, Berthiaume, LG, *Regulation of co- and post-translationally myristoylation of proteins during apoptosis: interplay of N-myristoyltransferases and caspases.* FASEB J., 2013. **27**(2): p. 811-821.
22. Rajala, R., Radhi, JM, Kakkar, R, Datla, RS, Sharma, RK, *Increased expression of N-myristoyltransferase in gallbladder carcinomas.* Cancer, 2000. **88**(9): p. 1992-1999.
23. Shrivastav, A., Sharma, AR, Bajaj, G, *et al*, *Elevated N-myristoyltransferase activity and expression in oral squamous cell carcinoma.* Oncol. Rep., 2007. **18**(1): p. 93-97.
24. Lu, Y., Selvakumar, P, Ali, K, *et al*, *Expression of N-myristoyltransferase in human brain tumors.* Neurochem. Res., 2005. **30**(1): p. 9-13.
25. Clegg, R., Gordge, PC, Miller, WR, *Expression of enzymes of covalent protein modification during regulated and dysregulated proliferation of mammary epithelial cells: PKA, PKC and NMT.* Adv. Enzyme Regul., 1999. **39**: p. 175-203.
26. Magnuson, B., Raju, RV, Moyana, TN, Sharma, RK, *Increased N-myristoyltransferase activity observed in rat and human colonic tumors.* J. Natl. Cancer Inst., 1995. **87**(21): p. 1630-1635.
27. Selvakumar, P., Smith-Windsor, E, Bonham, K, Sharma, RK, *N-myristoyltransferase 2 expression in human colon cancer: cross-talk between the calpain and caspase system.* FEBS Lett., 2006. **580**(8): p. 2021-2026.
28. Bonnet, D., Dick, JE, *Human acute myeloid leukemia is organized as a hierarchy that originates from a primitive hematopoietic cell.* Nat. Med., 1997. **3**(7): p. 730-737.
29. Krause, D., Van Etten, RA, *Right on target: eradicating leukemic stem cells.* Trends Mol. Med., 2007. **13**(11): p. 470-481.
30. Misaghian, N., Ligresti, G, Steelman, LS, *et al*, *Targeting the leukemic stem cell: the Holy Grail of leukemia therapy.* Leukemia, 2009. **23**(1): p. 25-42.
31. Ravandi, F., Estrov, Z, *Eradication of leukemia stem cells as a new goal of therapy in leukemia.* Clin. Cancer Res., 2006. **12**(2): p. 340-344.
32. Mikesch, J., Steffen, B, Berdel, WE, Serve, H, Muller-Tidow, C, *The emerging role of Wnt signalling in the pathogenesis of acute myeloid leukemia.* Leukemia, 2007. **21**(8): p. 1638-1647.
33. Austin, T., Solar, GP, Ziegler, FC, Liem, L, Matthews, W, *A role for the Wnt gene family in hematopoiesis: expansion of multilineage progenitor cells.* Blood, 1997. **89**(10): p. 3624-3635.
34. van den Berg, D., Sharma, AK, Bruno, E, Hoffman, R, *Role of the members of the Wnt gene family in human haematopoiesis.* Blood, 1998. **89**: p. 3189-3202.
35. Reya, T., Duncan, AW, Ailles, L, *et al*, *A role for Wnt signalling in self-renewal of haematopoietic stem cells.* Nature, 2003. **423**(6938): p. 409-414.

36. Goyama, S., Huang, G, Kurokawa, M, Mulloy, JC, *Posttranslational modifications of RUNX1 as potential anticancer targets.* Oncogene, 2015. **34**(27): p. 3483-3492.
37. Zhao, L., Cannons, JL, Anderson, S, *et al*, *CBFB-MYH11 hinders early T-cell development and induces massive cell death in the thymus.* Blood, 2007. **109**(8): p. 3432-3440.
38. Chin, D., Watanabe-Okochi, N, Wang, CQ, Tergaonkar, V, Osato, M, *Mouse models for core binding factor leukemia.* Luekemia, 2015. **29**(10): p. 1970-1980.
39. Licht, J., *AML1 and the AML1-ETO fusion protein in the pathogenesis of t(8;12) AML.* Oncogene, 2001. **20**(40): p. 5660-5679.
40. Cai, Q., Jeannet, R, Hua, WK, *et al*, *CBFβ-SMMHC creates aberrant megakaryocyte-erythroid progenitors prone to leukemia-initiation in mice.* Blood, 2016. **128**(11): p. 1503-1515.
41. Kuo, Y., Landrette, SF, Heilman, SA, *et al*, *CBF-SMHCC induces distinct abnormal myeloid progenitors able to develop acute myeloid leukemia.* Cancer Cell, 2006. **9**(1): p. 57-68.
42. Heath, E., Chan, SM, Minden, MD, Murphy, T, Shlush, LI, Schimmer, AD, *Biological and clinical consequences of NPM1 mutations in AML.* Leukemia, 2017. **31**(4): p. 798-807.
43. McShane, L., Altman, DG, Sauerbrei, W, Taube, SE, Gion, M, Clark, GM, *REporting recommendations for tumor MARKer prognostic studies (REMARK).* Br. J. Cancer, 2005. **93**: p. 387-391.
44. Dores, G., Devesa, SS, Curtis, RE, Linet, MS, Morton, LM, *Acute leukemia incidence and patient survival among children and adults in the United States, 2001-2007.* Blood, 2012. **119**(1): p. 34-43.
45. Siegel, R., Naishadham, D, Jermal, A, *Cancer statistics, 2012.* CA Cancer J. Clin. , 2012. **1**: p. 10-29.
46. Kaleem, Z., Crawford, E, Pathan, MH, *et al*, *Flow cytometric analysis of acute leukemias. Diagnostic utility and critical analysis of the data.* Arch. Pathol. Lab. Med., 2003. **127**(1): p. 42-48.
47. Byrd, J., Mrozek, K, Dodge, RK, *et al*, *Pretreatment cytogenetic abnormalities are predictive of induction success, cumulative incidence of relapse, and overall survival in adult patients with de novo acute myeloid leukemia: results from the Cancer and Leukemia Group B (CALGB 8461).* Blood, 2002. **100**(13): p. 4325-4336.
48. Yamamoto, Y., Kiyoi, H, Nakano, Y, *et al*, *Activating mutation of D835 within the activation loop of FLT3 in human hematologic malignancies.* Blood, 2001. **97**(8): p. 2434-2439.
49. https://genome.ucsc.edu/cgi-bin/hgTracks?db=hg38&lastVirtModeType=default&lastVirtModeExtraState=&virtModeType=default&virtMode=0&nonVirtPosition=&position=chr10%3A15102584-15168693&hgsid=593037429_uXonwID0jZmxzo8yET1ka54TRUaM.

Tables

Variable	Patients		NMT1 MFI (t-test *p* value)			NMT2 MFI (t-test *p* value)		
	N	%	Bulk	CD34+	CD34+38-	Bulk	CD34+	CD34+38-
Total N	N = 105							
Excluded N	1	1						
Included N	N = 104							
Age at Diagnosis (Median)	67.1 yrs							
> 65 yrs	56	54	0.425	0.331	0.395	0.674	0.245	0.605
Gender								
Male	71	68	0.971	0.924	0.880	0.167	0.094	0.099
Female	33	32						
Medical History								
MPN	10	10	0.380	0.514	0.458	0.051	**0.016**	**0.001**
Chemotherapy	8	8	0.435	0.400	0.477	0.717	0.962	0.942
Radiation	5	5	0.505	0.505	0.604	0.241	0.147	0.316
MDS	3	3	nil	nil	nil	0.413	0.596	0.441
Total WBC At Diagnosis (Median)								
Peripheral WBC	13.8 x 10^9 / L							
Periperal Blasts	33% of TNC							
BM Blasts	54% of TNC							
Cytogenetics								
Normal	42	40	0.058	0.053	0.059	0.173	**0.032**	**0.010**
Complex	16	15	0.496	0.510	0.549	0.370	0.345	0.211
t(v;11)	8	8	0.562	0.598	0.567	0.107	0.586	0.985
inv(16)	6	6	nil	nil	nil	**< 0.001**	**< 0.001**	**0.025**
t(v;21)	4	4	0.972	0.888	0.694	0.945	0.784	0.641
t(9;22)	1	1						
Molecular								
NPM1	29	28	0.750	0.586	0.873	**0.002**	**0.004**	0.164
FLT3-ITD	20	19	0.569	0.537	0.372	0.351	0.196	0.838
JAK2	5	5	0.549	0.742	0.639	0.098	0.179	0.213
BCR/ABL	2	2						
c-KIT	1	1						
CEBPA	1	1						
ELN Risk Group								
Favorable	23	22						
Intermediate	57	55						
Adverse	22	21						
Unknown	2	2						

Table 5.2.1 - Baseline patient characteristics and associations with NMT1 and NMT2 MFI

A total of 105 patients were recruited and were analyzed by FACS, with 44 being analyzed for both NMT1 and NMT2, and 61 analyzed for NMT2 alone. The population had a median age of 67.1 years, and was male predominant. Median peripheral WBC at diagnosis was 13.8 x 10^9 / L, with a median bone marrow blast count of 54% of total nucleated cells (TNC). The most common cytogenetic profile was normal (n = 42), with the second most common being complex cytogenetics (n = 16). Several core binding factor rearrangements were identified, including inv(16) (n = 8) and t(v;21) (n = 4). Additionally, several MLL rearrangements were identified, with t(v;11) (n = 8). The most commonly identified molecular abnormalities were NPM1 (n = 29) and FLT3-ITD (n = 20). The ELN risk groups were evenly balanced between favorable (n = 23), intermediate (n = 57), and unfavorable (n = 22).

Variable		Patients N	Patients %
Therapy			
	IDAC	55	95
	Azacytidine	13	
	LDAC	5	
	LDAC + Volasertib (Clinical Trial)	4	
	SGI1-110 (Clinical Trial)	9	
Induction		58	56
Response (IDAC)			**of N = 58**
	CR/iCR	46	79
	RD	8	14
	Death	4	7
Allo-SCT			
	Allo-HSCT	29	50
Relapse			
	Relapse	20	34
RFS			
	RFS Event	24	41
	Median RFS [Range]	1.31 yrs [0.10 - 1.48 yrs]	
OS			**of N = 104**
	OS Event	59	57
	Median OS [Range]	0.95 yrs [0.00 - 1.88 yrs]	
Follow-up			
	Median FU [Range]	1.54 yrs [0.11 - 3.53 yrs]	

Table 5.2.2 - Patient treatment and outcomes

58 patients received upfront induction chemotherapy, with most receiving a standard idarubicin and cytarabine (IDAC) regimen (n = 55). Of those treated with palliative regimens, 13 received azacytidine and 5 received low dose cytarabine (LDAC) as upfront therapy. A total of 46 patients who received induction chemotherapy achieved either a complete remission (CR) or complete remission with incomplete recovery (iCR). Allogenic hematopoietic stem cell transplant (Allo-SCT) was performed on 29 patients. A total of 20 patients had relapsed at last follow-up, with 24 having had an event per the relapse-free survival (RFS) composite outcome with a median RFS of 1.31 years, defined as the time from AML diagnosis to disease relapse or death. A total of 59 patients had met the overall survival (OS) outcome with a median OS of 0.95 years, defined as the time from AML diagnosis to death. Median follow-up for this cohort is 1.54 years.

ROC for OS and NMT2 CD34+38- MFI			
NMT2 CD34+38- MFI	Sensitivity	Specificity	Youden's J
1.01	0.82	0.55	0.37
1.03	0.79	0.55	0.34
1.05	0.75	0.55	0.30
1.10	0.71	0.55	0.26
1.14	0.71	0.60	0.31
1.15	0.68	0.60	0.28
1.17	0.64	0.70	0.34
1.20	0.57	0.70	0.27
1.24	0.54	0.75	0.29
1.26	0.50	0.75	0.25
1.28	0.50	0.80	0.30
1.30	0.46	0.80	0.26
1.31	0.43	0.85	0.28
1.34	0.39	0.85	0.24
1.37	0.36	0.85	0.21
1.43	0.32	0.90	0.22
1.53	0.25	0.90	0.15
1.61	0.21	0.95	0.16
1.68	0.18	0.95	0.13
1.72	0.14	0.95	0.09
1.78	0.11	0.95	0.06
1.94	0.11	1.00	0.11
2.09	0.07	1.00	0.07
2.37	0.04	1.00	0.04
3.61	0.00	1.00	0.00

Table 5.6.1 - Sensitivity versus specificity table for the optimized NMT2 receiver operator curve - NMT2 MFI for CD34+38- blasts, intermediate-risk only, with respect to OS

Sensitivity versus specificity is displayed for different cut-off values of NMT2 CD34+38- MFI with respect to overall survival (Curve F, Fig 5.6.7). Youden's J statistic, calculated as [(sensitivity + specificity) - 1] is also displayed as a measure of the overall performance of the test at different cutoff values. Two optimization peaks are demonstrated at an NMT2 MFI of 1.17, which optimizes sensitivity at the expense of specificity, and 1.28, which optimizes specificity at the expense of sensitivity.

A

Relapse-free Survival (All ELN risk groups)

	Univariate Analysis			Multivariate Analysis		
Variable	HR	95% CI	p-value	HR	95% CI	p-value
ELN Adverse-Risk (vs Int or Favorable)	3.361	[1.320 - 8.559]	**0.011**	3.076	[1.158 - 8.169]	**0.024**
Age > 65	0.670	[0.199 - 2.250]	0.517	0.866	[0.247 - 3.034]	0.822
Peripheral WBC > 20 x 10^9 /L	1.763	[0.790 - 3.935]	0.167	1.546	[0.668 - 3.574]	0.309
Bulk Blast NMT2 MFI > 1.28	1.211	[0.498- 2.944]	0.673	0.964	[0.374 - 2.484]	0.940

B

Overall Survival (All ELN risk groups, induction ONLY)

	Univariate Analysis			Multivariate Analysis		
Variable	HR	95% CI	p-value	HR	95% CI	p-value
ELN Adverse-Risk (vs Int or Favorable)	6.141	[2.360 - 15.983]	**< 0.001**	5.813	[2.192 - 15.413]	**< 0.001**
Age > 65	1.539	[0.548 - 4.320]	0.413	1.087	[0.335 - 3.534]	0.889
Peripheral WBC > 20 x 10^9 /L	1.879	[0.741 - 4.768]	0.184	1.418	[0.524 - 3.837]	0.491
Bulk Blast NMT2 MFI > 1.28	0.883	[0.286 - 2.728]	0.829	0.875	[0.259 - 2.955]	0.829

C

Overall Survival (All ELN risk groups)

	Univariate Analysis			Multivariate Analysis		
Variable	HR	95% CI	p-value	HR	95% CI	p-value
ELN Adverse-Risk (vs Int or Favorable)	2.390	[1.374 - 4.158]	**0.002**	2.232	[1.277 - 3.902]	**0.005**
Age > 65	3.847	[2.154 - 6.873]	**< 0.001**	3.805	[2.107 - 6.870]	**< 0.001**
Peripheral WBC > 20 x 10^9 /L	1.673	[1.003 - 2.791]	**0.049**	1.902	[1.902 - 1.123]	**0.017**
Bulk Blast NMT2 MFI > 1.28	1.263	[0.716 - 2.226]	0.420	1.296	[0.729 - 2.305]	0.377

Table 5.6.2 - NMT2 Cox-regression for RFS and OS in all ELN risk groups with NMT2 MFI in bulk blasts

Univariate and multivariate Cox regression analyses are displayed for relapse-free survival (A), overall survival in patients undergoing induction only (B), and overall survival in all patients (C). ELN adverse-risk was a significant variable for relapse-free survival in both univariate (HR 3.361, 95% CI 1.320 - 8.559, p = 0.011) and multivariate (HR 3.076, 95% CI 1.158 - 8.169, p = 0.024) analysis. ELN adverse-risk was also significant for overall survival in patients undergoing induction on univariate (HR 6.141, 95% CI 2.360, p < 0.001) and multivariate (HR 5.813, 95% CI 2.192 - 15.413, p < 0.001) analysis. Overall survival in all patients showed significance on univariate analysis for the variables ELN adverse-risk (HR 2.390, 95% CI 1.374 - 4.158, p = 0.002), age > 65 (HR 3.847, 95% CI 2.154 - 6.873, p < 0.001), and peripheral WBC > 20 x 10^9 /L (HR 1.673, 95% CI 1.003 - 2.791, p = 0.049). This was retained on multivariate analysis for ELN adverse risk (HR 2.232, 95% CI 1.277 - 3.902, p = 0.005), age > 65 (HR 3.805, 95% CI 2.107 - 6.870, p < 0.001), and peripheral WBC > 20 x 10^9 /L (HR 1.902, 95% CI 1.902 - 1.123, p = 0.017). The proportional hazards assumption was inspected visually and found to be valid in Kaplan-Meier curves 5.6.11 A, D, B, and C, but not for curves E and F.

A

Relapse-free Survival (ELN intermediate-risk ONLY)

	Univariate Analysis			Multivariate Analysis		
Variable	HR	95% CI	p-value	HR	95% CI	p-value
Age > 65	0.776	[0.167 - 3.599]	0.746	1.207	[0.239 - 6.093]	0.820
Peripheral WBC > 20 x 10^9 /L	2.655	[0.809 - 8.718]	0.107	5.433	[1.196 - 24.686]	**0.028**
Bulk Blast NMT2 MFI > 1.28	2.840	[0.823 - 9.798]	0.099	6.200	[1.348 - 28.529]	**0.019**

B

Overall Survival (ELN intermediate-risk and induction ONLY)

	Univariate Analysis			Multivariate Analysis		
Variable	HR	95% CI	p-value	HR	95% CI	p-value
Age > 65	1.041	[0.209 - 5.176]	0.961	1.968	[0.325 - 11.937]	0.461
Peripheral WBC > 20 x 10^9 /L	2.924	[0.698 - 12.249]	0.142	4.308	[0.842 - 22.038]	0.079
Bulk Blast NMT2 MFI > 1.28	2.661	[0.628 - 11.278]	0.184	3.403	[0.773 - 14.985]	0.105

C

Overall Survival (ELN intermediate-risk ONLY)

	Univariate Analysis			Multivariate Analysis		
Variable	HR	95% CI	p-value	HR	95% CI	p-value
Age > 65	5.230	[2.131 - 12.838]	**< 0.001**	5.618	[2.207 - 14.299]	**< 0.001**
Peripheral WBC > 20 x 10^9 /L	2.302	[1.126 - 4.706]	**0.022**	2.676	[1.250 - 5.730]	**0.011**
Bulk Blast NMT2 MFI > 1.28	2.683	[1.313 - 5.485]	**0.007**	1.789	[0.839 - 3.814]	0.132

Table 5.6.3 - NMT2 Cox-regression for RFS and OS in ELN intermediate-risk patients with NMT2 MFI in bulk blasts

Univariate and multivariate Cox regression analyses are displayed for relapse-free survival (A), overall survival in patients undergoing induction only (B), and overall survival (C) in ELN intermediate-risk only patients. No variables were significant for relapse-free survival on univariate analysis. On multivariate analysis for relapse-free survival, peripheral WBC > 20 x 10^9 (HR 5.433, 95% CI 1.196 - 24.686, p = 0.028) and bulk blast NMT2 MFI > 1.28 (HR 6.200, 95% CI 1.348 - 28.529, p = 0.019) were significant. No variables were significant on univariate or multivariate analysis for overall survival in intermediate-risk patients undergoing induction only. On univariate analysis for overall survival in all intermediate-risk patients, age > 65 (HR 5.230, 95% CI 2.131 - 12.838, p < 0.001), peripheral WBC > 20 x 10^9 /L (HR 2.302, 95% CI 1.126 - 4.706, p = 0.022), and bulk blast NMT2 MFI > 1.28 (HR 2.683, 95% CI 1.313 - 5.485, p = 0.007) were significant. On multivariate analysis for overall survival in all intermediate-risk patients age > 65 (HR 5.618, 95% CI 2.207 - 14.299, p < 0.001) and peripheral WBC > 20 x 10^9 /L (HR 2.676, 95% CI 1.250 - 5.730, p = 0.011) were significant. The proportional hazards assumption was inspected visually and found to be valid in Kaplan-Meier curves 5.6.11 A, D, B, and C, but not for curves E and F.

A **Relapse-free Survival (ELN intermediate-risk ONLY)**

Variable	OR	95% CI	p-value
NMT2 Bulk Blast MFI	67.409	[0.959 - 4737.185]	0.052
NMT2 CD34+ Blast MFI	13.979	[0.497 - 393.261]	0.121
NMT2 CD34+38- Blast MFI	13.384	[0.533- 336.019]	0.115

B **Overall Survival (ELN intermediate-risk and induction ONLY)**

Variable	OR	95% CI	p-value
NMT2 Bulk Blast MFI	37.102	[0.642 - 2145.082]	0.081
NMT2 CD34+ Blast MFI	13.631	[0.513 - 362.271]	0.119
NMT2 CD34+38- Blast MFI	18.144	[0.563 - 585.009]	0.102

C **Overall Survival (ELN intermediate-risk ONLY)**

Variable	OR	95% CI	p-value
NMT2 Bulk Blast MFI	10.923	[1.091 - 109.318]	**0.042**
NMT2 CD34+ Blast MFI	8.801	[0.861- 89.916]	0.067
NMT2 CD34+38- Blast MFI	7.275	[1.064 - 49.757]	**0.043**

Table 5.6.4 - Logistic regression for RFS and OS in ELN intermediate-risk AML with respect to NMT2 MFI as a continuous variable for bulk, CD34+, and CD34+38- blasts

Logistic regression of NMT2 MFI are displayed with respect to relapse-free survival for intermediate-risk patients in the bulk blast population (OR 67.409, 95% CI 0.959 - 4737.185, p = 0.052), CD34+ blast population (OR 13.979, 95% CI 0.497 - 393.261, p = 0.121), and CD34+38- blast population (OR 13.384, 95% CI 0.533 - 336.019, p = 0.115) is displayed (A). Logistic regression of NMT2 MFI with respect to overall survival for intermediate risk patients who underwent induction is displayed in the bulk blast population (OR 37.102, 95% CI 0.642 - 2145.082, p = 0.081), CD34+ blast population (OR 13.631, 95% CI 0.513 - 362.271, p = 0.119), and CD34+38- blast population (OR 18.144, 95% CI 0.563 - 585.009, p = 0.102) is also displayed (B). Logistic regression of NMT2 MFI with respect to overall survival for intermediate-risk patients is displayed in the bulk blast population (OR 10.923, 95% CI 1.091 - 109.318, p = 0.042), CD34+ blast population (OR 8.801, 95% CI 0.861 - 89.916, p = 0.067), and CD34+38- blast population (OR 7.275, 95% CI 1.064 - 49.757, p = 0.043) is also displayed (C).

Figures

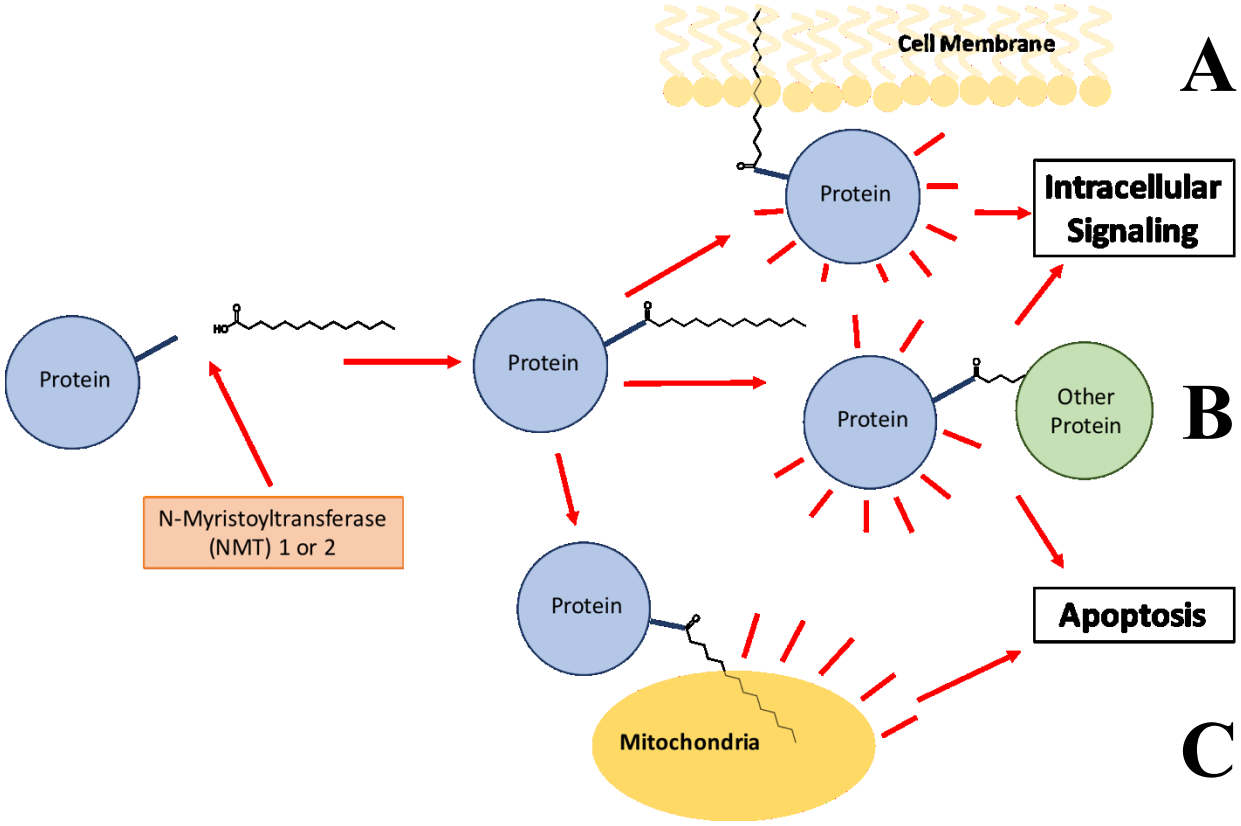

Figure 2.1.1 - Simplified schematic of protein regulation by myristoylation and N-myristoyltransferase 1 (NMT1) and NMT2

A basic overview of the mechanisms by which myristoylation regulates protein function is presented. NMT covalently attaches the 14-carbon fatty acid myristate co-translationally to an N-terminal glycine with a myristoylation consensus sequence after removal of the initiator methionine. Alternatively, myristoylation can occur post-translationally after caspase cleavage results in the exposure of an internal glycine with a cryptic myristoylation sequence. The myristoyl moiety is weakly hydrophobic, and can result in reversible targeting of a protein to the cellular membrane (A) or permanent targeting with a cooperating second signal. This will typically facilitate protein activity by concentration at the membrane and co-localization with other membrane dwelling proteins. Myristoylation can also result in protein-protein interactions (B), or targeting of a protein to the mitochondria, as in the case of BiD. Proteins regulated by myristoylation are largely involved in either intracellular signalling or apoptosis, and myristoylation is known to modulate these functions *in vivo*.

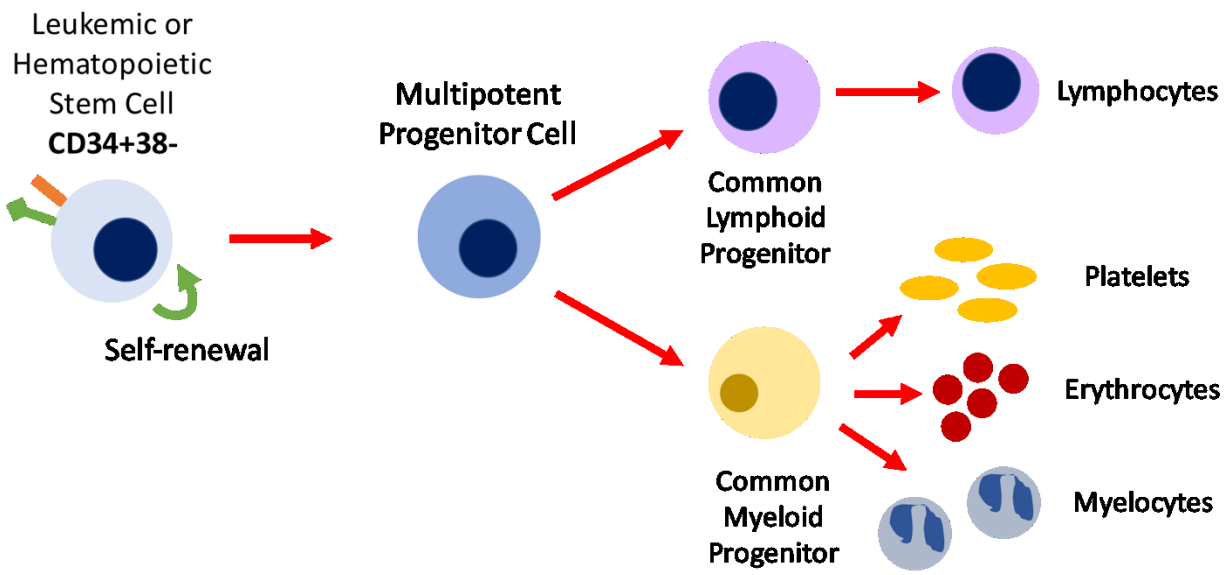

Figure 2.2.1 - Simplified schematic of the hematopoietic differentiation cascade, and the role of leukemic stem cells (LSCs)

A basic schematic overview of the hematopoietic differentiation cascade is presented, demonstrating the presence of primitive self-renewing precursor cells, either hematopoietic stem cells or their counterpart LSC, which display the CD34+38- cell surface marker profile. These cells lose these markers, in addition to losing the capacity for self-renewal, when they progress to multipotent progenitor cells, which subsequently commit to either the myeloid or lymphoid differentiation pathways.

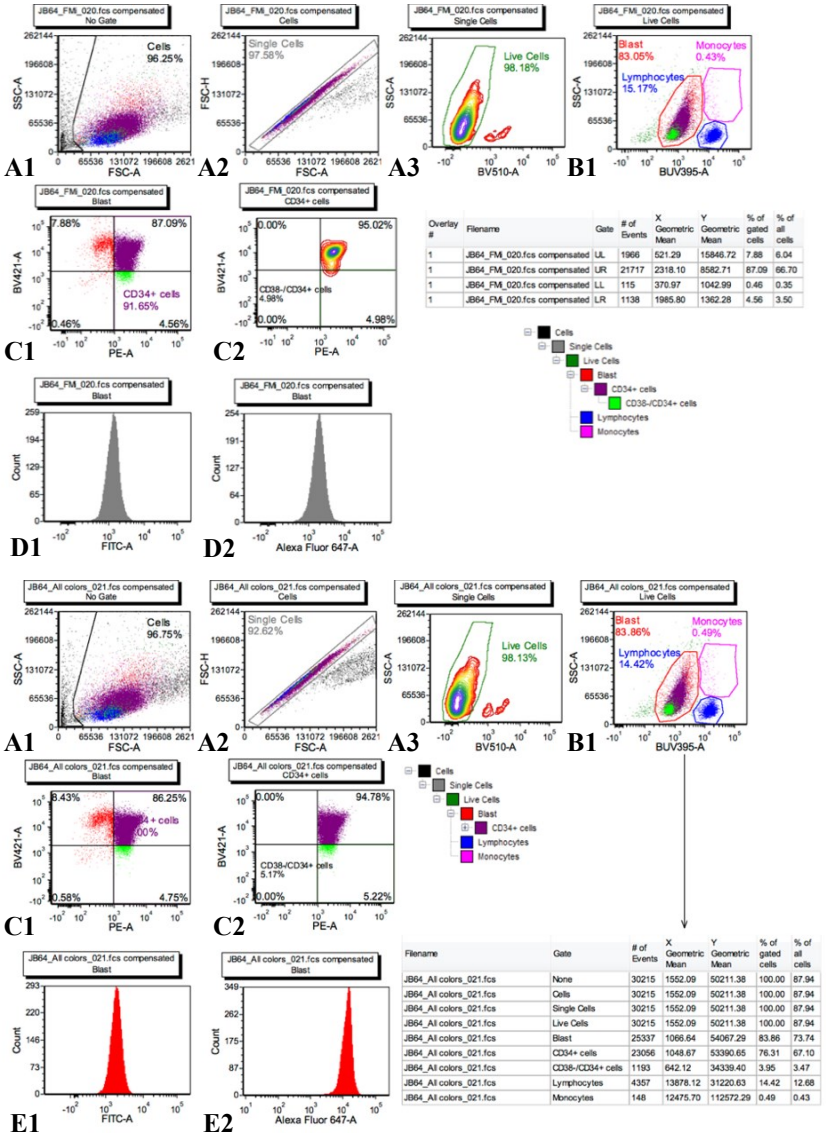

Figure 5.1.1 - Sample FACS data for NMT1 and 2 for AML patient marrow aspirate

Bone marrow aspirate or peripheral blood, either from a biobank maintained at -60°C or freshly obtained samples, were analyzed by multicolor fluorescent activated cell sorting (FACS). These were then gated for single, live cells with side scatter (SSC) vs forward scatter (FSC) and vs BV510, respectively (A1-3). Blasts, mature lymphocytes and monocytes were then gated with SSC vs CD45-BUV395 (B1). Primitive blast populations, defined as either CD34+ or CD34+38- immunophenotypes, were then gated with a two-parameter density plot generated with CD38-BV421 vs CD34-PE (C1-2). Histograms were generated for intracytoplasmic staining of IgGk-FITC or IgGk-Alexa Fluor 647 (D1-2) and anti-NMT2-FITC or anti-NMT1-Alex Fluor 647 (E1-2). Analysis was performed on approximately 1 x 10^6 cells in 100 µL buffer with a human Fc block applied, and application of IntraPrep permeabilization reagent for intracellular staining.

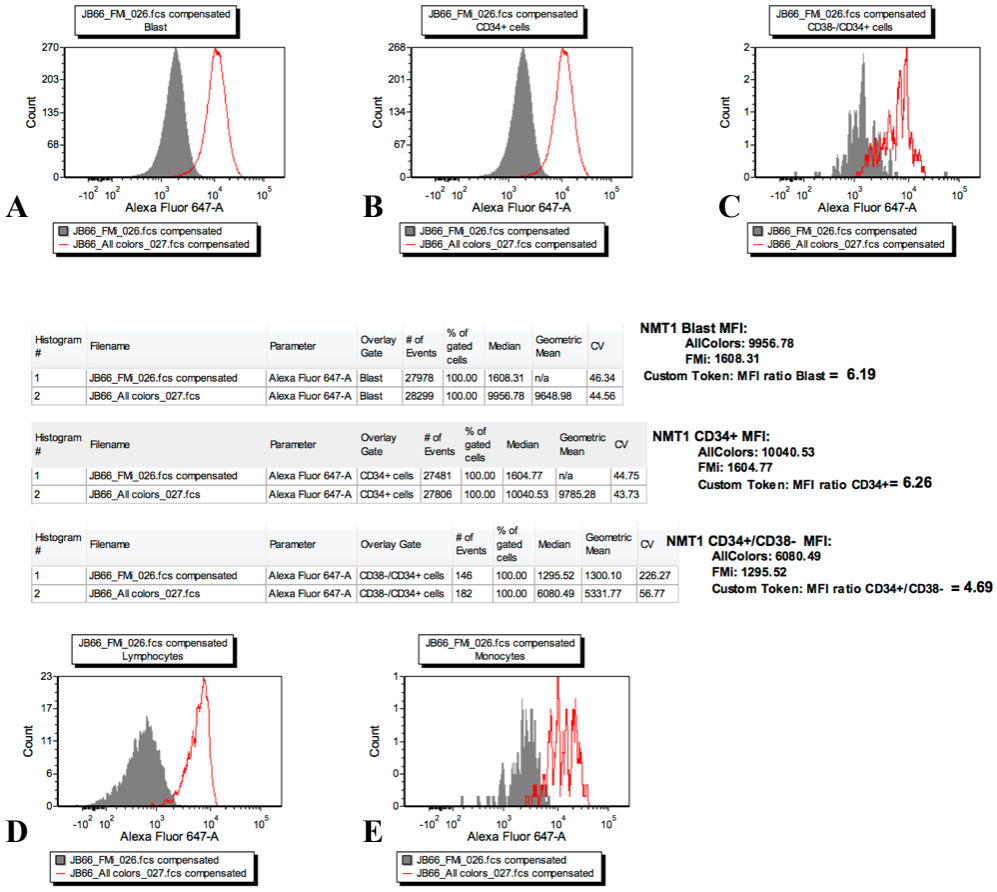

Histogram #	Filename	Parameter	Overlay Gate	# of Events	% of gated cells	Median	Geometric Mean	CV
1	JB66_FM_026.fcs compensated	Alexa Fluor 647-A	Blast	27978	100.00	1608.31	n/a	46.34
2	JB66_All colors_027.fcs	Alexa Fluor 647-A	Blast	28299	100.00	9956.78	9648.98	44.56

NMT1 Blast MFI:
AllColors: 9956.78
FMi: 1608.31
Custom Token: MFI ratio Blast = 6.19

Histogram #	Filename	Parameter	Overlay Gate	# of Events	% of gated cells	Median	Geometric Mean	CV
1	JB66_FM_026.fcs compensated	Alexa Fluor 647-A	CD34+ cells	27481	100.00	1604.77	n/a	44.75
2	JB66_All colors_027.fcs	Alexa Fluor 647-A	CD34+ cells	27806	100.00	10040.53	9785.28	43.73

NMT1 CD34+ MFI:
AllColors: 10040.53
FMi: 1604.77
Custom Token: MFI ratio CD34+= 6.26

Histogram #	Filename	Parameter	Overlay Gate	# of Events	% of gated cells	Median	Geometric Mean	CV
1	JB66_FM_026.fcs compensated	Alexa Fluor 647-A	CD38-/CD34+ cells	146	100.00	1295.52	1300.10	226.27
2	JB66_All colors_027.fcs	Alexa Fluor 647-A	CD38-/CD34+ cells	182	100.00	6080.49	5331.77	56.77

NMT1 CD34+/CD38- MFI:
AllColors: 6080.49
FMi: 1295.52
Custom Token: MFI ratio CD34+/CD38- = 4.69

Histogram #	Filename	Parameter	Overlay Gate	# of Events	% of gated cells	Median	Geometric Mean	CV
1	JB66_FM_026.fcs compensated	Alexa Fluor 647-A	Lymphocytes	2334	100.00	580.67	n/a	59.59
2	JB66_All colors_027.fcs	Alexa Fluor 647-A	Lymphocytes	2034	100.00	5763.96	5245.33	38.56

NMT1 Lymphocytes MFI:
AllColors: 5763.96
FMi: 580.67
Custom Token: Lymphocytes= 9.93

Histogram #	Filename	Parameter	Overlay Gate	# of Events	% of gated cells	Median	Geometric Mean	CV
1	JB66_FM_026.fcs compensated	Alexa Fluor 647-A	Monocytes	77	100.00	2296.36	2065.71	48.49
2	JB66_All colors_027.fcs	Alexa Fluor 647-A	Monocytes	98	100.00	11528.43	11548.03	55.44

NMT1 Monocytes MFI:
AllColors: 11528.43
FMi: 2296.36
Custom Token: Monocytes =5.02

Figure 5.1.2 - Sample NMT1 FACS histograms for AML patient marrow aspirate

Sample histograms of cell count vs fluorescence of anti-NMT1-Alexa Fluor 647 antibody, plotted in red, or vs anti-IgGk-Alexa Fluor 647 isotype control, plotted in grey. Histograms were generated for gates including: Bulk blast (A), CD34+ (B), CD34+38- (C), lymphocyte (D), and monocyte (E). Gates were defined as per described in figure legend 5.1.1.

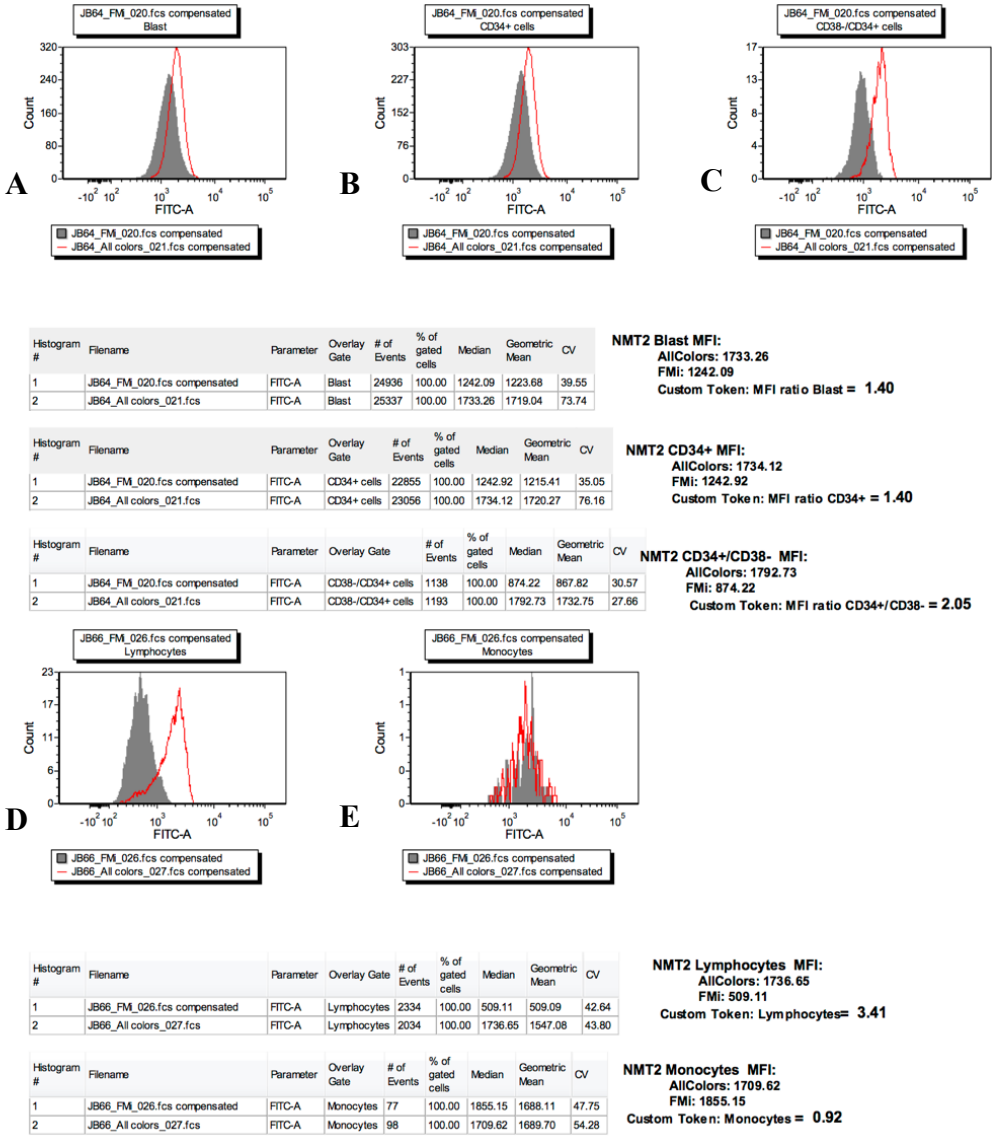

Figure 5.1.3 - Sample NMT2 FACS histograms for AML patient marrow aspirate

Sample histograms of cell count vs fluorescence of anti-NM2-FITC antibody, plotted in red, or vs anti-IgGk-FITC isotype control, plotted in grey. Histograms were generated for gates including: Bulk blast (A), CD34+ (B), CD34+38- (C), lymphocyte (D), and monocyte (E). Gates were defined as per described in figure legend 5.1.1.

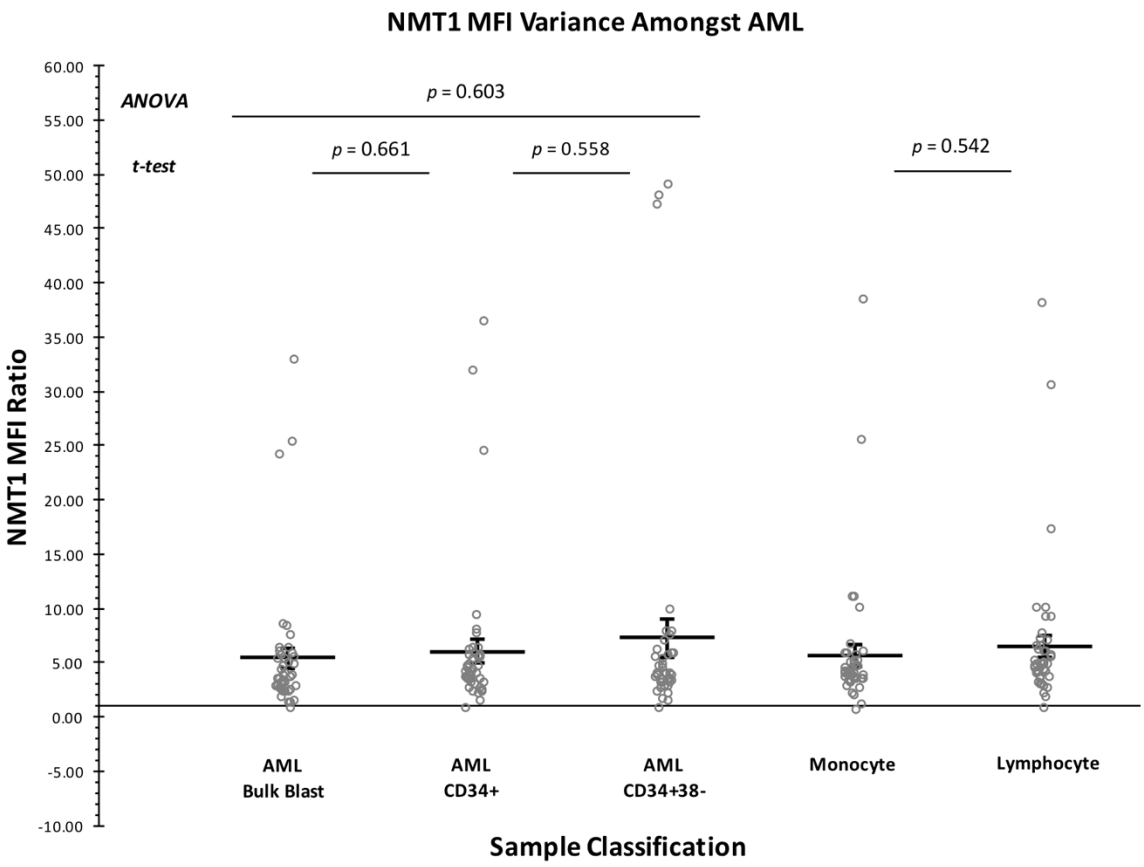

Figure 5.3.1 - NMT1 MFI variation amongst lymphocytes, monocytes, and AML bulk, CD34+, and CD34+38- blasts

NMT1 MFI is displayed for all patients with biobanked marrow aspirate (n = 44). NMT1 MFI did not vary amongst AML bulk blast populations (mean MFI = 5.39 ± 0.96) versus CD34+ blasts (mean MFI = 6.02 ± 1.07, p = 0.661), or CD34+ blasts versus CD34+38- blasts (mean MFI = 7.23 ±1.79, p = 0.558). NMT1 MFI also did not vary between the three groups. (p = 0.603) No variation was observed between mature monocytes (mean MFI = 5.66 ± 1.00) versus lymphocytes (mean MFI = 6.53 ± 1.02, p = 0.542).

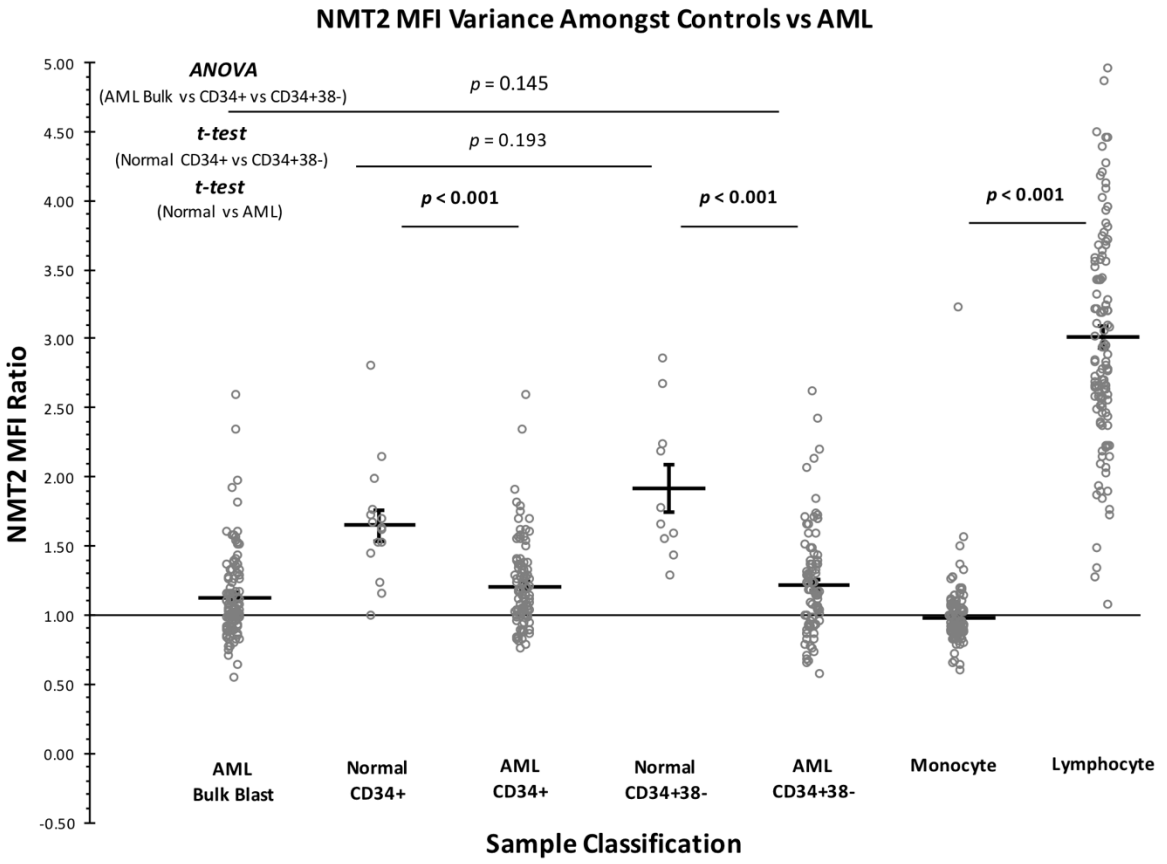

Figure 5.3.2 - NMT2 MFI variation amongst lymphocytes, monocytes, and AML bulk, CD34+, and CD34+38- blasts

NMT2 MFI is displayed for a cohort of normal patients who underwent marrow biopsy for non-AML indications (n = 16), in addition to patients with a new diagnosis of AML (n = 104). NMT2 MFI was significantly higher in normal samples versus their AML counterparts in the CD34+ population (mean MFI = 1.65 ± 0.11, $p < 0.001$) and the CD34+38- population (mean MFI = 1.91 ± 0.17, $p < 0.001$). NMT2 MFI was not significantly different between normal CD34+ and CD34+38- cells ($p = 0.193$). NMT2 MFI did not vary significantly between the AML bulk blasts (mean MFI = 1.13 ± 0.03), CD34+ blasts (mean MFI = 1.21 ± 0.03), and CD34+38- blasts (mean MFI 1.22 ± 0.04) ($p = 0.145$). NMT2 MFI was significantly lower in mature monocytes (mean MFI = 0.98 ± 0.03) versus mature lymphocytes (mean MFI = 3.01 ± 0.08, $p < 0.001$).

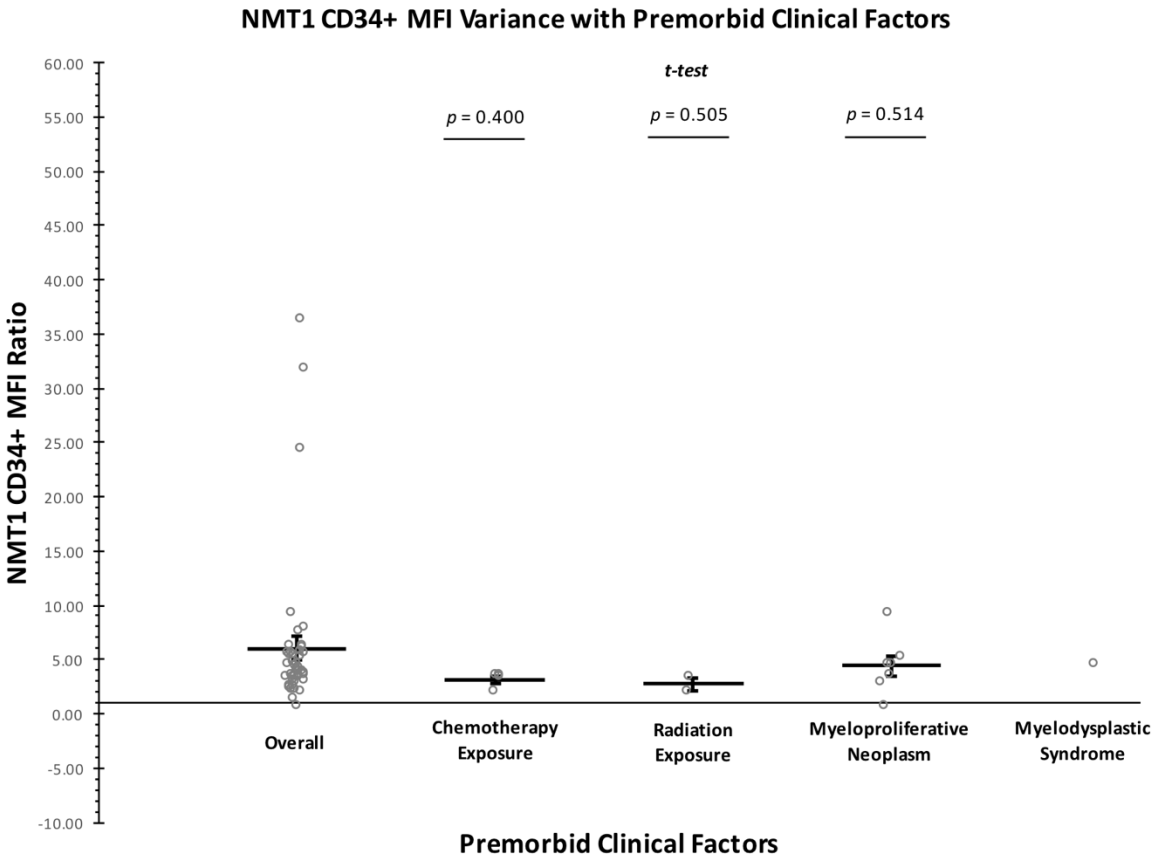

Figure 5.3.3 - NMT1 CD34+ blast MFI variation with premorbid patient clinical characteristics

NMT1 MFI is displayed for the overall population of patients with biobanked samples (median MFI = 6.02 ± 1.07, n = 44). NMT1 MFI was not statistically different for patients who had received antecedent chemotherapy (mean MFI = 3.13 ± 0.36, p = 0.400) or radiation therapy (mean MFI = 2.70 ± 0.63, p = 0.505) versus those who had not. NMT1 MFI was also not statistically different for patients with an antecedent MPN (mean MFI = 4.39 ± 0.988, p = 0.514). Only one patient who had NMT1 measured had an antecedent MDS (MFI = 4.55).

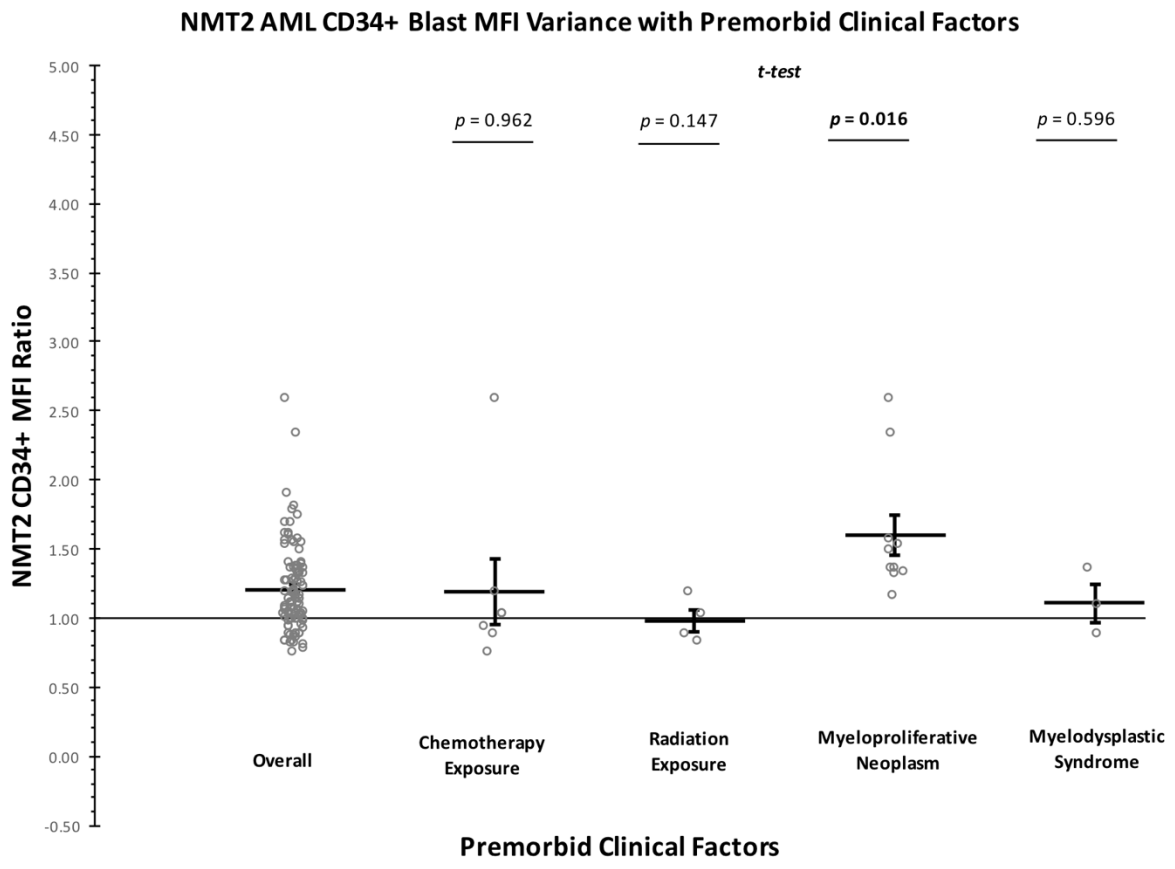

Figure 5.3.4 - NMT2 CD34+ blast MFI variation with premorbid patient clinical characteristics

NMT2 MFI is displayed for the overall population of patients with a new diagnosis of AML (mean MFI = 1.21 ± 0.03, n = 104). NMT2 MFI was not statistically different for patients who had received antecedent chemotherapy (mean MFI = 1.20 ± 0.24, p = 0.962) or radiation therapy (mean MFI = 0.98 ± 0.08, p = 0.147) versus those who had not. NMT2 MFI was statistically higher for patients with an antecedent MPN (mean MFI = 1.60 ± 0.15, p = 0.016). However, this was non-significant after application of the Bonferroni correction (p = (0.016 * 6) = 0.096). NMT2 MFI was not statistically different for patients with an antecedent MDS (mean MFI = 1.11 ± 0.14).

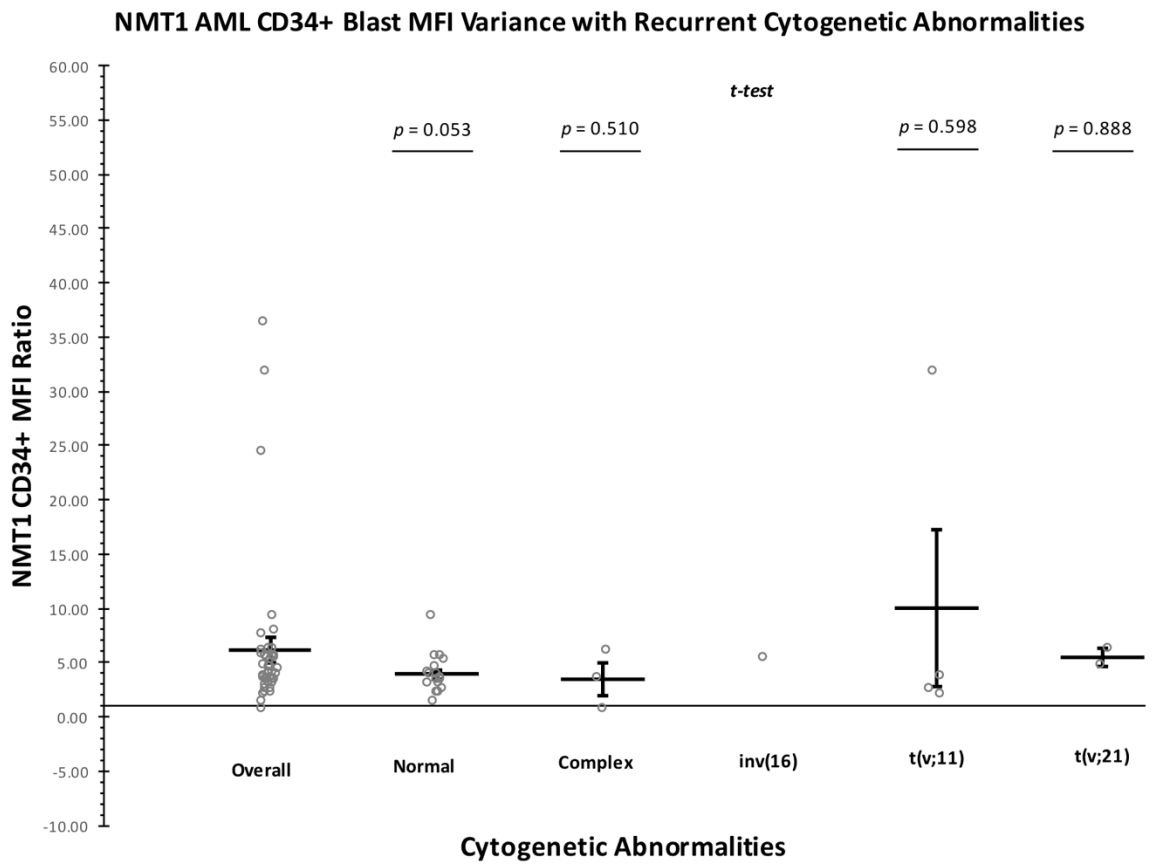

Figure 5.3.5 - NMT1 CD34+ blast MFI variation with recurrent cytogenetic abnormalities

NMT1 MFI is displayed for the overall population of biobanked patients who had a bone marrow biopsy at diagnosis (mean MFI = 6.15 ± 1.12, n = 43). NMT1 MFI was not significantly different for patients with normal (mean MFI = 3.91 ± 0.44, p = 0.053) or complex cytogenetics (mean MFI = 3.45 ± 1.52, p = 0.510). NMT1 MFI was not statistically different amongst patients with recurrent cytogenetic abnormalities t(v;11) (mean MFI = 10.04 ± 7.27, p = 0.598) or t(v;21) (mean MFI = 5.44 ± 0.81, p = 0.888). Only one patient had NMT1 MFI measured with inv(16) (MFI = 5.41).

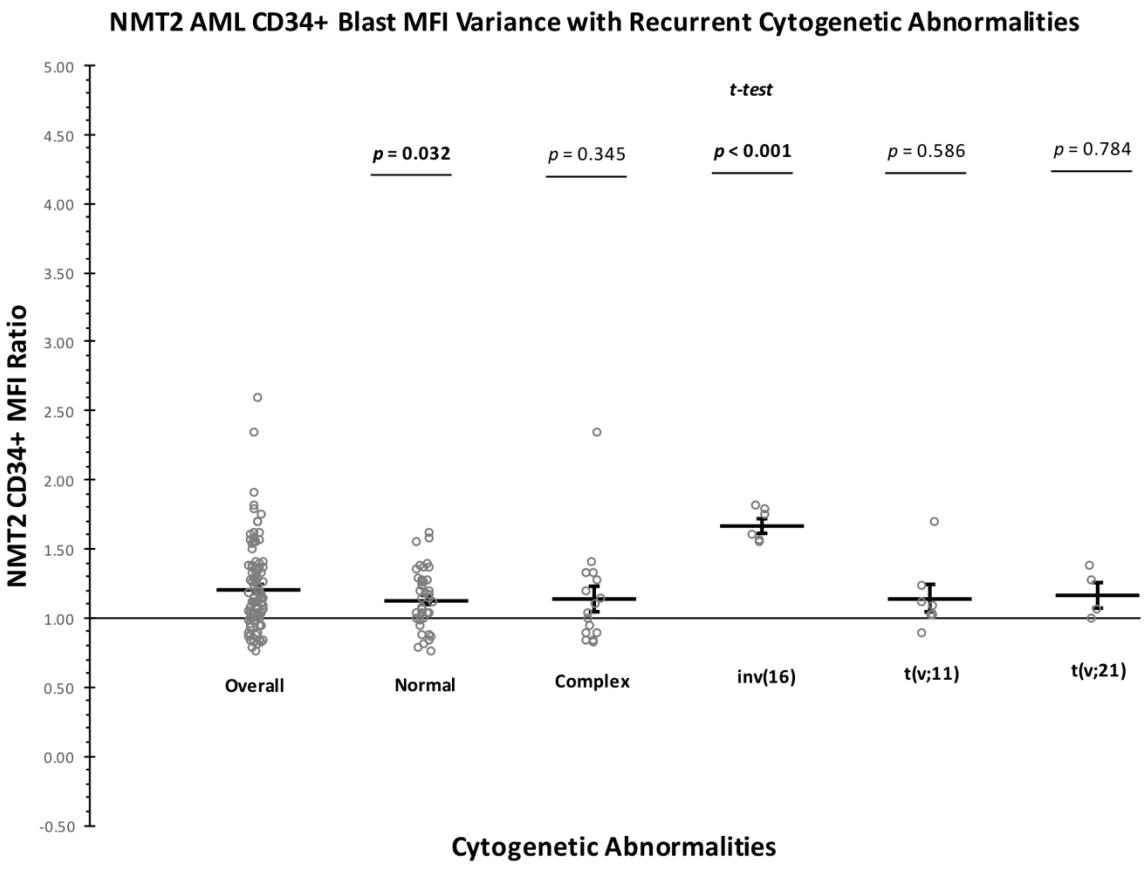

Figure 5.3.6 - NMT2 CD34+ blast MFI variation with recurrent cytogenetic abnormalities

NMT2 MFI is displayed for the overall population of patients who had a bone marrow biopsy at diagnosis (mean MFI = 1.21 ± 0.03, n = 102). NMT2 MFI was statistically lower for patients with normal cytogenetics (mean MFI = 1.13 ± 0.04, p = 0.032). However, this was non-significant after application of the Bonferroni correction (p = (0.032 * 6) = 0.192). NMT2 MFI was not statistically different in patients with complex cytogenetics (mean MFI = 1.14 ± 0.09, p = 0.093). NMT2 MFI was statistically higher in patients with the recurrent cytogenetic abnormality inv(16) (mean MFI = 1.67 ± 0.05, p < 0.001). This remained significant after application of the Bonferroni correction (p = (0.001 * 6) = 0.006). NMT2 MFI was not statistically different in patients with the recurrent cytogenetic abnormalities t(v;11) (mean MFI = 1.14 ± 0.10, p = 0.586) or t(v;21) (mean MFI = 1.17 ± 0.09, p = 0.784).

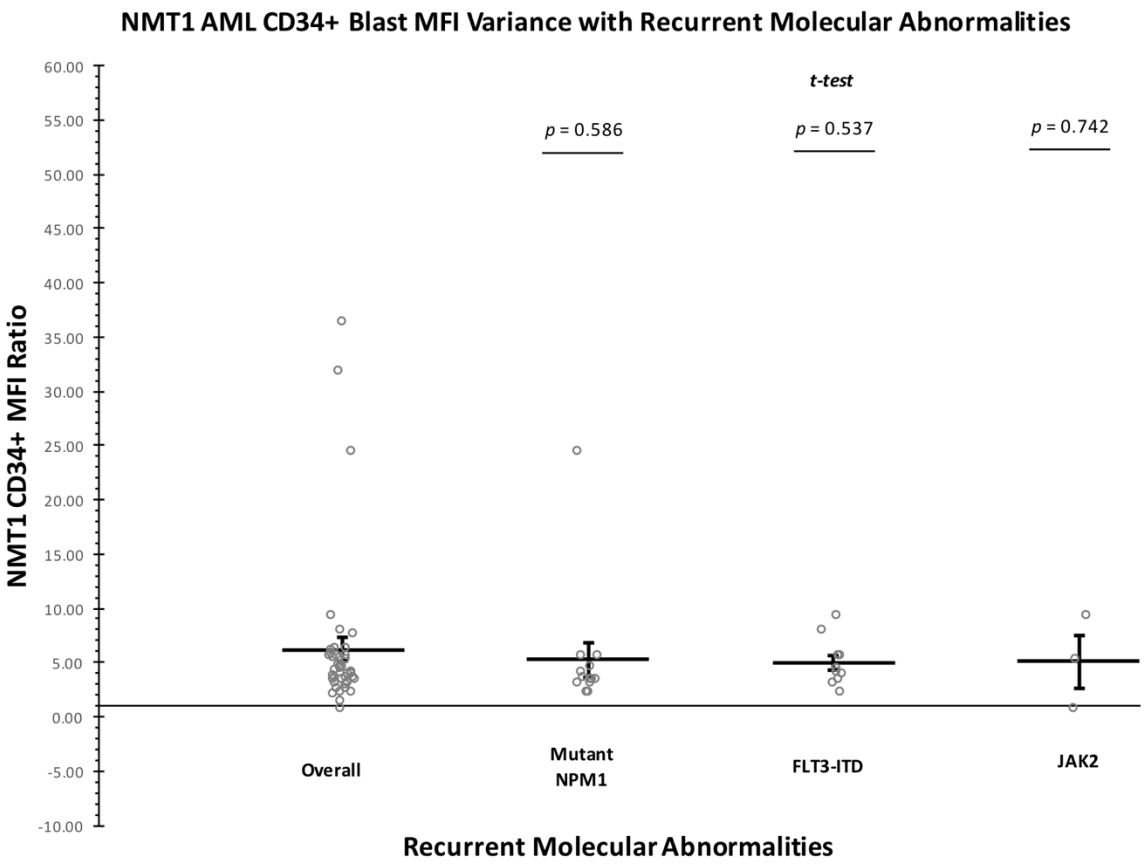

Figure 5.3.7 - NMT1 CD34+ blast MFI variation with recurrent molecular abnormalities

NMT1 MFI is displayed for the overall population of biobanked patients who had a bone marrow biopsy at diagnosis (mean MFI = 6.15 ± 1.12, n = 43). NMT1 MFI was not statistically different for patients with the recurrent molecular abnormalities NPM1 (mean MFI = 5.24 ± 1.63, p = 0.586), FLT3-ITD (mean MFI = 4.91 ± 0.71, p = 0.537), or JAK2 (mean MFI = 5.09 ± 2.46, p = 0.742).

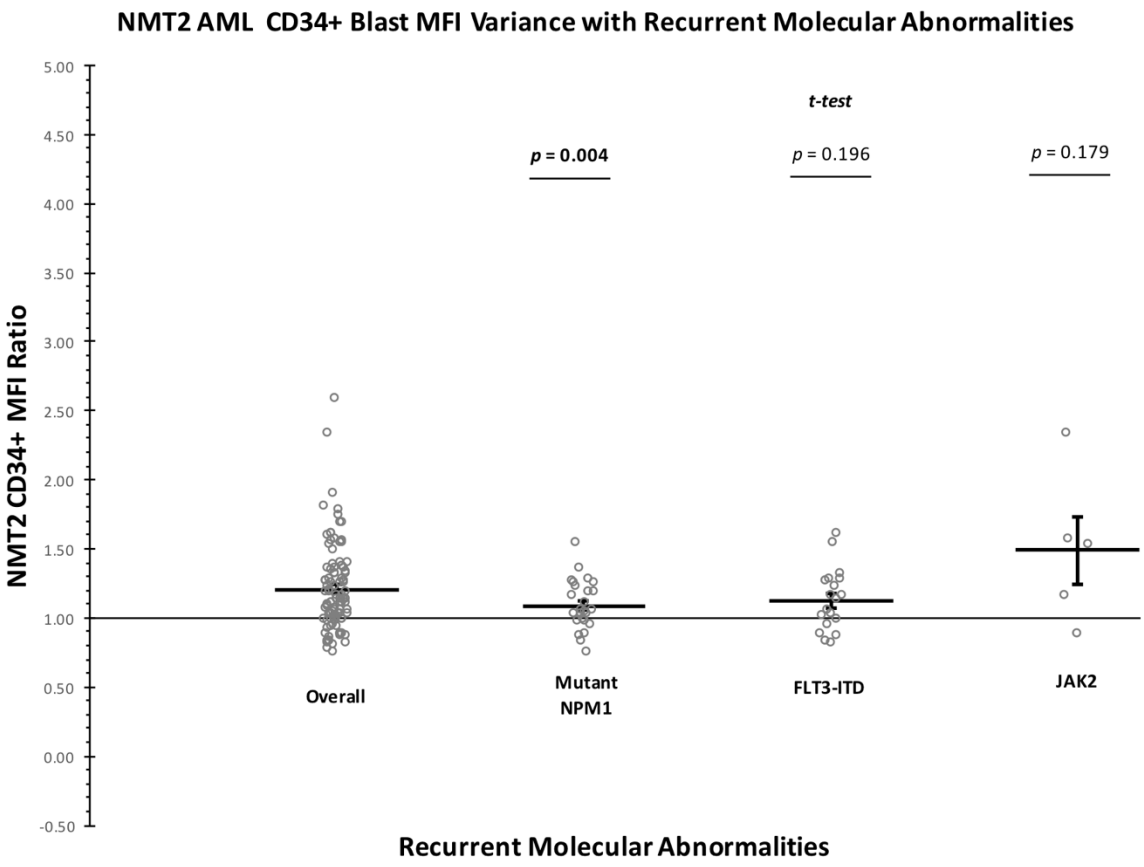

Figure 5.3.8 - NMT2 CD34+ blast MFI variation with recurrent molecular abnormalities

NMT2 MFI is displayed for the overall population of patients who had a bone marrow biopsy at diagnosis (mean MFI = 1.21 ± 0.03, n = 102). NMT2 MFI was statistically lower in patients with the recurrent molecular abnormality NPM1 (mean MFI = 1.09 ± 0.04, p = 0.004). This remained significant after application of the Bonferroni correction (p = (0.004 * 6) = 0.024). NMT2 MFI was not statistically different for patients with the recurrent molecular abnormalities FLT3-ITD (mean MFI = 1.13 ± 0.05, p = 0.196) or JAK2 (mean MFI = 1.49 ± 0.25, p = 0.179).

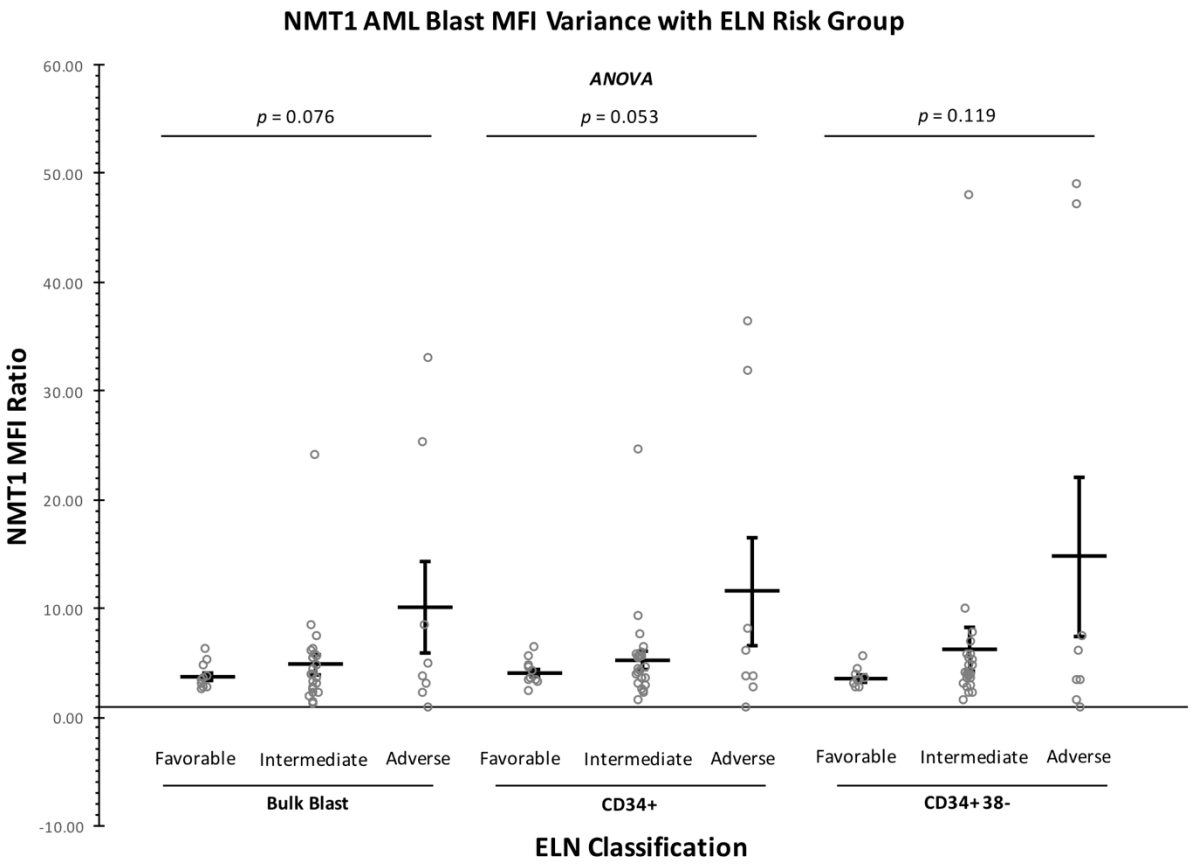

Figure 5.4.1 - NMT1 MFI variation with ELN risk group for bulk, CD34+, and CD34+38- blasts

NMT1 MFI is displayed for all biobanked patients who had a bone marrow biopsy at diagnosis (n = 43). NMT1 MFI for bulk blast populations was not statistically different between favorable-risk (mean MFI = 3.70 ± 0.39), intermediate-risk (mean MFI = 4.82 ± 0.92), and unfavorable-risk (mean MFI = 10.09 ± 4.26) (p = 0.076). NMT1 MFI for CD34+ blast populations were also not statistically different between favorable-risk (mean MFI = 4.03 ± 0.38), intermediate-risk (mean MFI = 5.23 ± 0.91), and unfavorable-risk (mean MFI = 11.58 ± 4.98) (p = 0.053). NMT1 MFI for CD34+38- blast populations were also not statistically different between favorable-risk (mean MFI = 3.54 ± 0.31), intermediate-risk (mean MFI = 6.23 ± 1.94), and unfavorable-risk (mean MFI = 14.74 ± 7.29) (p = 0.119).

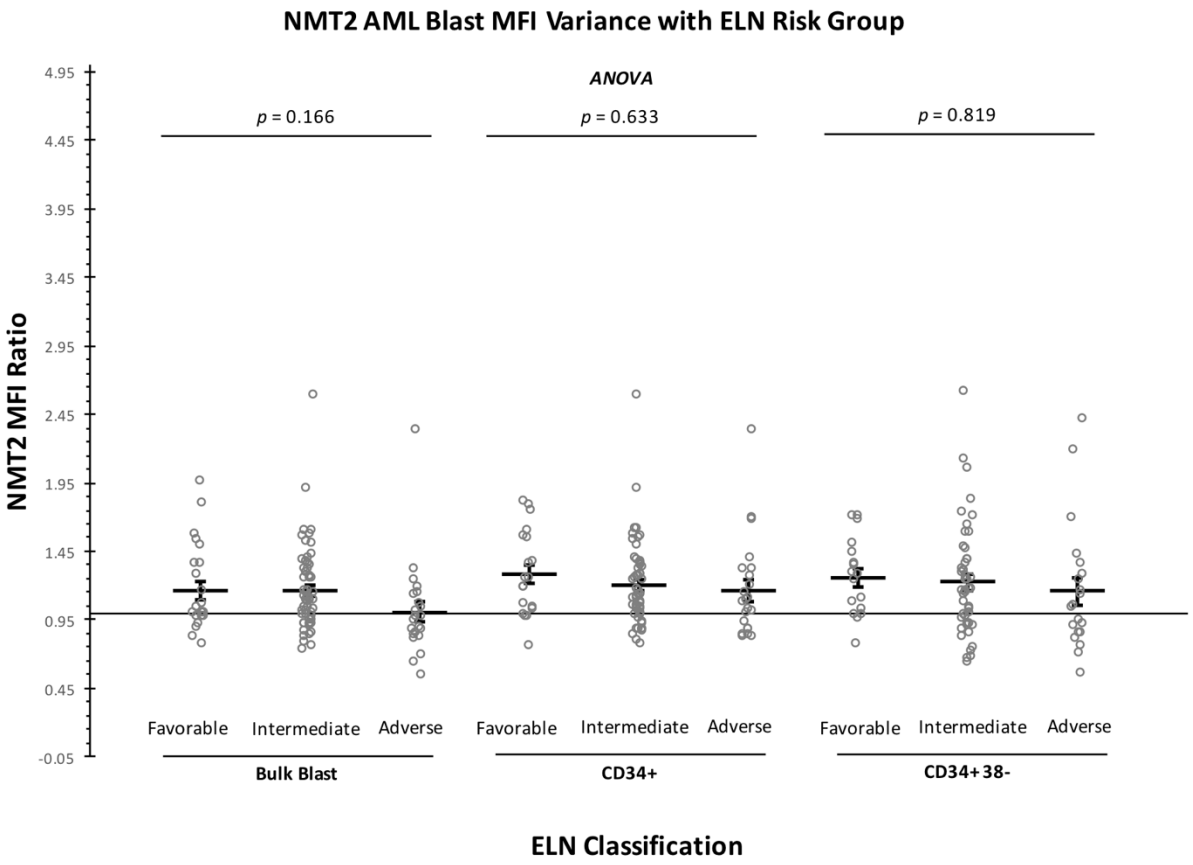

Figure 5.4.2 - NMT2 MFI variation with ELN risk group for bulk, CD34+, and CD34+38- blasts

NMT2 MFI is displayed for all patients who had a bone marrow biopsy at diagnosis (n = 102). NMT2 MFI for bulk blast populations was not statistically different between favorable-risk (mean MFI = 1.17 ± 0.07), intermediate-risk (mean MFI = 1.17 ± 0.04), and unfavorable-risk (mean MFI = 1.01 ± 0.08) (p = 0.166). NMT2 MFI for CD34+ blast populations were also not statistically different between favorable-risk (mean MFI = 1.28 ± 0.07), intermediate-risk (mean MFI = 1.20 ± 0.04), and unfavorable-risk (mean MFI = 1.16 ± 0.08) (p = 0.633). NMT2 MFI for CD34+38- blast populations were also not statistically different between favorable-risk (mean MFI = 1.26 ± 0.07), intermediate-risk (mean MFI = 1.23 ± 0.06), and unfavorable-risk (mean MFI = 1.16 ± 0.10) (p = 0.819).

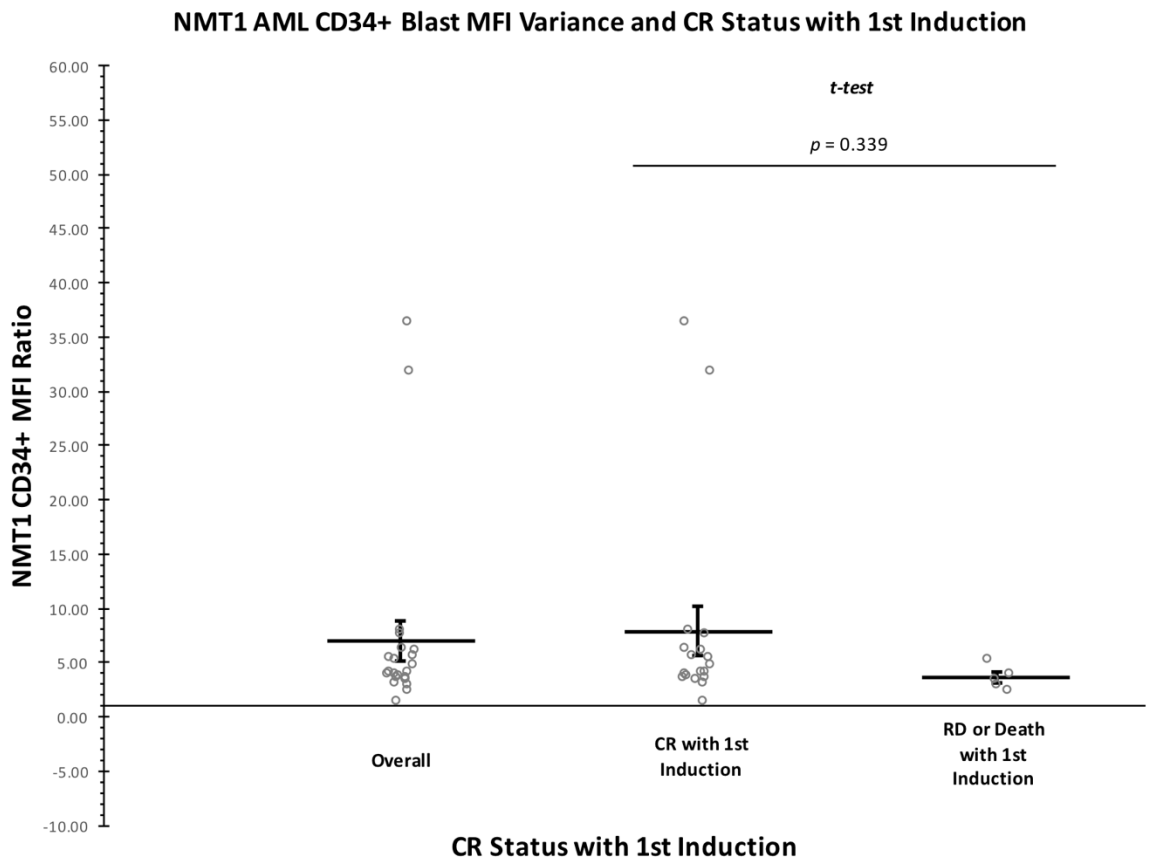

Figure 5.5.1 - NMT1 CD34+ blast MFI variation by achievement of CR1 with 1st induction chemotherapy

NMT1 MFI is displayed for all biobanked patients who underwent induction chemotherapy (mean MFI = 6.93 ± 1.82, n = 23). NMT1 MFI was not statistically different between patients who achieved CR or iCR with first induction chemotherapy (mean MFI = 7.87 ± 2.28) versus patients who had RD or death (mean MFI = 3.56 ± 0.50) (p = 0.339).

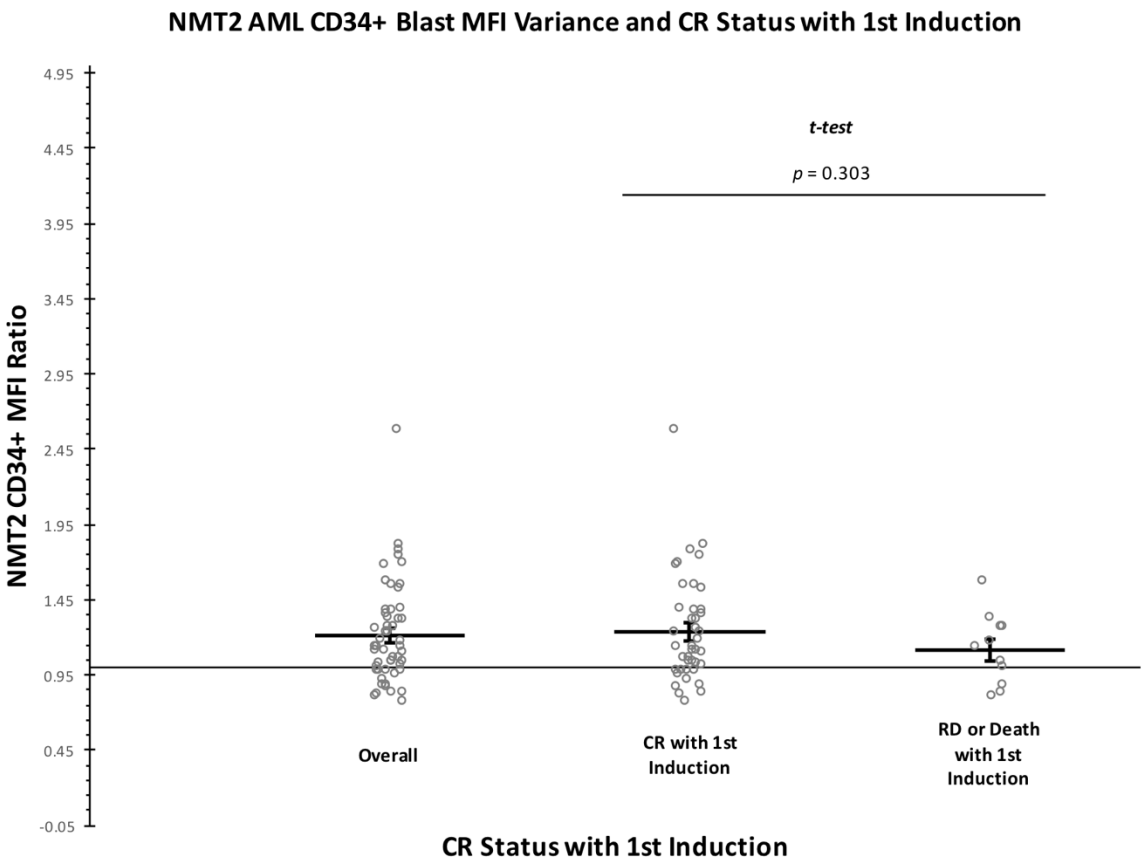

Figure 5.5.2 - NMT2 CD34+ blast MFI variation by achievement of CR1 with 1st induction chemotherapy

NMT2 MFI is displayed for all patients who underwent induction chemotherapy (mean MFI = 1.21 ± 0.05, n = 58). NMT2 MFI was not statistically different between patients who achieved CR or iCR with first induction chemotherapy (mean MFI = 1.23 ± 0.06) versus patients who had RD or death (mean MFI = 1.12 ± 0.07) (p = 0.303).

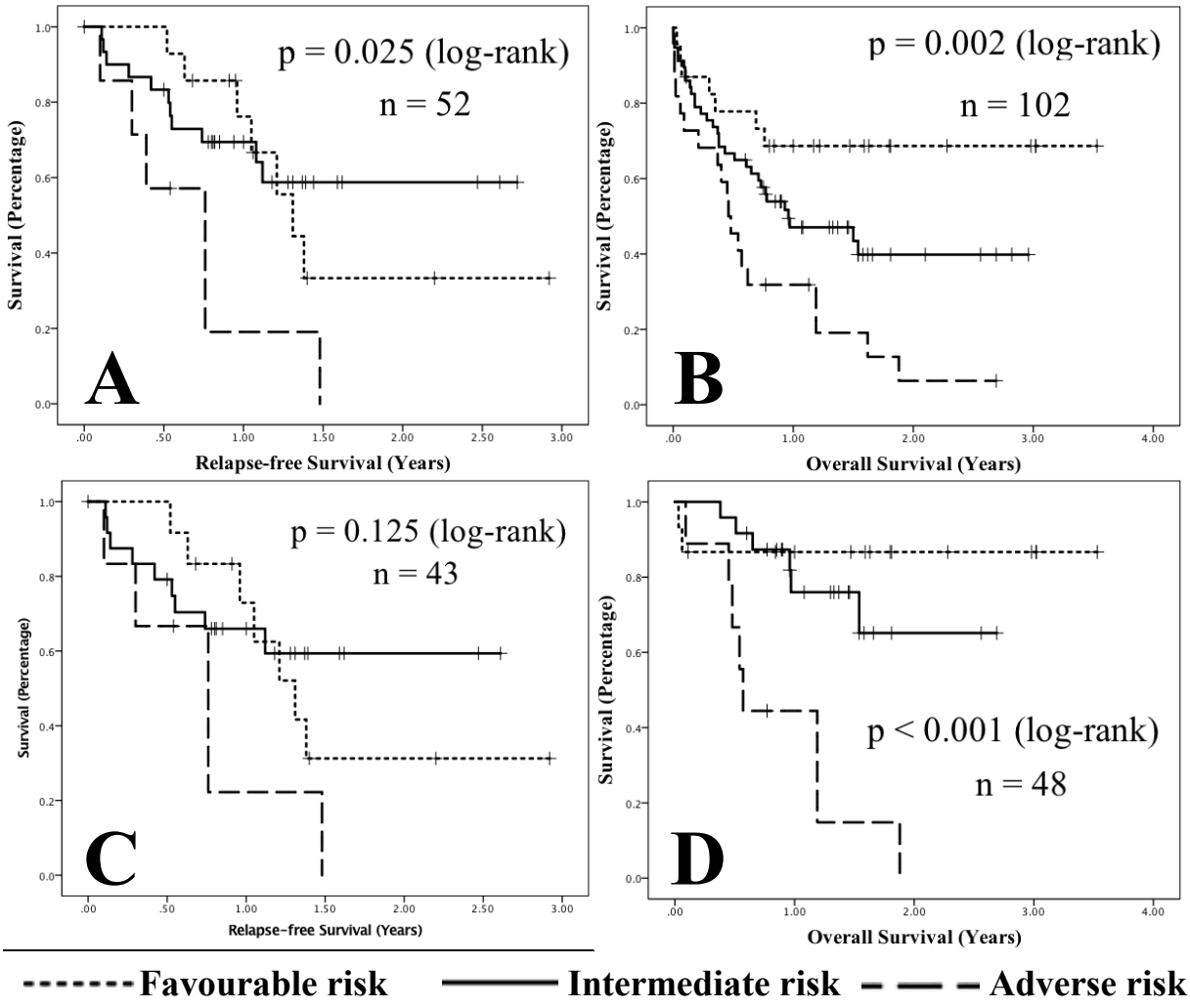

Figure 5.6.1 - Survival by Kaplan-Meier analysis with respect to ELN risk group

Kaplan-Meier survival curves are displayed for relapse-free survival (A) ($p = 0.025$, $n = 52$) and overall survival (B) ($p = 0.002$, $n = 102$) with stratification by ELN risk group for the applicable overall population that underwent a bone marrow biopsy. Survival curves are also displayed for the patients of age < 65 with respect to relapse-free survival (C) ($p = 0.025$, $n = 43$) and overall survival (D) ($p < 0.001$, $n = 48$).

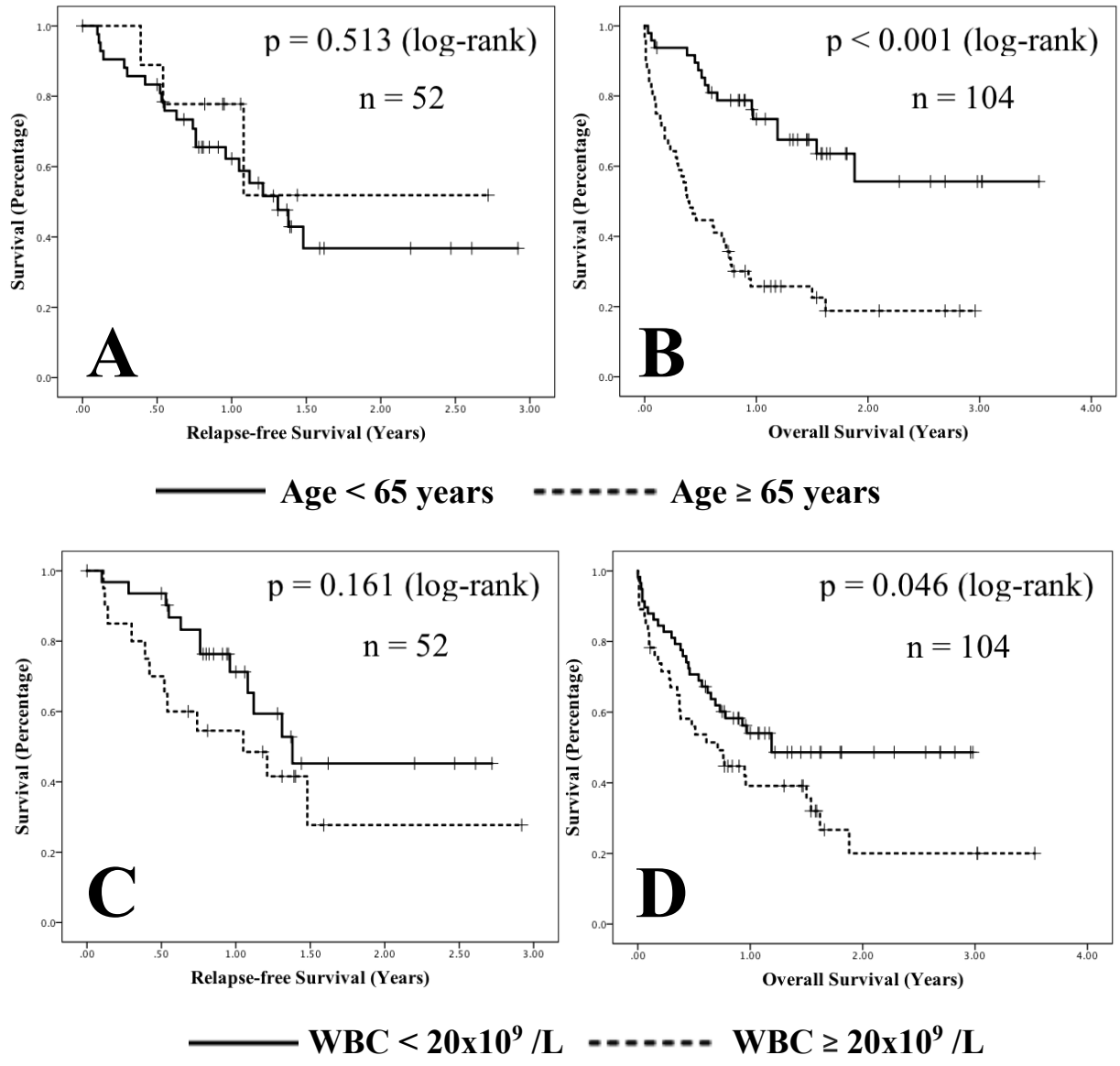

Figure 5.6.2 - Survival by Kaplan-Meier analysis with respect to age and WBC at diagnosis
Kaplan-Meier survival curves are displayed for relapse-free survival (A) ($p = 0.513$, $n = 52$) and overall survival (B) ($p < 0.001$, $n = 104$) with stratification by age greater than 65 at diagnosis. Survival curves are also displayed for relapse-free survival (C) ($p = 0.161$, $n = 52$) and overall survival (D) ($p = 0.046$, $n = 104$) with stratification by peripheral white blood cell count (WBC) greater than 20 x 10^9 /L at diagnosis.

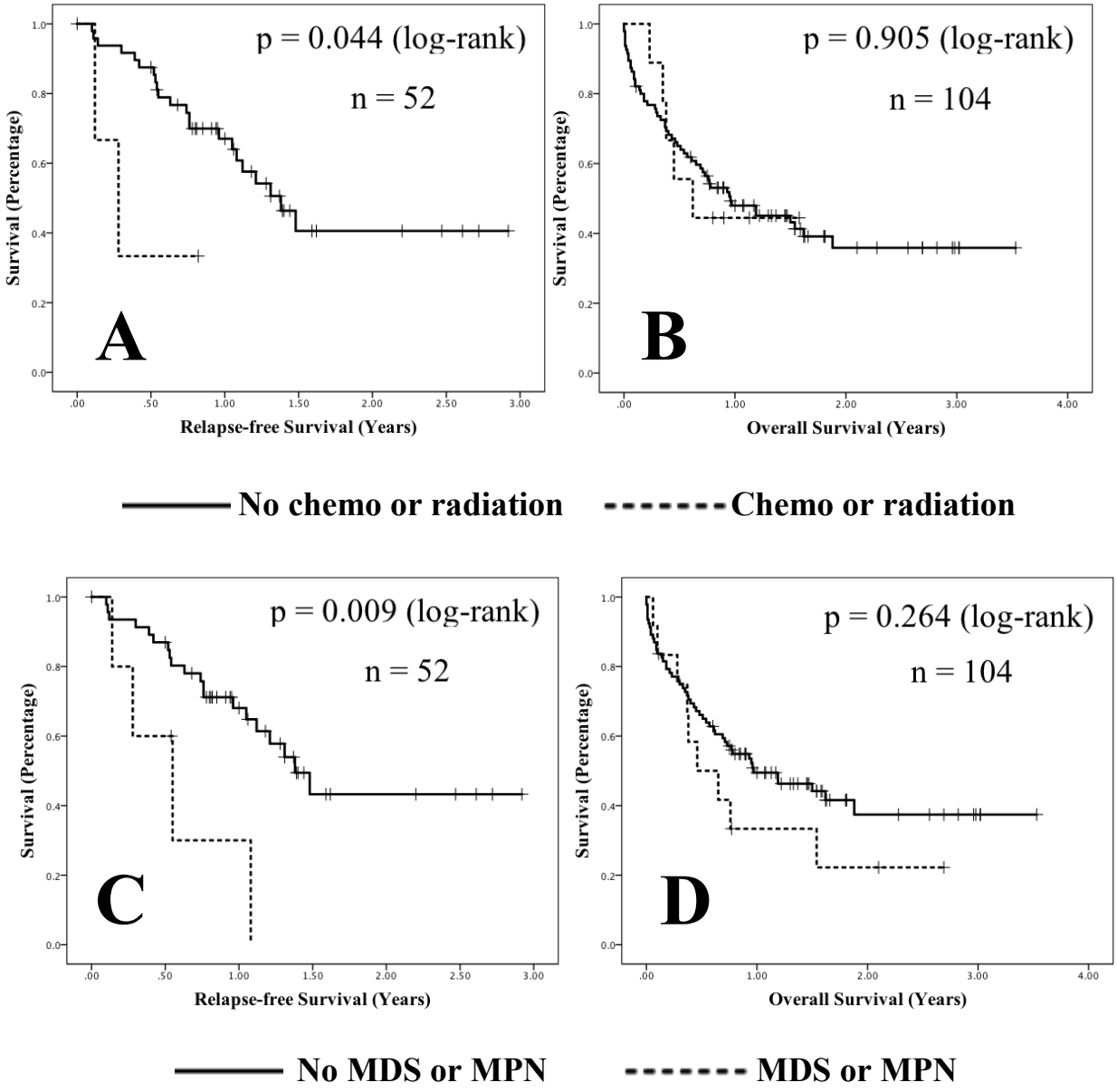

Figure 5.6.3 - Survival by Kaplan-Meier analysis with respect to antecedent MDS, MPN, chemotherapy, or radiation exposure

Kaplan-Meier survival curves displayed for relapse-free survival (A) (p = 0.044, n = 52) and overall survival (B) (p = 0.905, n = 104) with stratification by antecedent exposure to chemotherapy or radiation therapy prior to AML diagnosis. Kaplan-Meier survival curves are also displayed for relapse-free survival (C) (p = 0.009, n = 52) and overall survival (D) (p = 0.264, n = 104) with stratification by an antecedent diagnosis of MDS or MPN.

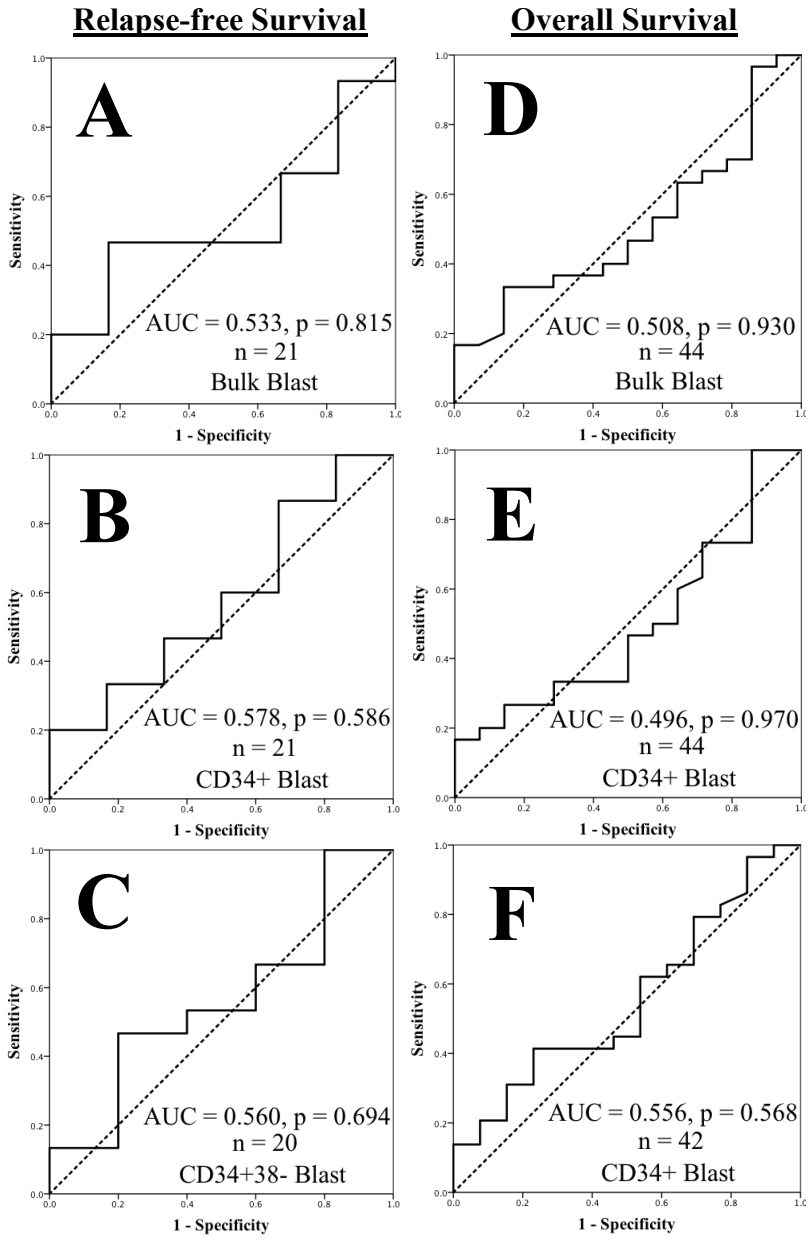

Figure 5.6.4 - Receiver operator curve of NMT1 for RFS and OS in bulk, CD34+, and CD34+38- blasts

Receiver operator curves are displayed for relapse free survival with respect to the bulk blast population (A) (AUC =0.533, p = 0.815, n = 21), CD34+ blast population (B) (AUC = 0.578, p = 0.586, n = 21), CD34+38- blast population (C) (AUC = 560, p = 0.694, n = 20). Receiver operator curves are also displayed for overall survival with respect to the bulk blast population (D) (AUC = 0.508, p = 0.930, n = 44), CD34+ blasts (E) (AUC = 0.496, p = 0.970, n = 44), and CD34+38- blasts (F) (AUC = 0.556, p = 0.568, n = 42).

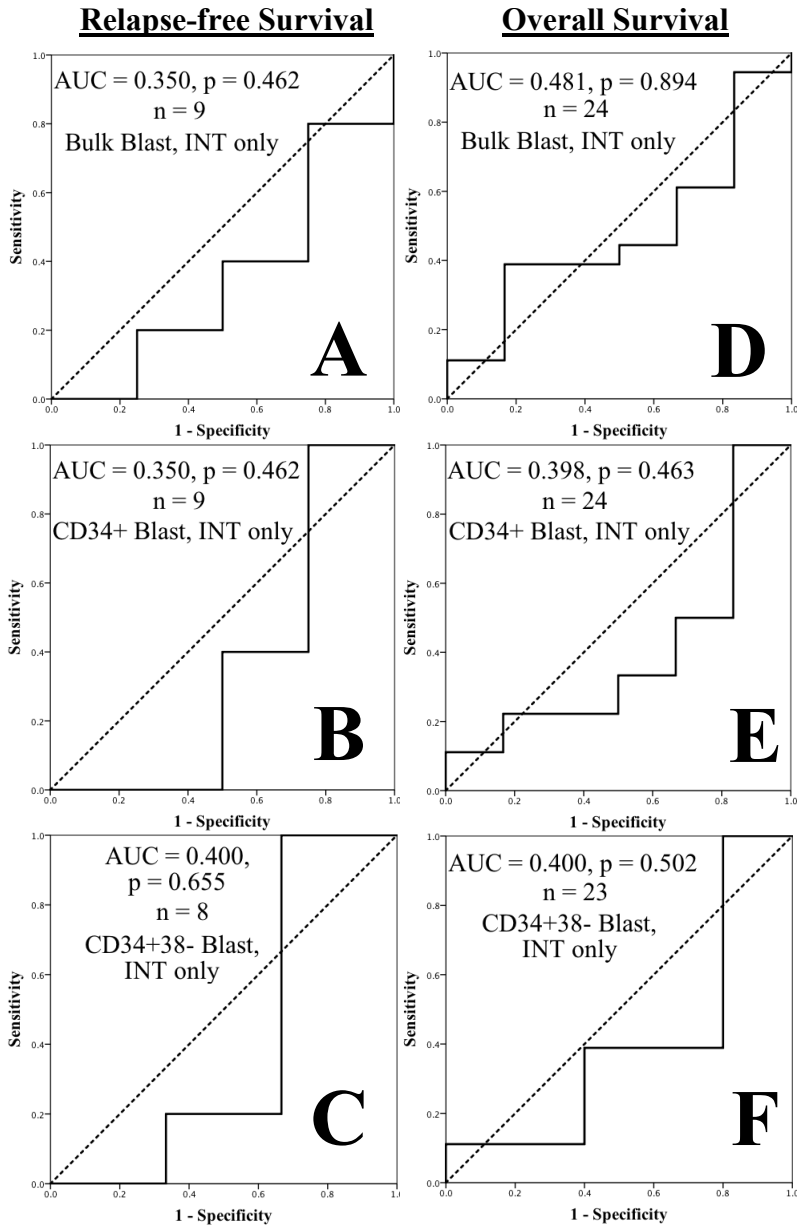

Figure 5.6.5 - Receiver operator curve of NMT1 for RFS and OS, intermediate-risk only in bulk, CD34+, and CD34+38- blasts

Receiver operator curves are displayed for relapse free survival in intermediate risk patients only with respect to the bulk blast population (A) (AUC = 0.350, p = 0.462, n = 9), CD34+ blast population (B) (AUC = 0.350, p = 0.462, n = 9), CD34+38- blast population (C) (AUC = 0.400, p = 0.655, n = 8). Receiver operator curves are also displayed for overall survival in intermediate risk patients only with respect the bulk blast population (D) (AUC = 0.481, p = 0.894, n = 24), CD34+ blasts (E) (AUC = 0.398, p = 0.463, n = 24), and CD34+38- blasts (F) (AUC = 0.400, p = 0.502, n = 23).

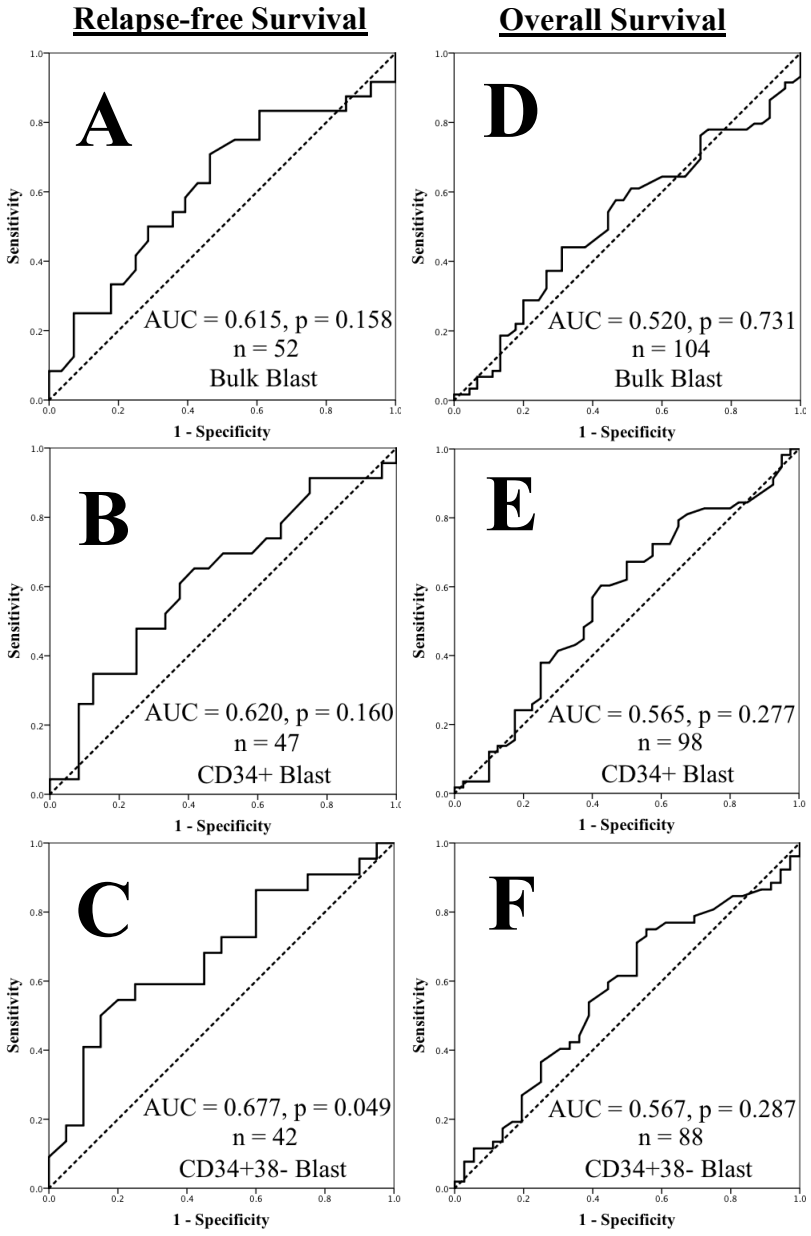

Figure 5.6.6 - Receiver operator curve of NMT2 for RFS and OS in bulk, CD34+, and CD34+38- blasts

Receiver operator curves are displayed for relapse free survival with respect to the bulk blast population (A) (AUC = 0.615, p = 0.158, n = 52), CD34+ blast population (B) (AUC = 0.620, p = 0.160, n = 47), CD34+38- blast population (C) (AUC = 0.677, p = 0.049, n = 42). Receiver operator curves are also displayed for overall survival with respect to the bulk blast population (D) (AUC = 0.520, p = 0.731, n = 104), CD34+ blasts (E) (AUC = 0.565, p = 0.277, n = 98), and CD34+38- blasts (F) (AUC = 0.567, p = 0.287, n = 88).

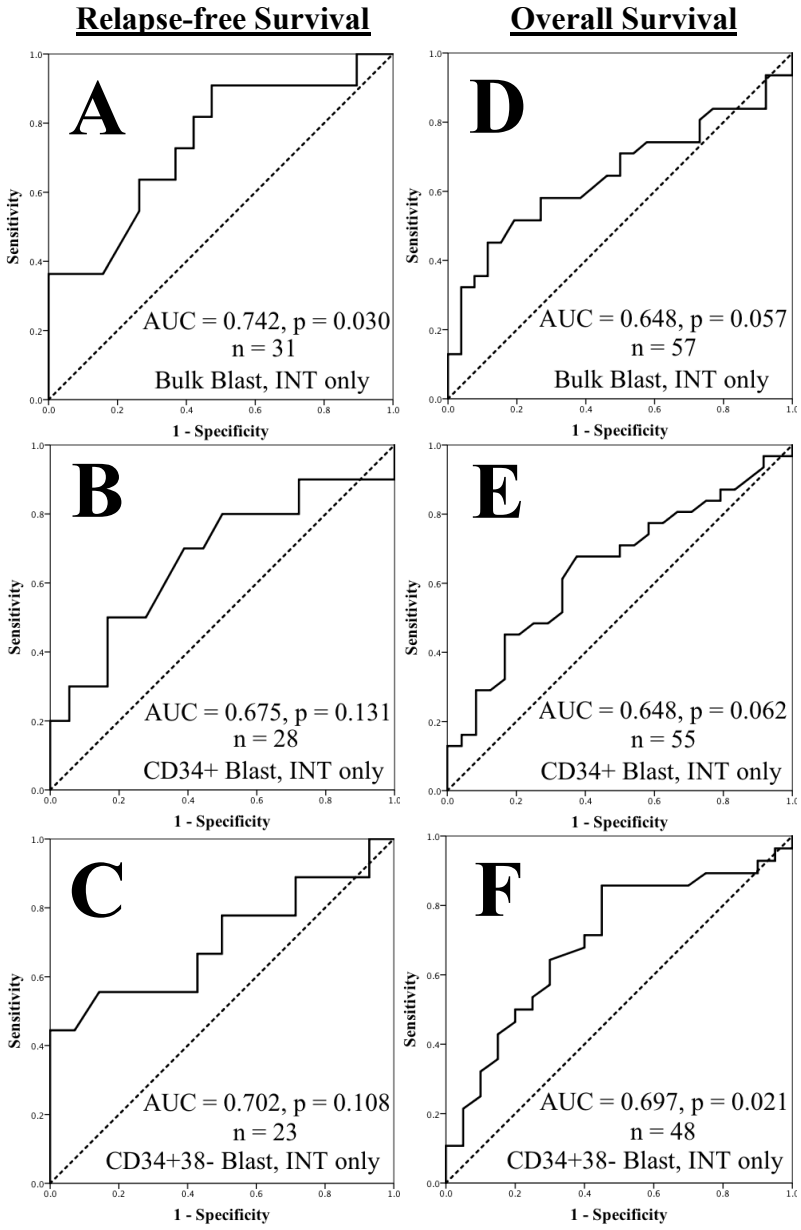

Figure 5.6.7 - Receiver operator curve of NMT2 for RFS and OS, intermediate-risk only in bulk, CD34+, and CD34+38- blasts

Receiver operator curves are displayed for relapse free survival in intermediate risk patients only with respect to the bulk blast population (A) (AUC = 0.742, p = 0.030, n = 31), CD34+ blast population (B) (AUC = 0.675, p = 0.131, n = 28), CD34+38- blast population (C) (AUC = 0.702, p = 0.108, n = 23). Receiver operator curves are also displayed for overall survival in intermediate risk patients only with respect the bulk blast population (D) (AUC = 0.648, p = 0.057, n = 57), CD34+ blasts (E) (AUC = 0.648, p = 0.062, n = 55), and CD34+38- blasts (F) (AUC = 0.697, p = 0.021, n = 48).

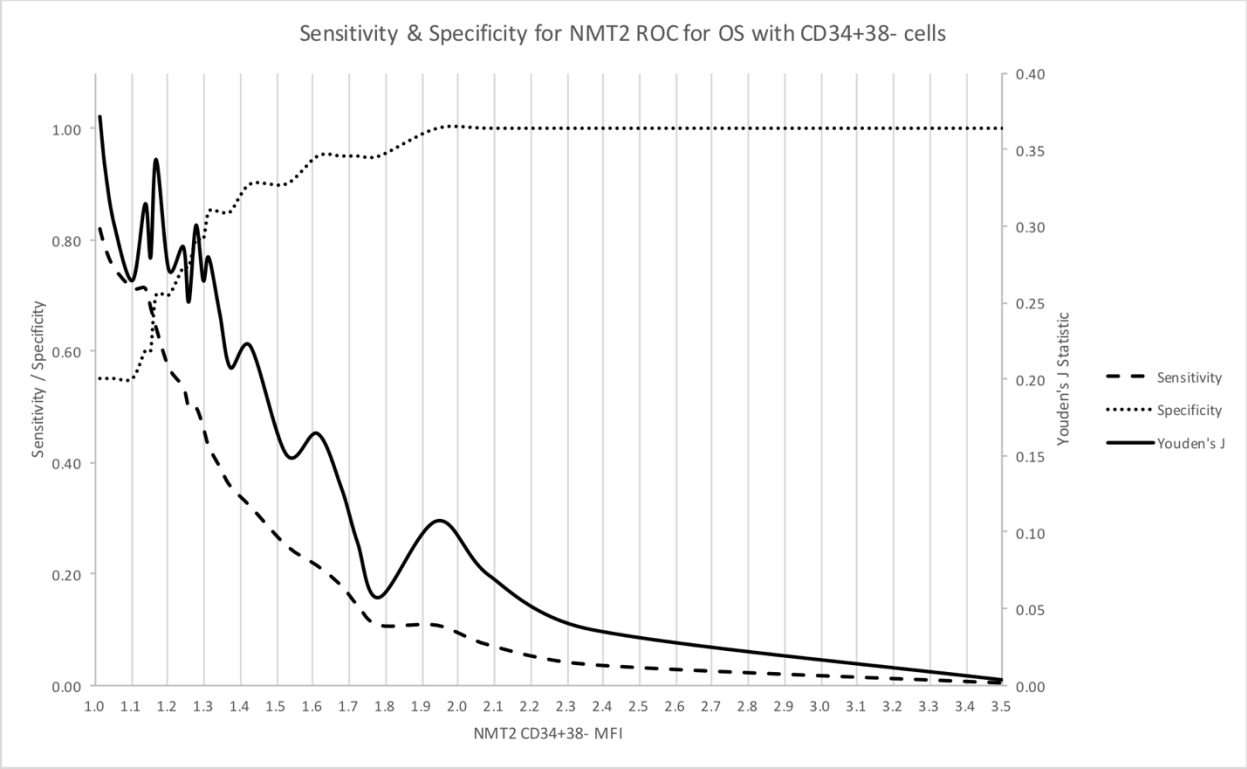

Figure 5.6.9 - Sensitivity versus specificity graph for the optimized NMT2 receiver operator curve - NMT2 MFI in CD34+38- blasts, intermediate-risk only, with respect to OS

Sensitivity versus specificity is displayed for different cut-off values, displayed on the x-axis, of NMT2 CD34+38- MFI with respect to overall survival. Sensitivity and specificity are plotted relative to the first y-axis in orange and blue, respectively. Youden's J statistic, calculated as [1 - (sensitivity + specificity)] is also displayed as a measure of the overall performance of the test at different cut-off values, represented by the red line relative to the second y-axis. Two optimization peaks are demonstrated at a NMT2 MFI of 1.17, which optimizes sensitivity at the expense of specificity, and 1.28, which optimizes specificity at the expense of sensitivity.

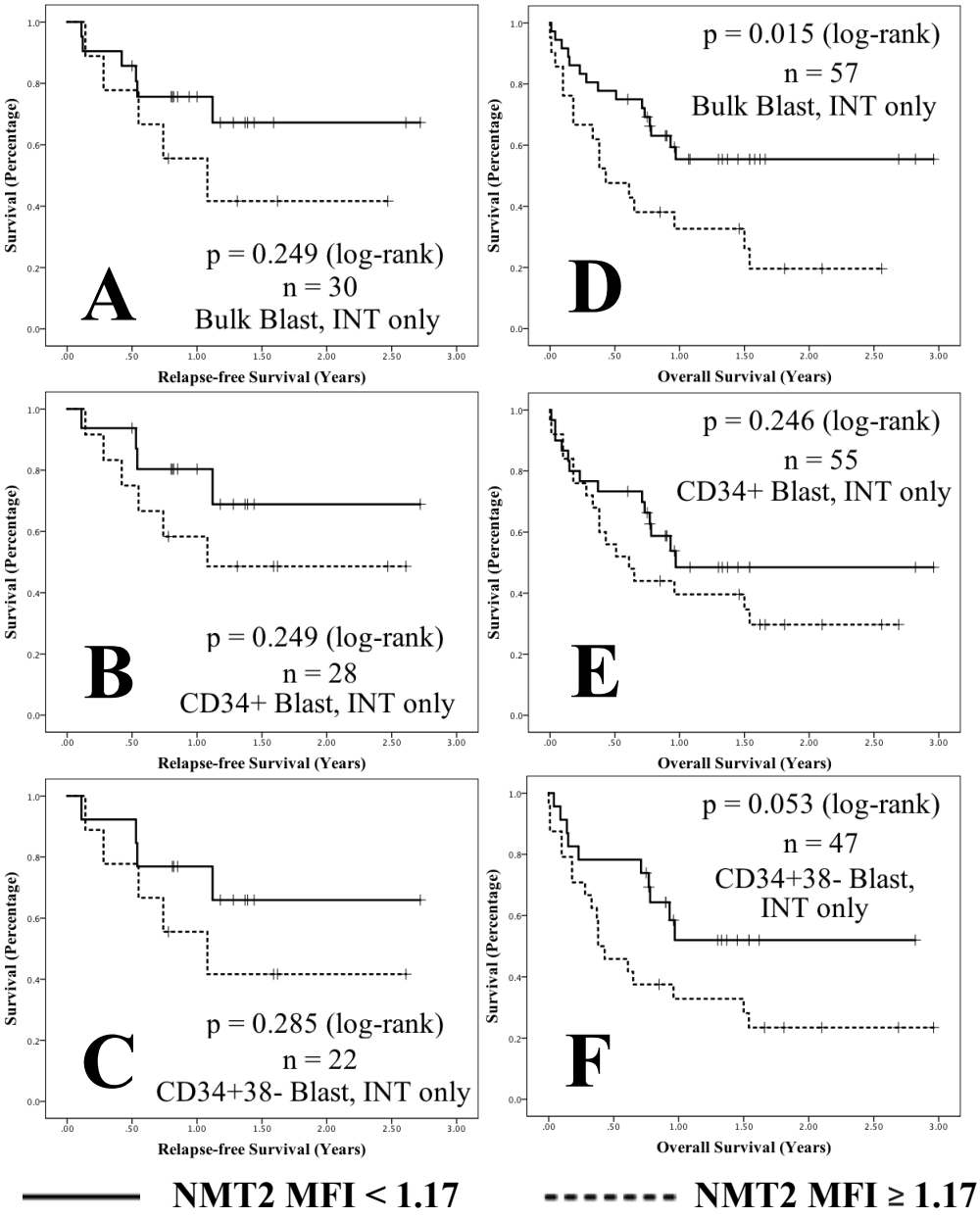

Figure 5.6.10 - Survival by Kaplan-Meier, intermediate-risk, NMT2 MFI > 1.17, in bulk, CD34+, and CD34+38- blasts

Kaplan-Meier survival curves are displayed for relapse-free survival for bulk blast (A) (p = 0.249, n = 30), CD34+ blast (B) (p = 0.249, n = 28), and CD34+38- blast populations (C) (p = 0.285, n = 22). Kaplan-Meier survival curves are also displayed for overall survival for bulk blast (D) (p = 0.015, n = 57), CD34+ (E) (p = 0.246, n = 55), and CD34+38- blast populations (F) (p = 0.053, n = 47). A higher sensitivity, lower specificity NMT2 MFI cut-off of 1.17 was used to dichotomize this population.

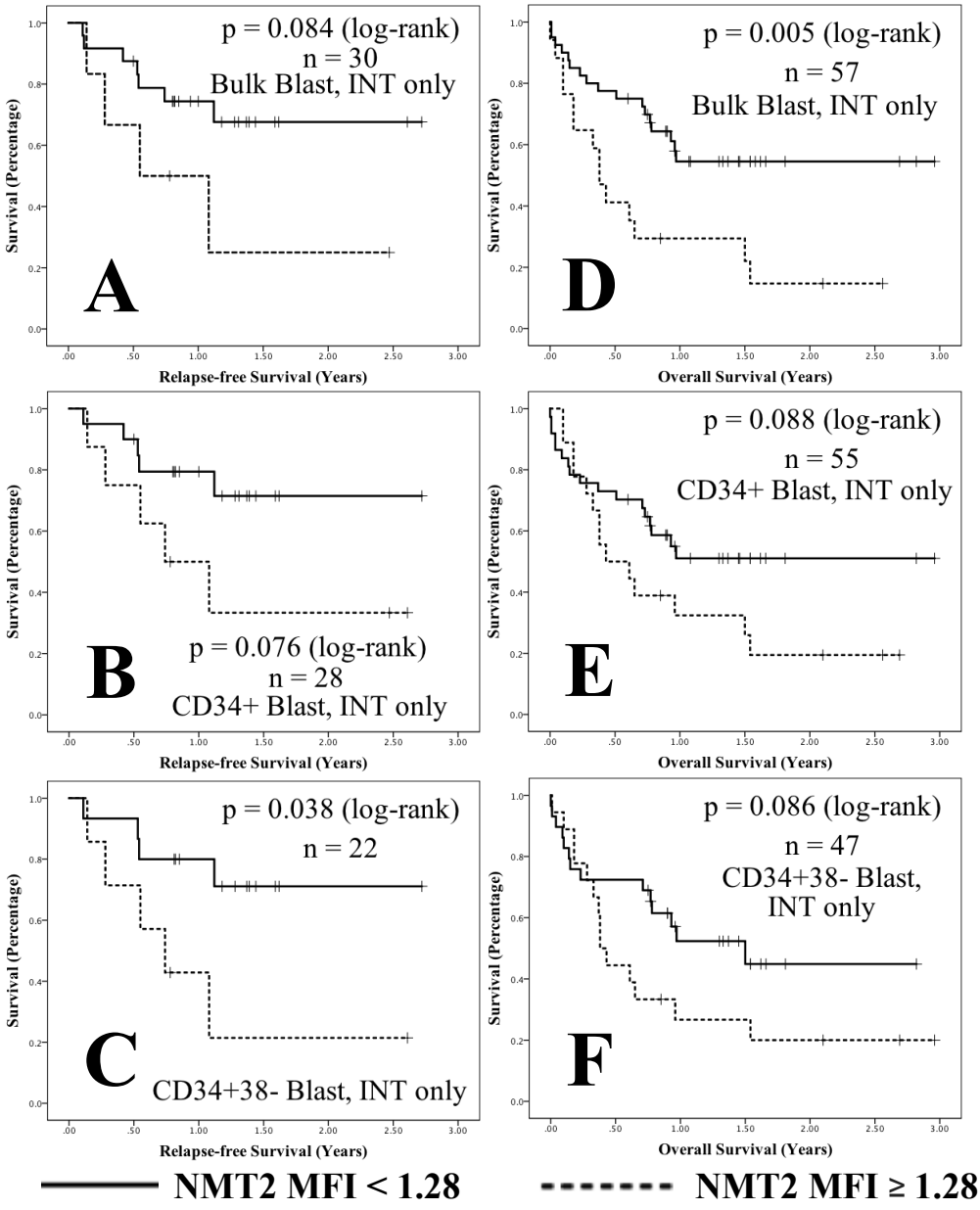

Figure 5.6.11 - Survival by Kaplan-Meier, intermediate-risk, NMT2 MFI > 1.28, in bulk, CD34+, and CD34+38- blasts

Kaplan-Meier survival curves are displayed for relapse-free survival for bulk blast (A) (p = 0.084, n = 30), CD34+ blast (B) (p = 0.076, n = 28), and CD34+38- blast populations (C) (p = 0.038, n = 22). Kaplan-Meier survival curves are also displayed for overall survival for bulk blast (D) (p = 0.005, n = 57), CD34+ (E) (p = 0.088, n = 55), and CD34+38- blast populations (F) (p = 0.086, n = 47). A lower sensitivity, higher specificity NMT2 MFI cut-off of 1.28 was used to dichotomize this population.

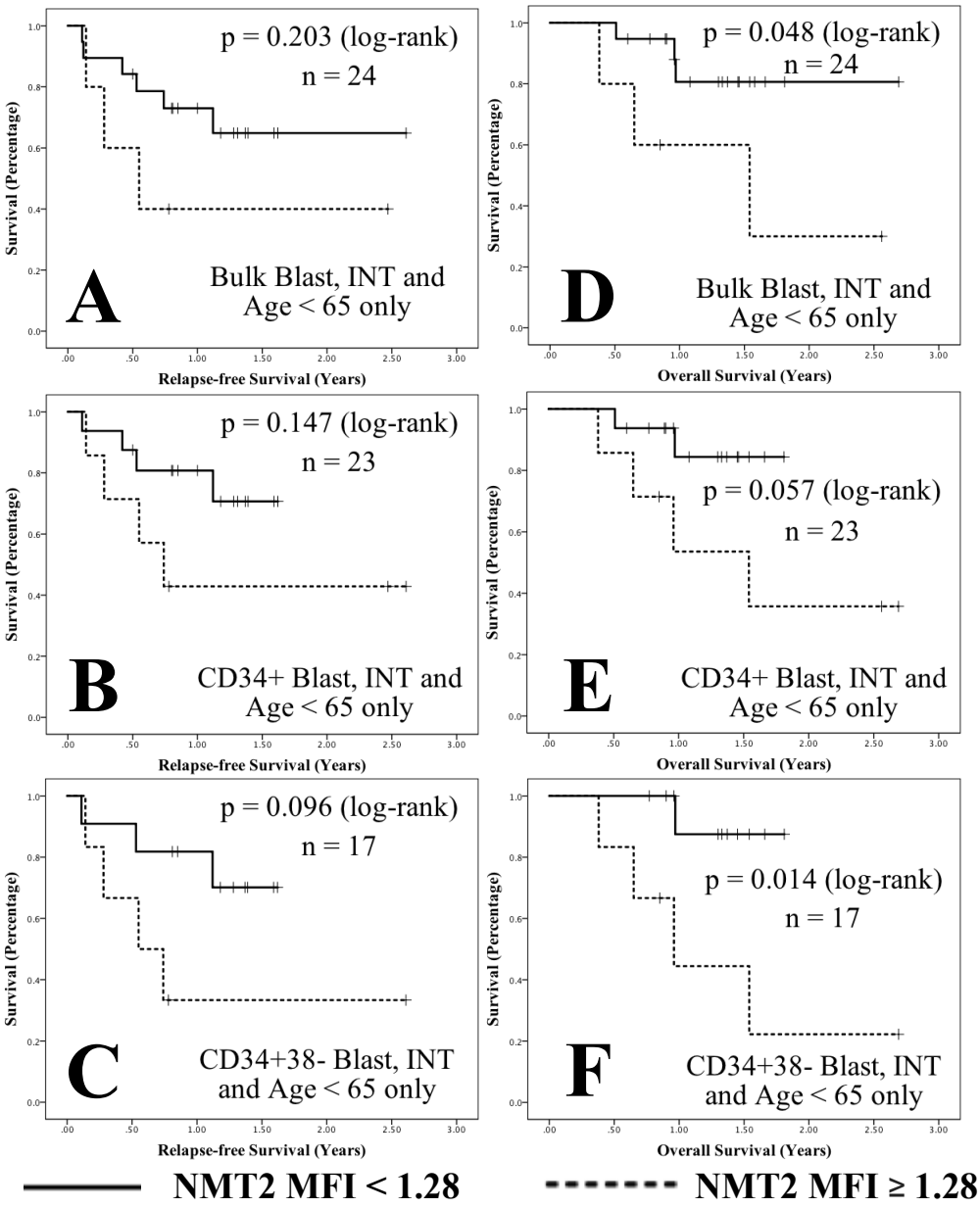

Figure 5.6.12 - Survival by Kaplan-Meier, intermediate-risk, age < 65, NMT2 MFI > 1.28, in bulk, CD34+, and CD34+38- blasts

Kaplan-Meier survival curves are displayed for relapse-free survival for bulk blast (A) (p = 0.203, n = 24), CD34+ blast (B) (p = 0.147, n = 23), and CD34+38- blast populations (C) (p = 0.096, n = 17). Kaplan-Meier survival curves are also displayed for overall survival for bulk blast (D) (p = 0.048, n = 24), CD34+ (E) (p = 0.057, n = 23), and CD34+38- blast populations (F) (p = 0.014, n = 17). A lower sensitivity, higher specificity NMT2 MFI cut-off of 1.28 was used to dichotomize this population.